Relations between ligand binding and activation gating in nicotinic acetylcholine receptors

Thesis

in partial fulfilment of the requirements for the degree of
doctor rerum naturalium (Dr. rer. nat.)

submitted to the Council of the Faculty of Medicine
at Friedrich Schiller University of Jena

by M.Sc. Neuroscience, Abhilasha Ladha
born on 17.06.1986 in Varanasi, Uttar Pradesh, India

Beziehungen zwischen Ligandenbindung und Aktivierungs in nikotinischen Azetylcholinrezeptoren

Dissertation

zur Erlangung des akademischen Grades

„doctor rerum naturalium“ (Dr. rer. nat.)

vorgelegt dem Rat der Medizinischen Fakultät

der Friedrich-Schiller-Universität Jena

von M.Sc. Neuroscience, Abhilasha Ladha

geboren am 17.06.1986 in Varanasi, Uttar Pradesh, Indien

Dissertation, Friedrich Schiller Universität Jena, [2018]

Gutachter / Reviewer:

1. **Prof. Dr. Klaus Benndorf**
   Institute of Physiology II, University Hospital Jena, Jena

2. **Prof. Dr. Ivan Vilotijević (Jun.-Prof.)**
   Institute of Organic chemistry and Macromolecular chemistry, FSU Jena, Jena

3. **Prof. Dr. Thomas Baukrowitz**
   Physiological Institute, Christian-Alberechts-University, Kiel

Tag der öffentlichen Verteidigung / Date of the public disputation: 30.10.2018

Contents

List of abbreviations

µm	- Micrometer
µM	- Micromolar
ACh	- Acetylcholine
AChRs	- Acetylcholine receptors
AgCl	- Silver chloride
A^o	- Angstrom
BASIC	- Bile acid-sensitive ion channel
BBS	- Borate buffered saline
BP filter	- Band-pass filter
Ca^{2+}	- Calcium ion
$CaCl_2$	- Calcium chloride
CFP	- Cyan fluorescent protein
cm	- Centimeter
CNG	- Cyclic nucleotide-gated ion channel
CNS	- Central nervous system
CO_2	- Carbon dioxide
cPCF	- Confocal patch-clamp fluorometry
cRNA	- Complementary ribonucleic acid
Cy3	- Cyanine 3
Cy3-ACh	- Cyanine 3-coupled ACh
Cy5	- Cyanine 5
Cys-loop	- Cysteine-loop
dCy3-ACh	- Non-sulfonated cyanine3-coupled ACh
DNA	- Deoxyribonucleic acid
Dy647 dye	- Dyomics647 dye
E. coli	- Escherichia coli
EC_{50}	- Half maximal effective concentration
ED	- Extent of desensitization
EDTA	- Ethylene diamine tetra acetic acid

EGTA	- Ethylene glycol-bis (β-aminoethyl ether)-N,N,N',N'-tetra acetic acid
EPB-Atto610	- Epibatidine-Atto610 dye
EPB-Cl-Cou	- Epibatidine-chloro-coumarin
EPB-Cou	- Epibatidine-coumarin
EPB-Cy3	- Epibatidine-cyanine3
EPB-Cy5	- Epibatidine-cyanine5
fACh	- Fluorescence tagged acetylcholinene
FCS	- Fetal calf serum
GPCRs	- G protein-coupled receptors
HCN2	- Hyperpolarization-activated cyclic nucleotide-gated channel
HEK 293	- Human embryonic kidney cell 293
HEPES	- 4-(2-hydroxyethyl)-1-piperazineethanesulfonic acid
KCl	- Potassium chloride
kDa	- Kilodalton
kHz	- Kilohertz
L-ACh	- Linker-coupled ACh
LP filter	- Low-pass filter
mAChRs	- Muscarinic type acetylcholine receptors
MEM	- Minimum essential media
$MgCl_2$	- Magnesium chloride
min	- Minute
ml	- Milliliter
mm	- Millimeter
mM	- Millimolar
mRNA	- Messenger ribonucleic acid
ms	- Millisecond
mV	- Millivolt
MWC model	- Monod-Wyman-Changeux model
MΩ	- Megaohm

nA	- Nanoampere
nAChRs	- Nicotinic acetylcholine receptors
NaCl	- Sodium chloride
nM	- Nanomolar
PBS	- Phosphate buffered saline
PCF	- Patch clamp fluorometry
PEG	- Polyethylenglycol
PNS	- Peripheral nervous system
ROI	- Region of interest
s	- Second
S.E.M.	- Standard error of the mean
SH-EP1	- S-type human epithelial cell line

Summary

Nicotinic acetylcholine receptors (nAChRs) are considered as the founding father of the pentameric ligand-gated ion channel superfamily (Changeux, 2012), containing highly diverse family members. nAChRs are involved in the cholinergic transmission of the central nervous system, the peripheral nervous system, and at the neuromuscular junction. Based on their primary site of expression, nAChRs are broadly classified as muscle-type, neuronal-type, and non-neuronal and non-muscle type nAChRs. The muscle-type nAChRs are expressed at the neuromuscular junction, where it mediates the fast-synaptic response upon acetylcholine (ACh) release from the α-motor neuron. They are large glycoproteins of 290 kDa molecular mass. The adult subtype of the receptor is an asymmetric pentamer formed by four distinct subunits α1, β1, δ, and ε subunits in the ratio 2:1:1:1 and has two binding sites, one at the αδ interface and another at the αε interface. The receptor can exist in different states: closed, open and desensitized. It is one of the most studied ion channels and the gating mechanism has been described intensively. However, the reciprocal relationship between activation state and agonist binding is still elusive. Herein, we adapted a challenging approach called confocal patch-clamp fluorometry (cPCF) to study state-dependent agonist binding and unbinding behavior in nAChRs under whole-cell conditions.

The main prerequisite for performing cPCF experiments was to find a suitable fluorescent agonist which can closely mimic the action of the native agonist acetylcholine and which functions in a concentration range suitable for fluorescence microscopy. For this reason, two other agonists of this receptor, nicotine, and carbachol, along with acetylcholine were functionally characterized and compared to find the best suitable ligand for synthesizing its fluorescent derivative. HEK 293 cells were used as the heterologous expression system. Functional characteristics such as concentration-response relationship, desensitization, recovery from desensitization and agonist-induced block were assessed and compared. Upon comparison, acetylcholine was found to be the most potent and efficient agonist for this receptor and was thus chosen for the synthesis of its fluorescent derivative. In this study, a novel fluorescence tagged ACh derivative, fACh, was identified which is an excellent congener of the native neurotransmitter agonist at adult muscle-type nAChRs. fACh was found to be similarly effective as ACh and even slightly more potent. Exposure of

transfected cells to fACh led to fluorescence signals that were absent in non-transfected control cells.

By performing cPCF recordings, allowing for monitoring agonist binding and channel gating in parallel, three different application approaches to gain more insight into the complex gating behavior of nicotinic receptors were suggested in the present study.

1. Monitoring agonist binding and unbinding. Both agonist binding and unbinding followed a biexponential time course. Whereas the fast components were found to be too fast to be resolved, slow processes could be studied with cPCF. The existence of two components might support the idea of αδ and αε binding sites having different affinities for the agonist.

2. Relating agonist binding to desensitization. When recording fluorescence intensity and current flow simultaneously, binding and desensitization behavior can be directly compared. Herein, a high similarity between the kinetics of binding and desensitization was found that supports the idea of an increase in binding affinity during desensitization.

3. Relating unbinding to recovery from desensitization. cPCF allows for studying ligand unbinding during the electrically silent process of recovery. We found that recovery from desensitization was already completed, while the process of ligand unbinding was still proceeding.

Together, the feasibility of employing fluorescent agonists to shed light on the activation mechanisms of the nAChRs and other members of the Cys-loop superfamily is demonstrated in the present study.

Zusammenfassung

Nikotinerge Azetylcholinrezeptoren (nAChRs) werden häufig als Gründungsväter der pentameren ligandengesteuerten Ionenkanalsuperfamilie angesehen (Changeux, 2012), eine vielfältig zusammengesetzte Gruppe ligandengesteuerter Ionenkanäle. Sie spielen eine wichtige Rolle in der cholinergen Transmission im zentralen und peripheren Nervensystem, sowie an der neuromuskulären Endplatte. Nach ihrem Expressionsort, werden sie in neuronale, muskuläre sowie nicht-neuronale/nicht-muskuläre Rezeptoren eingeteilt. Der muskuläre nAChR an der postsynaptischen Membran der neuro-muskulären Endplatte vermittelt die schnellen synaptischen Antworten, ausgelöst durch Azetylcholinfreisetzung durch ein α-Motoneuron. Es handelt sich bei diesen Kanalproteinen um große Glykoproteine von 290 kDa Molekulargewicht. Die adulte Form ist ein asymmetrisches Pentamer, dass sich aus vier unterschiedlichen Untereinheiten zusammensetzt: α1, β1, δ, und ε im Verhältnis 2:1:1:1. Es weist zwei Bindungsstellen auf, eine zwischen den Untereinheiten α1 und δ, die andere zwischen α1 und ε.

nAChRs können in verschiedenen Aktivitätszuständen vorliegen: geschlossen, offen und desensitiviert. Obwohl es sich bei diesem Rezeptor um den am intensivsten untersuchten Ionenkanal handelt und der Aktivierungsmechanismus durch verschiedene experimentelle Ansätze beobachtet wurde, ist die reziproke Beziehung zwischen Agonistbindung und Aktivierungszustand nicht aufgeklärt. Eine geeignete Technik für diese Fragestellung ist die konfokale Patch-Clamp-Fluorometrie, eine Methode, die konfokale Fluoreszenzmikroskopie und Patch-Clamp-Techniken miteinander kombiniert, um mit Hilfe eines Fluorophor-markierten Agonisten Bindungs- und Aktivierungsverhalten parallel zu beobachten. In der vorliegenden Arbeit wurde die cPCF so modifiziert, dass sie für die whole-cell-Konfiguration unter Verwendung von HEK293-Zellen als heterologes Expressionssystem anwendbar ist.

Eine wichtige Voraussetzung für die Anwendung der cPCF ist ein Fluorophor-markierter Agonist, der eine ähnliche Wirkung hervorruft, wie der native Agonist Azetylcholin und in einem Konzentrationsbereich arbeitet, der für die Anwendung in der Fluoreszenzmikroskopie geeignet ist. Aus diesem Grund wurden zunächst drei Agonisten, Azetylcholin, Nikotin und Carbachol, funktionell charakterisiert, um deren aktivierendes Verhalten an adulten muskulären Rezeptoren in HEK293-Zellen unter whole-cell-Bedingungen zu studieren. Die Konzentrations-Aktivierungs-Beziehung,

das Desensitivierungsverhalten, die Erholung von der Desensitivierung sowie der Agonisten-induzierte Block wurden erhoben und verglichen. Azetylcholin hat sich als der am besten geeignete Agonist unter den drei getesteten herausgestellt und wurde daher als Agonist für die Fluorophor-Markierung herangezogen. Unterstützt durch Kooperationspartner (Plested-Labor, FMP Berlin und ChiroBlock GmbH Wolfen) wurde die Synthesestrategie entwickelt und realisiert. Wir konnten zeigen, dass das fluoreszierende Derivat (fACh) ähnlich effizient ist und eine geringfügig höhere Potenz im Vergleich zu ACh aufweist. Nach Applikation verursacht fACh an nAChR-exprimierenden HEK293-Zellen ein spezifisches Fluoreszenzsignal, welches nicht in nicht-transfizierten Kontrollzellen auftrat.

Durch die Anwendung der cPCF, die die parallele Beobachtung der Agonistenbindung und die damit in reziproker Beziehung stehende Kanalaktivierung erlaubt, konnten drei Applikationen vorgeschlagen werden, die zu einem besseren Verständnis des komplexen nAChR-Verhaltens beitragen können.

1. *Agonistenbindung und -entbindung.* Sowohl die Agonistenbindung als auch die Entbindung folgte einem biexponentiellen Zeitverlauf. Während sich die schnelle Komponente als zu schnell erwies, um mit den hier verwendeten Methoden aufgelöst zu werden, konnte die langsame Komponente gut beschrieben werden. Das Auftreten zweier Komponenten könnte auf unterschiedliche Affinitäten der αδ- und αε- Bindungsstellen hindeuten, wie bereits aus früheren elektrophysiologischen Arbeiten vermutet.

2. *Beziehung zwischen Agonistenbindung und Desensitivierung.* Durch die parallele Aufzeichnung der Fluoreszenzänderung und des Stromflusses können Bindungs-verhalten und Desensitivierungsverhalten direkt miteinander in Beziehung gesetzt werden. Somit konnte in der vorliegenden Arbeit gezeigt werden, dass während der Desensitivierungsphase das Fluoreszenzsignal mit gleicher Kinetik ansteigt, was als Ausdruck einer desensitivierungsinduzierten Affinitätssteigerung interpretiert werden kann. Dies wurde auf Grund früherer elektrophysiologischer Arbeiten vermutet und kann nun direkt ausgelesen werden.

3. Beziehung zwischen Agonistenentbindung und Erholung von der Desensitivierung. Die Anwendung der cPCF erlaubt es, Ligandenbindung auch an elektrophysiologisch nicht zu fassende Aktivitätszustände zu beobachten, wie sie zum Beispiel während

der Erholung von der Desensitivierung auftreten. In dieser Arbeit fanden wir eine kürzere Zeitkonstante für den Prozess der Erholung als für den Prozess der Agonistenentbindung. Dies könnte darauf hindeuten, dass eine erneute Kanalaktivierung bereits möglich ist, während die Entbindung des zweiten Liganden noch nicht abgeschlossen ist.

Zusammenfassend konnte gezeigt werden, dass Fluorophor-gekoppelte Agonisten ein geeignetes Werkzeug sind, um mit Hilfe der konfokalen Patch-Clamp-Fluorometrie unter Anwendung der whole-cell-Konfiguration den Aktivierungsmechanismus nikotinerger Azetylcholinrezeptoren zu untersuchen. Bei Vorhandensein geeigneter Agonisten kann diese Methode auf andere Cys-Loop-Rezeptoren übertragen werden.

1. Introduction

1.1. Acetylcholine receptors

Acetylcholine receptors (AChRs) are integral membrane proteins, which respond to a direct binding of the ligand acetylcholine (ACh), and hence, are categorized as ligand-gated ion channels. In 1914, Sir Henry Dale classified two types of ACh receptors, metabotropic muscarinic ACh receptors and ionotropic nicotine ACh receptors. This distinction was based on the receptors' sensitivities to different agonists: muscarine, a toxin from the mushroom *Amanita muscaria* and nicotine, an alkaloid found in leaves of *Nicotiana tabacum*, respectively. Both muscarine and nicotine mimic responses typical for ACh.

The muscarinic type (mAChRs), a member of the G-protein coupled receptor (GPCRs) family, mediates its slow metabolic responses by activating a cascade of intracellular pathways whereas nicotinic receptors (nAChRs) are ligand-gated ion channels of the 'Cys-loop' superfamily that mediate fast synaptic responses. However, both receptors share the similar property of being activated by the endogenous ligand ACh and are expressed in both, neuronal and non-neuronal cell-types.

1.2. Nicotinic ACh receptors

nAChRs are prototypes for the pentameric ligand-gated ion channels (Celie et al., 2004). They are non-selective cation channels (Gündish and Eibl, 2012; Reitstetter et al., 1999) and are characterized by unique combinations of 17 homologous subunits, i.e. α1- α10, β1- β4, δ, ε, and γ (Lukas et al., 1999; Kalamida et al., 2007; Wu and Lukas, 2011; Gündish and Eibl, 2012). An evolutionary phylogenetic tree of nicotinic ACh receptor subunits is shown in Figure 1.

Based on their primary site of expression, nAChRs are broadly classified as muscle-type nAChRs, neuronal-type nAChRs, and non-neuronal / non-muscle type nAChRs. Muscle-type nAChRs are exclusively found at the neuromuscular junction and fetal extrajunctional sites (Lustig, 2006; Kalamida et al., 2007; Gündish and Eibl, 2012). Neuronal-type nAChRs are present in CNS, PNS, and ganglions (Gotti and Clementi, 2004; Lustig, 2006; Kalamida et al., 2007; Gündish and Eibl, 2012), while non-neuronal and non-muscle type are present in keratinocytes, bronchial epithelial cells,

aortic endothelial cells, macrophages, and lymphocytes (Lindstrom, 1997; Nguyen et al., 2000; Peng et al., 2004; Lustig, 2006; Kalamida et al., 2007; Gündish and Eibl, 2012).

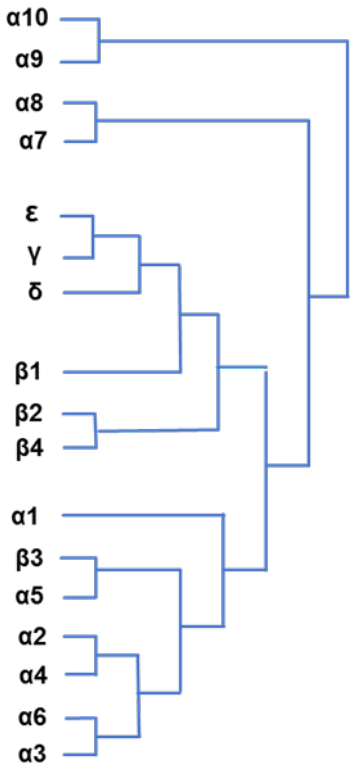

Figure 1. An evolutionary phylogenetic tree of nicotinic ACh receptor subunits
The dendrogram illustrates the apparent evolutionary distance between subunits of the nicotinic ACh receptor. The ancestral or precursors of α-subunits (ligand binding subunits) and β-subunits (non-ligand binding subunits) were most probably homologs of nAChR α9 or α10 (adapted from Lustig, 2006).

nAChRs subtypes mediate various important physiological, pathophysiological, and therapeutic functions (Lustig, 2006; Kalamida et al., 2007; Gündish and Eibl, 2012). They are involved in regulating the release of neurotransmitter, synaptic transmission, cell excitability, neuronal networking, and integrations as well as in regulating pain, hunger, anxiety, sleep, and arousal (Lindstrom, 1997; Changeux and Edelstein, 2001; Gotti and Clementi, 2004; Lustig, 2006). Impairment of nAChR function also leads to a variety of diseases and disorders, such as myasthenia gravis, Alzheimer's disease,

Parkinson disease, depression, schizophrenia, obesity, tobacco dependence, epilepsy, and some form of skin disorders (Lustig, 2006; Gündish and Eibl, 2012).

1.3. Muscle-type nicotinic ACh receptors

The muscle-type nAChR is a large glycoprotein of 290 kDa molecular mass (Francis and Papke, 1996; Prince et al., 2002; Unwin, 2005). It exists in an asymmetric pentamer formed by four distinct subunits, α1, β1, δ, and ε in the ratio of 2:1:1:1 (Figure 2A). In fetal form, γ subunit is present instead of ε subunit (Auerbach, 2015). The receptor contains two binding sites: αδ and αε. These subunits assemble to form a pore that allows cations to cross the cell membrane. Each subunit exhibits a large N-terminal extracellular domain (Francis and Papke, 1996; Prince et al., 2002; Unwin, 2005; Wonnacott and Barik, 2007), a membrane-spanning domain (Reynolds and Karlin, 1978; Lindstrom et al., 1979; Saitoh et al., 1980; Raftery et al., 1980; Kistler et al., 1982; Giraudat et al., 1982; Francis and Papke, 1996; Unwin, 2005; Wonnacott and Barik, 2007), and a smaller intracellular domain (Francis and Papke,1996; Prince et al., 2002; Unwin, 2005).

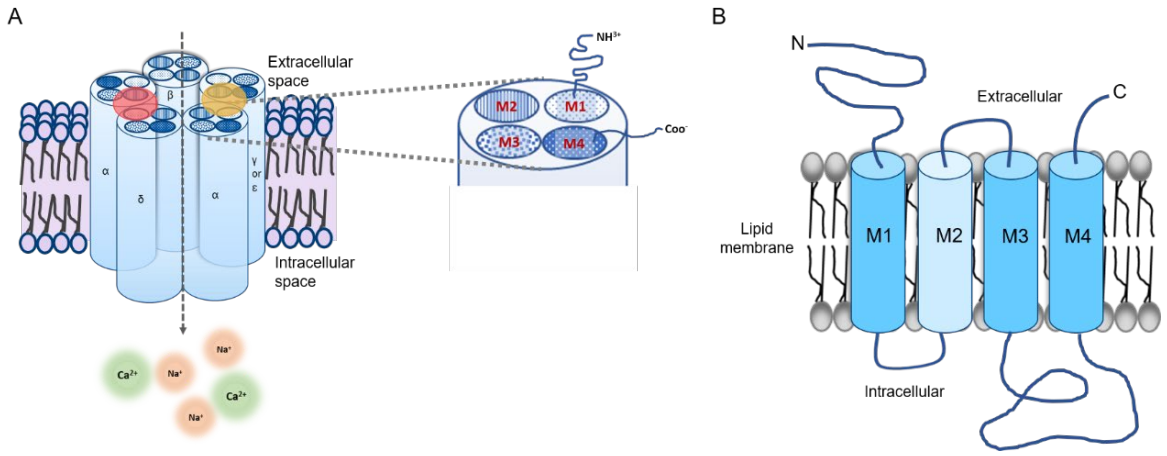

Figure 2. Illustration of the heteropentameric muscle-type nAChR

(A) The figure shows the arrangement of five subunits that form a pore, which allows the exchange of cations across the cell membrane. Circles in red and yellow represent the two binding sites at the αδ and αε interface, respectively. Each subunit is made up of four transmembrane domains shown in patterned circles. (B) The cartoon represents the putative

transmembrane organization of a single nAChR subunit. All four transmembrane domains (M1-M4) are represented.

1.3.1. Molecular architecture of the muscle-type nicotinic ACh receptors

The extracellular ligand binding domain of each nAChR subunit is organized around a curled β-sandwich consisting of two sets of β-sheets, which are joined via a disulfide bridge (Brejc et al., 2001). This disulfide bridge forms a so-called 'Cys-loop', the signature sequence of the ligand-gated ion channel family (Figure 3). Extracellular domains of nAChRs contain two ligand-binding sites: one at the αδ interface, while another at the αε interface (Prince et al., 2002). These sites allow for binding of ligands to the channel and mediate channel functions. However, the question is still to be addressed whether these two binding sites are identical (Colquhoun and Ogden, 1988; Akk and Auerbach, 1996; Salamone et al., 1999) or non-identical (Arias, 2000; Unwin, 2005; Kalamida et al., 2007; Wonnacott and Barik, 2007) concerning of ligand affinity. Each binding site is formed by the combination of two separate parts: one is called the 'principal component' (segments of α subunit) and the other is called the 'complementary component' (segments of non-α subunit). Two cysteine residues, Cys 128 and Cys 148 located in the α subunit (*Torpedo*) form a disulfide bridge that helps in agonist binding and channel opening (Wonnacott and Barik, 2007). While α1, δ, and ε subunits play a role in ligand binding, β1 helps in clustering of the nAChRs (Kalamida et al., 2007). Apart from full agonists (i.e. ACh), partial agonists (e.g., decamethonium), as well as competitive antagonists (e.g., α-bungarotoxin) can also bind to the primary binding sites (αδ and αε) of the channel. However, there is another binding site(s) for non-competitive agonists (e.g., catharanthine) and allosteric modulators (e.g., galantamine) (Akk and Steinbach, 2005; Wonnacott and Barik, 2007; Papke et al., 2010; Arias et al., 2010; Papke, 2014).

The membrane-spanning domain of each subunit of the nAChR is composed of four transmembrane α helical segments (M1-M4) (Unwin, 2005; Kalamida et al., 2007) (Figure 2B). The M2 segment of each subunit of the nAChR mainly contributes to the lining of the channel pore, while the extracellular ends of the M1 segment of each subunit possibly have a smaller contribution in the lining of the channel pore.

(Changeux et al., 1992; Arias, 1996; Miyazawa et al., 1999; Prince et al., 2002). Segments M1, M3, and M4 shield the inner ring formed by M2 α helical segments from membrane lipids by coiling around each other (Unwin, 2005; Kalamida et al., 2007).

The intracellular domain of each subunit of the nAChR consists of the large cytoplasmic M3-M4 loop containing a curved α-helix. The length of the loop is different for different subunits ranging from 110 to 270 amino acids. Intracellular loops possess an abundance of negatively charged amino acids that favor the influx of cations (Na^+, K^+, and Ca^{2+}) (Unwin, 2005).

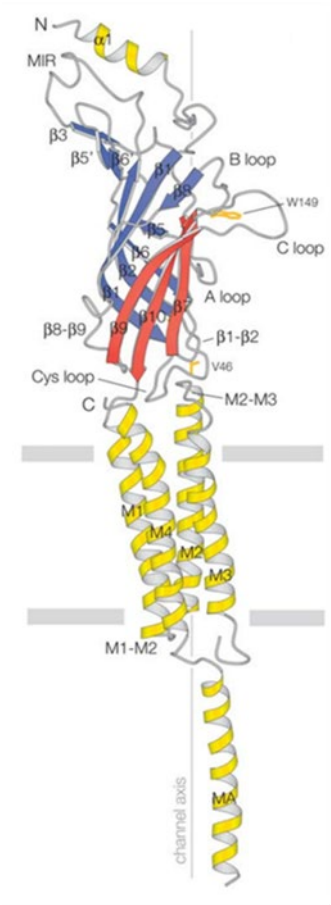

Figure 3. Electron microscopy structure of a single subunit (α) of *Torpedo marmorata* nAChR at 4 A° resolution

Ribbon structure of a side view of the α subunit is illustrated. The transmembrane domains (M1-M4) are shown in yellow, β-sandwich are shown in red (outer) and blue (inner).

Functionally important A, B, C, β1- β2 and Cys loops are also represented. MA (yellow) is a curved α- helix present in intracellular domain (adapted and modified from Unwin, 2005).

1.3.2. Gating behavior of muscle-type nicotinic ACh receptors

Muscle-type nAChRs are allosteric proteins that exist in multiple interconvertible conformational states (Papke, 2014): resting or closed state, activated or open state, and desensitized states (Katz and Thesleff, 1957; Sakmann et al.,1980; Neubig et al.,1982; Heidmann et al., 1983; Jackson, 1989; Auerbach, 1993; Hess, 1993; Karlin and Akabas, 1995). However, the existence and an exact number of possible substates are still a matter of debate. The allosteric mechanism which leads the receptor to undergo conformational changes is known as gating (Perutz, 1989). The main functional states of adult muscle-type nAChRs are shown in Figure 4.

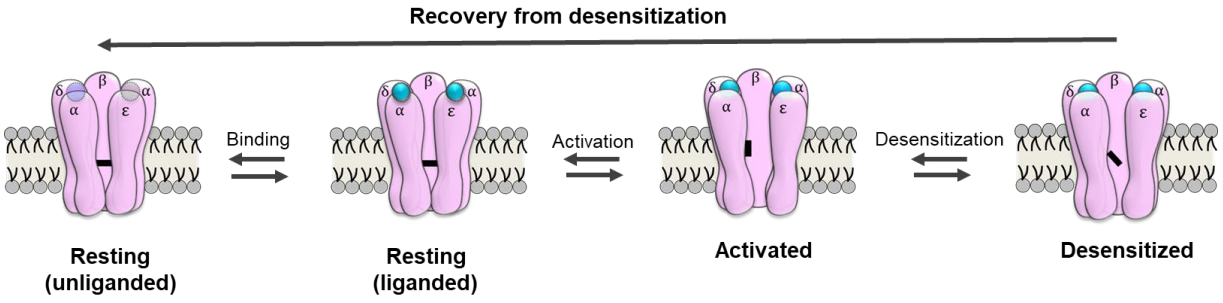

Figure 4. Functional states of the adult muscle-type nAChR

Illustrations of the different functional states: resting and unliganded, resting and liganded, activated, and desensitized state. In the absence of a ligand, the channel exists in the closed state (resting unliganded state). When a ligand binds to the receptor (resting liganded state), the gate of the channel opens due to conformational changes in the receptor. This is defined as an activated state. Upon prolonged exposure of the ligand, the channel enters into the desensitized state. The ligand is shown in green color. A horizontal gray bar in the channel lumen represents closure of the channel gate, the tilted gray bar represents a different conformation of the gate which does not allow passage of ions through the pore.

The ‘resting’ or ‘closed state’ exists when the gate of the receptor is closed in the absence of ligands at the binding sites. The closed state is the most stable state, however, spontaneous openings without ligands being bound are possible to a low

extent (Karlin and Akabas, 1995; Karlin, 2002). Binding of ligands to the binding sites provokes the channel to undergo tertiary conformational changes, resulting in a metastable state called 'open' or 'activated state' (Kalamida et al., 2007). This leads to a movement of ions across the cell membrane. The transient opening of the channel occurs within tens of microseconds (Wu et al., 1994; Yamodo et al, 2010). However, prolonged presence of agonist at binding sites for hundreds of milliseconds triggers the channel to enter into a 'desensitized state'. Amongst the liganded states, the desensitized state is the most stable state and has the highest affinity for ligands; howbeit, access of ions in the pore is prohibited (Karlin and Akabas, 1995; Karlin, 2002). The channel enters into the closed state again when unbinding of ligands is completed. The stoichiometry of the receptor, types of ligands (agonists, antagonists, and allosteric modulators), and occupancy of binding sites regulate the equilibrium between different functional states (Papke, 2014).

Resting state of the receptor

The resting or closed state is a non-conducting state as there is no ionic movement across the channel due to the closure of the pore. Electron microscopic studies of *Torpedo marmorata* nAChRs at 4 A^{o} resolution revealed that the presence of bulky hydrophobic side chains and a smaller separation between M2 helices make the pore constricted enough that the passage of ions is hindered.

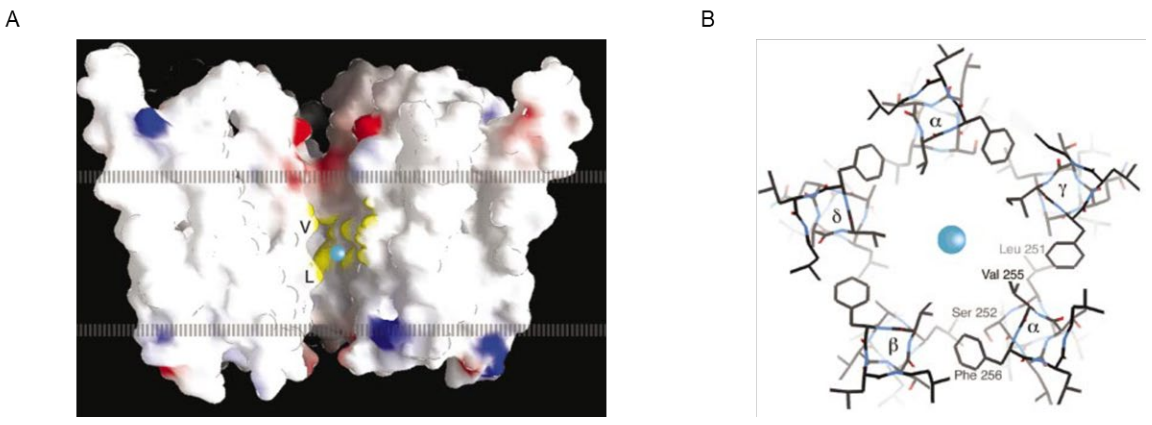

Figure 5. Overview of the pore in the closed conformational state of the receptor

(A) The image represents the molecular surface of the pore domain. Circles in red and dark blue represent highly positively charged and highly negatively charged areas, respectively. Yellow circles show the hydrophobic area containing the gate of the pore. (B) The model represents symmetrical arrangements of side chains that form the gate of the channel. The blue sphere indicates a sodium ion in both A and B (adapted from Miyazawa et al., 2003).

Additionally, side-to-side interactions of hydrophobic amino acids of neighboring M2 helices form a tight hydrophobic girdle (Figure 5). Hence, the energetic barrier created by the girdle prevents the ionic permeation during resting state (Miyazawa et al., 2003).

Open state of the receptor

Ligand binding facilitates the conformational change in the receptor entering into the conducting or open state. It is interpreted that upon ligand binding, the two sets of β-sheets in the α subunit exert alternative conformations facilitating the activation of the channel. This allosteric change entails 15^{o} rotational movement of the inner β-sheets. The twisting movement weakens side to side hydrophobic interactions, which otherwise are responsible for the constricted pore. The helices 'collapse' back and make alternative hydrophobic contact with the outer protein wall. As a consequence, the channel skips to the 'open state' (Miyazawa et al., 2003) (Figure 6).

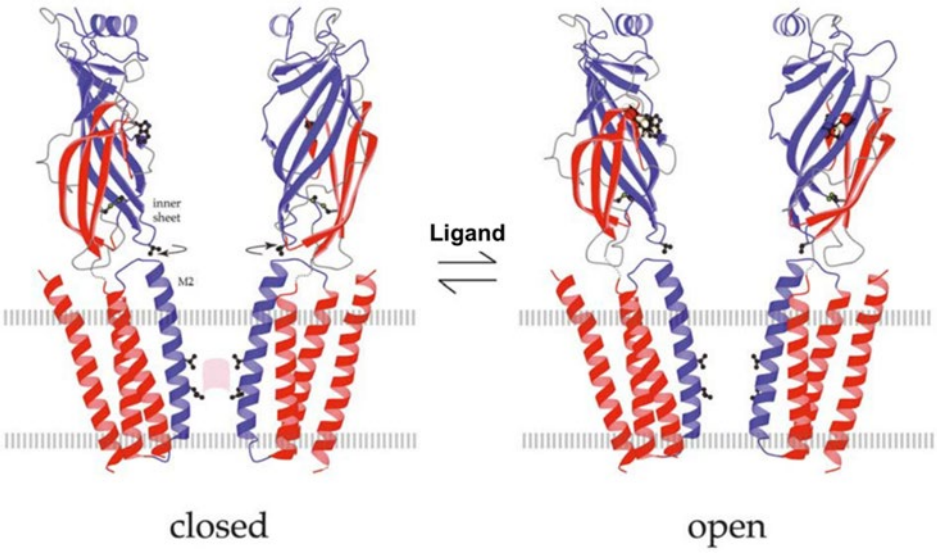

Figure 6. Illustration of closed (left) and open (right) channel conformation

Binding of the ligand to the binding sites leads to a 15° rotational movement, which is transmitted to the gate via M2 helices. Rotation destabilizes the gate and leads the helices to adopt an alternative configuration where they can move freely, resulting in a weakening of side to side hydrophobic interactions. Consequently, helices collapse and lead to the opening of the ion channel. The relevant moving part is shown in gray. Arrows denote the alternative conformations of β-sheets. Pink patch on the left represents the gate. Broken horizontal gray lines display the membrane surface (adapted and modified from Unwin, 2003).

Although the structural mechanism by which ligand binding leads to channel opening is known, it is still a matter of debate whether ligand binding at one binding site can open the channel (Jha and Auerbach, 2010; Williams et al., 2011) or two binding sites must be occupied for channel opening (Cash and Hess, 1980; Sine and Taylor, 1980; Stroud and Moore, 1985; Arias, 2000; Wonnacott and Barik, 2007).

Desensitized state of the receptor

Desensitization of nAChRs was first described by Katz and Thesleff in 1957. The desensitized state exists under kinetically distinguishable protein conformations (Heidmann and Changeux, 1980; Neubig and Cohen 1980; Reitstetter et al., 1999; Elenes and Auerbach, 2002; Elenes et al., 2006). It is a high-affinity albeit non-conducting state that occurs spontaneously upon prolonged exposure to the agonists. Additionally, channels can also undergo desensitization without channel activation and thus by surpassing the open state (Magleby and Pallotta, 1981; Reitstetter et al., 1999). Desensitization plays a key role in synaptic plasticity (Galzi and Changeux, 1994; Reitstetter et al., 1999) and in nicotine dependence of smokers (Lukas et al., 1996; Reitstetter et al., 1999). Inaccurate desensitization of the receptor leads to pathophysiological problems, such as myasthenia gravis and congenital myasthenic syndrome (Giniatullin et al., 2005; Kalamida et al., 2007). The duration of agonist application as well as the concentration of agonist, regulate the desensitization process (Wang and Sun, 2005).

The receptor can exist in several different states of desensitization, but the exact number of states and their properties are still undetermined (Reitstetter et al., 1999; Elenes and Auerbach, 2002). Despite this fact, desensitization is often classified into two states: ‘fast’ and ‘slow’ (Neubig et al., 1980; Boyd and Cohen, 1980; Yu et al.,

2009). The ‘fast’ or ‘classical desensitization’ follows the activation and occurs within tens of milliseconds. It generally takes place upon medium to high (µM to mM) concentrations of agonist application. However, ‘slow’ or ‘high-affinity desensitization’ takes place upon agonist application in nM to µM range and occurs in seconds to minutes range (Changuex and Edelstein, 1998; Dahan et al., 2004; Giniatullin et al., 2005) (Figure 7).

In comparison to activation, the mechanism of desensitization is poorly understood (Elenes and Auerbach, 2002; Giniatullin et al., 2005; Yu et al., 2009). Structural changes in the receptor during binding and activation has been nicely deduced (Unwin, 1995; Brejc et al., 2001), but locations and conformational changes that drive the channel into the desensitized state are still unclear.

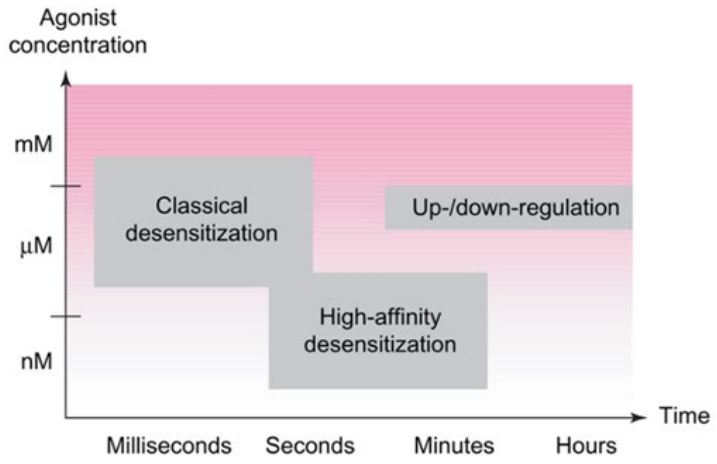

Figure 7. Different states of desensitization

Classical desensitization is fast (in ms - s range) that occurs upon application of an agonist in the µM to mM range, whereas high-affinity desensitization is slow (in s-min range). It occurs upon application of an agonist in the nM to mM range (adapted from Giniatullin et al., 2005).

Block of muscle-type nicotinic ACh receptors

The block of the muscle-type nAChRs by barbiturates and local anesthetics was first reported by Adams (1976) and Ruff (1976). In addition to the antagonists, open channel block of nAChRs by agonists such as ACh, nicotine, carbamylcholine, suberyldicholine (Sine and Steinbach, 1984; Ogden and Colquhoun, 1985; Maconochie and Steinbach, 1995), decamethonium (Adams and Sakmann, 1978; Marshall et al., 1991), tetraethylammonium, tetramethylammonium (Akk and

Steinbach, 2003), and choline (Grossman and Auerbach, 2000; Purohit and Grossman, 2006; Lape et al., 2009) has been constantly reported.

The mechanism behind the transient blocking of the receptor by agonists is still obscure. It is predicted that during the open channel block, the interruption in ionic flow is a result of physically plugging the pore by the open channel blockers (Prince et al., 2002), which hints towards the presence of an extra binding site inside the pore other than the two binding sites in the extracellular channel portion (Maconochie and Steinbach, 1995). This was concluded from the fact that the access to the binding site inside the pore is only possible when the channel is present in the activated state. The location of the binding site is predicted to lie within the membrane field (Prince et al., 2002). Removal of agonists from the pore site leads to unblocking (reopening), whereas removal from the classical binding sites leads to the closure of the channel (Neher and Steinbach, 1978).

1.3.3. Agonists and antagonists of muscle-type nAChRs

It is widely known that muscle-type nAChRs are activated upon binding of endogenous ligand ACh at binding sites located in the extracellular domain. Surprisingly, several other ligands can also bind to the same binding sites and regulate the gating of the nAChRs. Agonists, such as epibatidine, carbamylcholine, nicotine, and choline are substances, which upon binding to the receptor, activate the receptor to produce a biological response (Arias, 2000; Wonnacott and Barik, 2007). Unlike agonists, antagonists inhibit a biological response by binding to a receptor. They are commonly classified as competitive antagonists and non-competitive antagonists. Competitive antagonists, such as α-bungarotoxin, d-tubocurarine, α-conotoxin MI, and lophotoxin bind at or near the agonist binding sites and compete with the agonists by preventing their access to the binding sites. Non-competitive antagonists or channel blockers, such as physostigmine, chlorpromazine, and galantamine are those which inhibit the function of the channel without inhibiting agonist binding. Their binding sites are located at different luminal and non-luminal domains (Arias, 2000; Wonnacott and Barik, 2007). Table 1 and Table 2 summarize various agonists, competitive antagonists, and non-competitive antagonists of muscle-type nAChRs (Cooper et al., 1996; Akk and Auerbach, 1999; Arias, 2000; Jonsson et al., 2006; Wonnacott and Barik, 2007; Kudryavtsev et al., 2015).

Table1: List of agonists of muscle-type nAChRs.

Agonists	Source of origin	Comments
ACh	Motor neuron, parasympathetic nervous system	Endogenous ligand
Choline	Plants and animal products	Essential nutrient
Nicotine	Natural alkaloid found in plants of *Solanaceae* family	Exogenous ligand
Epibatidine	Natural alkaloid secreted by *Epipedobates* frogs	Exogenous ligand
Cytisine	Natural alkaloid found in plants of *Fabaceae* family	Exogenous ligand
Anatoxin-a	Bicyclic amine alkaloid found in cyanobacteria	Exogenous ligand
Lobeline	Natural alkaloid found in plants of *Lobelia* family	Exogenous ligand
Muscarine	Natural alkaloid found in mushroom species *Amanita muscaria*	Exogenous ligand
Carbamylcholine	Synthetic choline ester and a positively charged quaternary ammonium compound	Exogenous ligand
Dimethylphenylpiperazinium iodide	Synthetic compound	Exogenous ligand
Oxotremorine-M	Synthetic compound	Exogenous ligand
Methacholine	Synthetic choline ester	Exogenous ligand
Succinylcholine	Synthetic compound	Exogenous ligand

Table 2: List of antagonists of muscle-type nAChRs.

Antagonists	Source of origin	Comments
α-Bungarotoxin	Found in venom of the snake *Bungarus multicinctus*	Competitive
α-conotoxin MI	Found in venom of the snail *Conus magus*	Competitive
d-tubocurarine	Mono-quaternary alkaloid found in the *Chondrodendron tomentosum* plant	Competitive

Coniine	An alkaloid found in *Conium maculatum* plant	Competitive
Pinnatoxins	A toxin derived from a dinoflagellate *Vulcanodinium rugosum*	Competitive
Lophotoxin	A neuromuscular toxin isolated from corals of *Lophogorgia* genus	Competitive
Decamethonium	A synthetic bis-quaternary ammonium compound	Competitive
Parncuronium	An amino steroid	Competitive
Benzoquinonium	Synthetic compound	Competitive
Physostigmine	A crystalline alkaloid obtained from Calabar bean	Non-competitive
Galantamine	A tertiary alkaloid obtained from plants of Amaryllidaceae family	Non-competitive
Histrionicotoxin	A poisonous alkaloid found in the skin of frog *Oophaga histrionica*	Non-competitive
Chlorpromazine	An antipsychotic drug; synthetic	Non-competitive

1.3.4. Physiological aspect of nAChRs at neuromuscular junction

A motor neuron and a motor endplate with a synaptic cleft (junctional gap) form a neuromuscular junction, which plays a key role in the contraction of skeletal muscles. nAChRs concentrated in the sarcolemma at the neuromuscular junction (Unwin, 2005) are involved in transferring the electrical impulses of α-motor neurons to muscle cells.

When the action potential reaches the nerve terminal, it depolarizes the terminal, which accelerates the opening of voltage-gated calcium channels. This leads to an increase in the intracellular calcium concentration, which triggers the release of ACh molecules from the axon terminal to the synaptic cleft. ACh molecules bind to nAChRs present at the motor endplate. Binding of ACh results in the opening of nAChRs, which leads to the inward current due to the movement of cations, and hence, the membrane gets depolarized. This depolarization causes opening of the voltage-gated sodium channels that result in eliciting action potentials. Elicited action potentials propagate along the sarcolemma and membrane of the T-tubules. This

triggers the release of stored calcium from the sarcoplasmic reticulum and ultimately leads to muscle contraction (Figure 8). When the calcium concentration returns to the normal level, it induces muscle fibers to relax (Slater, 2017).

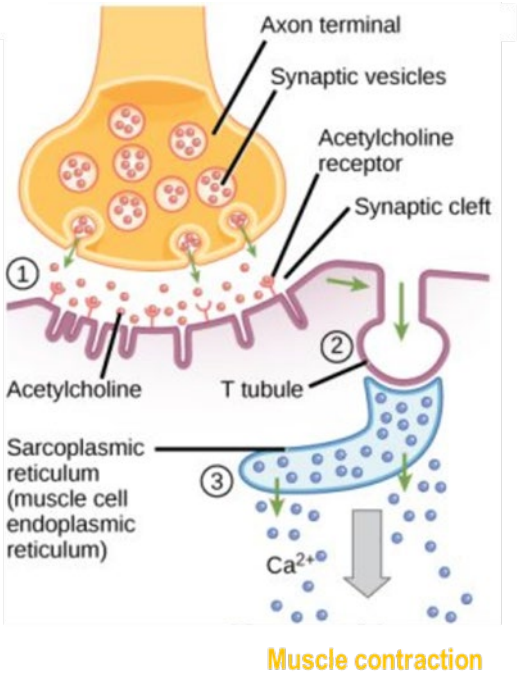

Figure 8. Events at the neuromuscular junction.

When action potentials reach the axon terminal: (1) ACh gets released and binds to the nAChRs present at the motor endplate. (2) Binding of ACh to nAChRs results in the opening of nAChRs. This leads to inward movement of cations that results in the generation of transient endplate potential and opening of voltage-dependent sodium channels. Opening of voltage-gated sodium channels results into elicitation of action potentials in the muscle fibers. These action potentials further propagate to the T-tubules. (3) In response to the transient voltage change, Ca^{2+} gets released from the sarcoplasmic reticulum and triggers muscle contraction (modified from Molnar and Gair, 2015).

1.3.5. Pathophysiological aspect of muscle-type nAChRs

Muscle-type nAChRs are eminent targets in several acquired and inherited diseases, such as myasthenia gravis and congenital myasthenic syndromes that cause impairment of neuromuscular transmission and muscle weakness (Kalamida et al., 2007).

Myasthenia gravis is a chronic autoimmune disorder in which autoantibodies are produced by white blood cells, which bind to the body's own muscle nAChRs and destroy them. Muscular weakness caused by the reduced efficiency of the neuromuscular junction and fatigue are symptoms of this disease. It can either be confined to a single muscle group or can be spread to several skeletal muscles (Kalamida et al., 2007).

Congenital myasthenia syndrome is an inherited disease caused by defective genes resulting in muscle fatigue due to deformity at the neuromuscular junction. Some of the naturally occurring 'gain of function' mutations, such as αG153S, αN217K, and εL221F in adult human muscle-type nAChRs are well-known (Engel et al., 1982; Oosterhuis et al., 1987; Engel et al., 1996; Abraham, 2003), which cause the congenital myasthenic syndrome. This syndrome is generally classified into two subtypes: slow channel syndromes and fast channel syndromes. These slow and fast channel syndromes are characterized by kinetic abnormalities of nAChR function. Slow channel syndromes arise due to the prolonged opening of the nAChR channel, causing abnormally slow decay of the synaptic currents. In contrast, fast channel syndromes arise from the abnormally fast decay of synaptic response because of brief channel opening due to decreased affinity for ACh and lower gating efficiency (Kalamida et al., 2007).

Another reason why muscle-type nAChRs involved in neuromuscular transmission are of pharmacological interest is their usability as an appropriate pharmacological target for muscle relaxants, such as rocuronium, rapacuronium, and 3-desacetyl rapacuronium (Paul et al., 2002). Muscle relaxants, in particular, neuromuscular blocking agents, work at the neuromuscular junction. They are basically classified as depolarizing blocking agents (e.g., succinylcholine) and non-depolarizing blocking agents (e.g., tubocurarine). Depolarizing agents are agonists that mimic ACh, while non-depolarizing agents competitively block or inhibit ACh binding to the nAChR. These muscle relaxants are co-administered with anesthesia during surgery to cause temporary paralysis.

2. Aim and objectives of the study

Many functional studies are committed to determining whether there are intermediate states between ligand binding and muscle-type nAChRs opening and between the opening and full desensitization. Complex kinetic models have been repeatedly proposed based on electrophysiological studies of muscle-type nAChRs to understand state-dependent relationships. Four examples are shown in Figure 10.

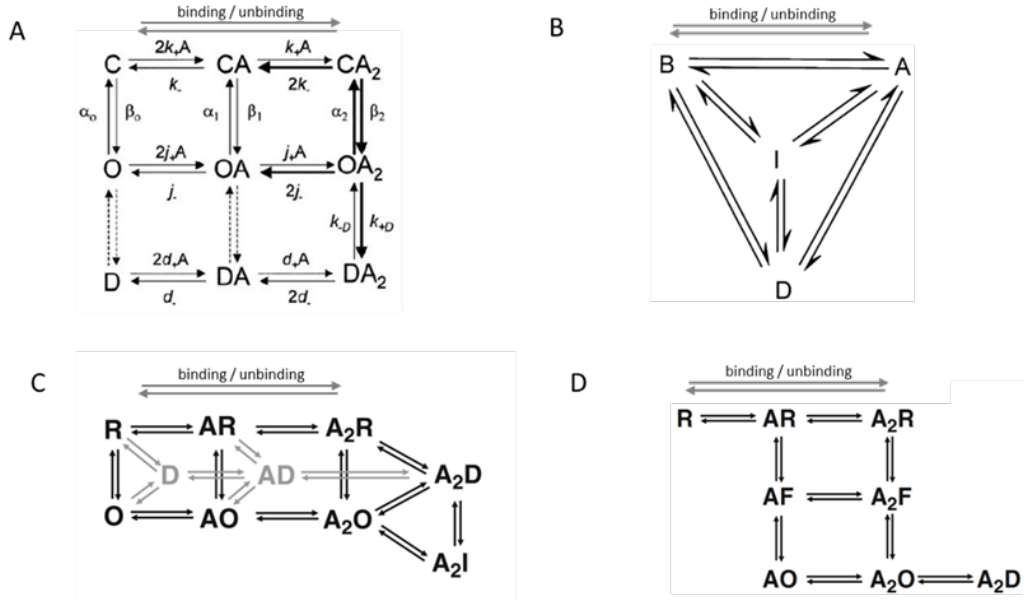

Figure 10. Schemes of kinetic models

(A) Kinetic model proposed by Grosman and Auerbach, 2001. C is the closed state, A is an activated state, O is an opened state, and D is a desensitized state. (B) The kinetic scheme proposed by Edelstein et al., 1996. B is a basal state (closed state), A is an active state, I is an initially inactivated state, and D is a desensitized state. (C) Illustration of a Monod-Wyman-Changeux (MWC) model for desensitization proposed by Lester, 2014. R is a resting state, A is an activated state, O is an open state, D is a desensitized state, and I is a structurally distinct state of desensitization. (D) Kinetic model proposed by Lape et al., 2009. R is a resting state, F is a flip state (intermediate state), O is an open state, and D is a desensitized state.

Although much is known about the structural and functional relationship of the receptor, the reciprocal relationship between ligand binding and channel gating is still elusive. Therefore, the aim of this study is to contribute to a further validation of these kinetic models so far based on electrophysiological recordings, by providing data on

ligand binding. For realizing this, adapting confocal patch-clamp fluorometry to whole-cell recording was required. The objectives of the present study are:

1. To accomplish experimental requirements for electrophysiological and/or fluorescent experiments.
2. To find a suitable ligand amongst available agonists for synthesizing its fluorescent derivative.
3. To synthesize the suitable fluorescent derivative.
4. To relate ligand binding and gating for the synthesized fluorescent derivative.

3. Materials and Methods

3.1. Plasmids amplification, extraction, and purification

Genes encoding adult human muscle-type nicotinic ACh receptor (nAChR) α_1, β_1, δ, and ε in the plasmid vector pcDNA3 (generous gift by Lucia Sivilotti, UCL, London) were used in experiments of the present study. Plasmids were amplified in *E. coli*, extracted, and purified by Karin Schoknecht, Dr. Gunter Ehrlich, and Prof. Dr. Thomas Zimmer (Institute of Physiology II, Jena, Germany).

3.2. Cell culture and transfection

3.2.1. Cell line

HEK 293 cells were used as a heterologous expression system. These cells are widely used in patch-clamp electrophysiology not only because they exhibit few endogenous channels but also because they have beneficial properties, such as a rapid division and easy maintenance. Furthermore, they can be transfected conveniently. The appropriate size of cells (about 20-30 µm in diameter) makes them suitable for the experimental needs of the present study.

3.2.2. Cell culture

HEK 293 cells (European Collection of Authenticated Cell Cultures, England) were initially grown in Petri dishes (100 x 20 mm; Greiner bio-one GmbH, Frickenhausen, Germany) and were maintained in Minimum Essential Media (MEM) with Earle's Salt and L-Glutamine (GIBCO BRL, Karlsruhe, Germany) containing 10% Fetal Calf Serum (FCS) (Biochrom GmbH, Berlin, Germany), 1% antibiotics (penicillin/streptomycin), and 1% non-essential amino acid in a humidified 5% CO_2 incubator at 37^{o}C. After achieving about 80-90 % cell confluence, cells were sub-cultured using Trypsin-EDTA (GIBCO, BRL, Karlsruhe, Germany) digestion.

3.2.3. Cell transfection

3.2.3.1. Calcium phosphate transfection method

HEK 293 cells were transiently transfected with calcium phosphate transfection method. The method is efficient for introducing foreign DNA plasmids in different cell types. The principle involves the introduction of DNA into cells by formation of a

calcium phosphate DNA co-precipitate. These precipitates are internalized by the cells via endocytosis leading to efficient expression of DNA (Graham and van der Eb, 1973).

3.2.3.2. Transfection procedure

Cells were trypsinized, diluted with culture medium and were seeded in a separate Petri dish (60 x 15 mm; Greiner bio-one GmbH, Frickenhausen, Germany), for overnight incubation. Next day, when 60-70% of cell confluence was achieved, the culture medium was exchanged with fresh medium 1 hour before transfection. Plasmids of adult human muscle-type nAChRs α_1, β_1, δ and ε were mixed in a ratio of 2:1:1:1, along with a CFP (cyan fluorescent protein) encoding plasmid (Clontech Laboratories, Inc. / Takara Bio, California, USA) as a cell transfection marker. A mixture of plasmids was then mixed with calcium chloride ($CaCl_2$) solution, borate buffered saline (BBS, pH 6.95) and water in a definite proportion, vortexed and incubated for 10 minutes at room temperature. After 10 minutes, the solution was poured evenly over the cells, which were incubated afterward in a temperature controlled humidified CO_2 incubator overnight.

After 12-14 hours of transfection, the culture medium was aspirated, and cells were washed three times with PBS to remove traces of transfection solution remaining after aspiration that may otherwise lead to toxic effects. Cells were re-trypsinized, re-diluted in culture medium and plated on coverslips coated with poly-*l*-lysine (0.5mg/ml) (Sigma-Aldrich Production GmbH, Steinheim, Germany) and placed in 24-well plates. Electrophysiological experiments were performed after one day of transfection.

3.2.3.3. Stoichiometry of adult muscle-type nAChRs

Numerous studies showed that adult muscle-type nAChRs exist in a heteropentameric form consisting of α, β, δ, and ε subunits in a 2:1:1:1 ratio (Gupta et al., 2016; Albuquerque et al., 2009). However, the formation of the functional receptor has also been reported when oocytes were injected with mRNA or cRNA of α, β, δ and ε subunits in a 1:1:1:1 ratio (J.Connolly et al., 1992; Yuan Liu and Paul Brehm, 1993;

HS Kachel et al., 2016). Therefore, an experiment was conducted to compare functional properties of the receptor in both cases.

HEK 293 cells were transfected with two different subunit ratios: α, β, δ and ε subunits in 2:1:1:1 ratio and in 1:1:1:1 ratio, respectively. Both transfections were done at the same time and on the next day, electrophysiological experiments were performed at both conditions. Cells were held at a potential of -60 mV and acutely exposed to 500 µM ACh in order to record transient inward ionic currents (for more details about the electrophysiological settings see below) (Figure 11A).

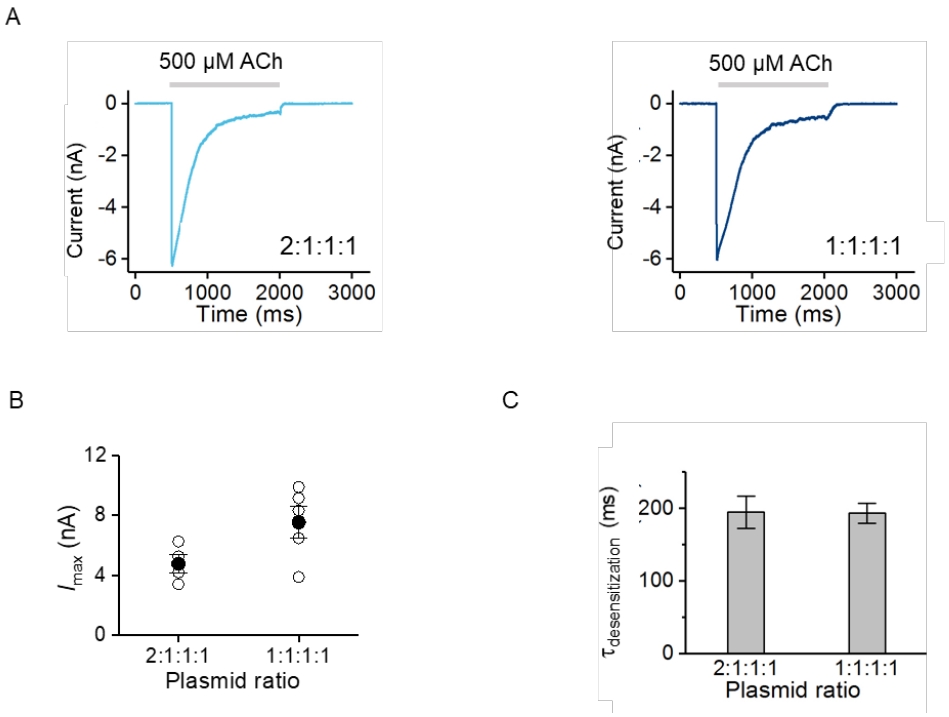

Figure 11. Influence of different plasmid ratios on the functional properties of the nAChR

(A) Representative current traces obtained from cells transfected with plasmid ratios 2:1:1:1 (light-blue) and 1:1:1:1 (dark-blue). Gray bar represents the period of ligand application (500 µM ACh). (B) Comparison between maximum current amplitude (I_{max}) obtained with different plasmid ratios. The difference in the maximum current amplitude obtained from the two-different plasmid ratios turned out to be insignificant (P=0.53). Black symbols represent means of 4 recordings (2:1:1:1 ratio) and 5 recordings (1:1:1:1 ratio), open symbols represent individual recordings. (C) Bar graph representing time course of desensitization, $\tau_{desensitization}$ (ms) obtained with two different plasmid ratios. No significant difference was found in the time

course of desensitization obtained from the two different plasmid ratios (P=0.96). Data are means ± S.E.M. of 4-5 cells.

Using 500 µM ACh, cells transfected with plasmids in the ratio 2:1:1:1 produced maximum current amplitude of 4.78 ± 0.62 nA (n=4) while those transfected with plasmids in the ratio 1:1:1:1 produced 7.55 ± 1.07 nA (n=5; P=0.62) (Fig. 11B). Further, receptor desensitization was fitted with a mono-exponential function in both cases. The time constants $\tau_{desensitization}$ were 194.85 ± 21.96 ms (n=4) for 2:1:1:1 plasmid ratio and 193.58 ± 13.92 ms (n=5; P=0.96) for 1:1:1:1 plasmid ratio (Figure 11C), respectively. Hence, functional properties of the receptor were found to be similar in both cases, indicating normal functioning of channels irrespective of the plasmid ratio.

3.3. Chemicals and Solutions

Ligands used to activate adult human muscle-type nAChRs were ACh chloride, nicotine, carbamylcholine chloride (all from Sigma-Aldrich Chemie GmbH, Steinheim Germany), and fACh, a fluorescent derivative of ACh (Chiroblock, Wolfen, Germany, Abcam, Cambridge, UK). Precursor compounds, i.e., chemically modified ACh derivatives, were provided by the Plested lab (FMP, Berlin). Stock solutions of a concentration of 50 mM were prepared in distilled water for all ligands and were stored at -20^{o}C. Solutions of desired concentration were obtained by diluting respective stock solution in control solution used for patch-clamp experiments. All chemicals used were of analytical grade.

Solutions used in patch-clamp experiments contained:

External bath solution (extracellular solution) (in mM): 115 NaCl, 30 KCl, 1 $MgCl_2$, 1.8 $CaCl_2$, 5.5 Glucose, 10 HEPES; pH 7.4

Internal or pipette solution (in mM): 0.5 NaCl, 115 KCl, 1 $MgCl_2$, 1.8 $CaCl_2$, 5.5 Glucose, 10 HEPES; pH 7.2

Control solution (vehicle control for ligands) (in mM): 150 NaCl, 2 KCl, 10 EGTA, 10 HEPES; pH 7.2

3.4. Patch-clamp experiments

3.4.1. Fabrication of patch-pipettes

Patch pipettes used for whole-cell patch clamp experiments were fabricated from borosilicate glass capillary tubes with an outer diameter and inner diameter of 2 mm and 1 mm, respectively (Hilgenberg GmbH, Malsfeld, Germany). Pipettes were pulled using a horizontal P-97 Flaming/Brown type micropipette puller (Sutter Instruments, Novato, USA) and were further fire polished with the help of an MF-830 Microforge fire-polisher (Narishige International USA, INC., New York, USA). Pipette resistance obtained after fire polishing was between 1-3 MΩ.

Patch pipettes used for confocal whole-cell patch-clamp fluorometry experiments were fabricated from filament-containing borosilicate glass capillary tubes (A-M Systems, Sequim, Washington, USA) with an outer and inner diameter of 1.5 mm and 1.12 mm, respectively, using a horizontal P-97 Flaming/Brown type micropipette puller (Sutter Instruments, Novato, USA). Pipette resistance was between 1-3 MΩ. Non-fire polished pipettes were used in these experiments. Specific reasons behind using different glass pipettes and avoiding fire polishing, in this case, are explained in the result section (refer 4.5.2).

For ligand application, double-barreled theta glass capillaries (Hilgenberg GmbH, Malsfeld, Germany) were fabricated using a P-97 Flaming/Brown type micropipette puller (Sutter Instruments, Novato, USA). Polyethylene tubes (Adtech Polymer Engineering LTD, Stroud, Glos, England) of an inner diameter of 0.3 mm, an outer diameter of 0.76 mm, and a length of around 2-3 cm were inserted in both barrels at the non-fabricated end of the application pipette and were tightly sealed by glue.

3.4.2. Patch-clamp recordings

The patch-clamp technique is a standard electrophysiological technique that allows for measuring ionic currents through channel proteins with high time-resolution, providing the advantage to study the physiological and pathophysiological functions of ion channels in excitable cells or tissues.

For basic electrophysiological experiments, the patch-clamp setup consisted of the following components: (1) an inverted microscope (Axiovert 100, Carl Zeiss MicroImaging GmbH, Jena, Germany) for cell visualization placed on a vibration-

isolation table (Newport, Irvine (CA), USA), (2) a Faraday cage, surrounding the setup, which isolates the system from electrical noise, (3) a patch-clamp amplifier (Axopatch 2B, Axon Instruments Inc., Foster City (CA), USA) controlled by the patch-clamp software ISO3 (MFK, Niederhnhausen, Germany) on a PC, (4) a micromanipulator (Luigs & Neumann Feinmechanik und Elektrotechnik GmbH, Ratingen, Germany) holding the amplifier head stage in connection with the pipette holder and the pipette, (5) CFP Filter set : BP 436/20 and 455 LP (Carl-Zeiss GmbH, Jena, Germany), (6) halogen lamp to visualize transfected fluorescent cells, (7) a piezo device (Physik Instrumente (PI) GmbH & Co. KG, Karlsruhe, Germany), to switch the application pipette forth and back, (8) a bath chamber, (9)) a piezo-driven application system for the application of ligands (tailor-made at the workshop of Institute of Physiology II, Jena, Germany), (10) a reference or bath electrode made of Ag/AgCl (Science Products GmbH, Hofheim, Germany), to set the zero current level that enables to observe changes in current while keeping the voltage constant, and (11) a recording electrode (Ag/AgCl wire) that allows electrical contact between the intracellular environment and the patch-clamp amplifier.

Voltage-clamp experiments were performed in the whole-cell mode with a slight modification to allow fast solution exchange across the cell membrane (discussed in result section 4.1). To attain a gigaseal between glass pipette and cell membrane, the pipette was brought into close contact with the cell and negative pressure was gently applied using a 5 ml syringe. Once a gigaseal was obtained, cells were ruptured by using the zap function of the amplifier which injects a large amount of current into the cell resulting in opening the membrane patch underneath the pipette tip. This provided access to the intracellular side of the cell, leading to the attainment of the whole-cell mode. Cells were then lifted-up and positioned in front of the double-barreled application pipette controlled by a piezo-device. Fast switches of this application pipette filled with control solution in one tube and ligand-containing solutions in the other tube were used to realize fast concentration jumps to the cell (Figure 12). This caused channel gating and resulted in the generation of ionic current. All recordings were done at -60 mV. Currents recorded were sampled at 5 kHz and filtered at 2 kHz.

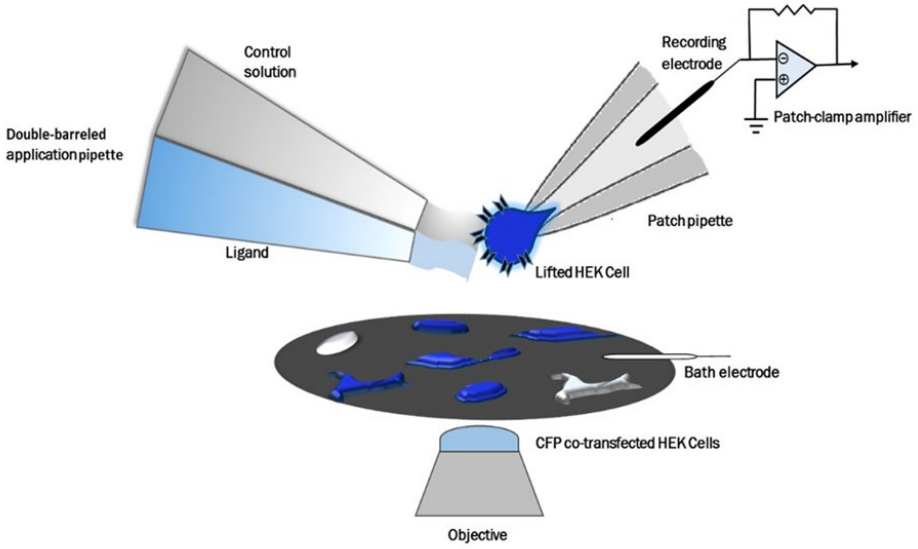

Figure 12. Patch clamp setup illustration

Scheme of an electrophysiological setup with a lifted HEK 293 cell in front of a double-barreled application pipette containing ligand and control solution is shown. A transfected HEK 293 cell (in blue; transfection marker: CFP) was lifted after attaining whole-cell configuration. Currents were recorded by a patch clamp amplifier.

To measure the speed of the fast switching between the solutions, HCN2 (hyperpolarization-activated cyclic nucleotide-gated channels) channels were used as a test system because these channels are voltage-activated and no ligand application is needed to activate the channel, which might have compromised the recording due to the binding of ligand. HCN2 channels expressed in HEK 293 cells were activated by applying a hyperpolarizing voltage pulse of -100 mV from a holding voltage of 0 mV. Fast jumps were realized between 100% and 10% permeating cation solution. The estimated solution exchange time (10%-90%) is 6.8 ms. (Figure 13).

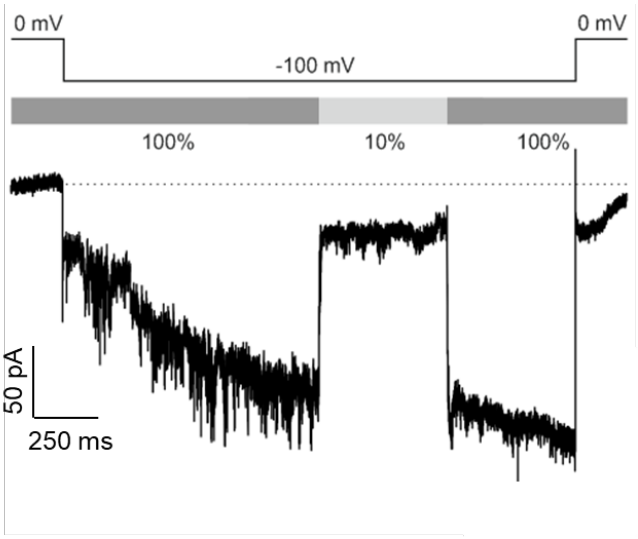

Figure 13. Monitoring of the speed of the solution exchange using piezo controlled application system.

HCN2 channels expressed in HEK 293 cells were activated by applying hyperpolarizing voltage jumps from 0 to -100 mV. A representative current trace obtained in response to fast concentration jumps realized between 100% (150 mM KCl) and 10% (15 mM KCl) permeating cation solution is shown. The rise time from 10% to 90% is 6.8 ms.

3.4.3. Confocal patch-clamp fluorometry

Confocal patch-clamp fluorometry (cPCF) is a combination of electrophysiological patch-clamp and confocal fluorescence microscopy. It enables simultaneous electrical and optical measurements that allow either monitoring conformational changes in real-time or monitoring ligand binding by either using fluorescently tagged receptors or fluorescently tagged ligands.

For cPCF, the standard electrophysiology set up can be used. Additional features of the setup were: (1) Confocal microscope (LSM 7 Duo+ LSM 710 scan head, Carl-Zeiss Microscopy GmbH, Jena, Germany); (2) C-Apochromat 40x water-immersion objective (Carl-Zeiss Microscopy GmbH, Jena Germany); (3) He/Ne 543 laser line, to excite fACh; (4) He/Ne 633 laser line, to excite the reference dye Dy647 (Dyomics GmbH, Jena, Germany); (5) Zen 2010 fluorescence imaging software (Carl Zeiss Microscopy GmbH, Jena, Germany).

For performing experiments, patch pipettes were adjusted around 45^{o} with respect to the bath chamber and the whole-cell configuration was achieved using 25x (NA=0.8)

Plan-Apochromat water immersion objective (Carl-Zeiss Microscopy GmbH, Jena, Germany). When whole-cell mode was obtained, cells were lifted-up and positioned in front of the double-barreled piezo-driven application pipette (refer Figure 12). After positioning, the objective was switched to 40x (NA=1.2) C-Apochromat water immersion objective (Carl-Zeiss Microscopy GmbH, Jena, Germany) for imaging. Fast solution exchange was realized with the help of forth and back jumps of the application pipette between fACh and control solution. Both solutions contained 1 µM of the reference dye, Dy647, (1) for focusing the cell and (2) also used in the mathematical analysis to subtract the background fluorescence caused by unbound fACh, from the channel-bound fraction (refer section 3.6).

Ionic currents were recorded at a membrane potential of -60 mV. The sampling rate was 10 kHz and the filter was set to 2 kHz. Optical measurements were performed simultaneously in the same cell. fACh and Dy647 dye were excited by the He/Ne laser lines 543 nm and 633 nm, respectively. The possibility of cross-talking between both dyes was neglectable because of their different absorption and emission spectra. The confocal slice thickness was 2 µm.

Change in fluorescence intensity during the ligand binding phase as well as during the wash-out phase was recorded. Obtained fluorescence data points were sampled with different sampling rates of 10 Hz and 1.3 Hz (The reason for choosing two different sampling rates is discussed further in results section 4.5.4.). All experiments in the present study were performed at 20-22°C.

3.5. The strategy for the synthesis of fluorescent ACh derivatives

ACh derivatives were synthesized with the help of collaborators in Berlin, Germany (Dr. Andrew J.R. Plested, Molecular Neuroscience, and Biophysics group, Medicinal Chemistry group, Leibniz- Institute of Molecular Pharmacology, Berlin, Germany and Dr. Vera Martos, Medicinal Chemistry group, Leibniz- Institute of Molecular Pharmacology, Berlin) along with the companies ChiroBlock GmbH (Bitterfeld-Wolfen, Germany) and Abcam (Cambridge, UK). The goal was to synthesize a fluorescent ligand for adult muscle-type nAChR which could closely mimic the action of its native ligand ACh. The basic approach was to couple a fluorophore to ACh via a linker, to avoid hindrance at the binding site as well as to retain the properties of the parent ligand (Baker et al., 2003; Middleton and Kellam, 2005; Middleton et al., 2007)

(Figure 14). It has been reported that the nature of the linker and the fluorophore, as well as the length of the linker, plays a key role in influencing the pharmacological as well as physicochemical properties of a parent ligand (Baker et al., 2010 and Rose et al., 2012). Therefore, choosing appropriate linkers and fluorophores was a key step for the strategy.

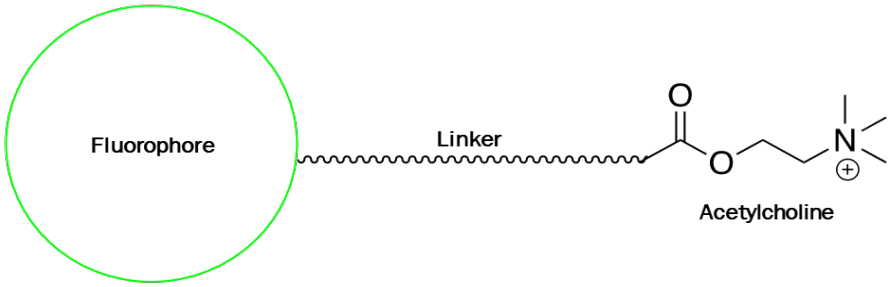

Figure 14. The strategy to synthesize the fluorescent ACh derivative
To synthesize a fluorescent derivative of ACh, the coupling of a suitable fluorophore to ACh via a linker was designed to avoid steric hindrance, which may be caused by the fluorophore when it is linked directly to ACh.

Since polyethylene glycol (PEG) is hydrophilic, non-toxic, and non-immunogenic, it was chosen as a linker in the present study. A cyanine dye was used as fluorophore because cyanine dyes are comparatively small, photostable, bright, and cause minimal interruption with biological samples (Leisle et al., 2016). The fluorescent ACh derivative (fACh) was obtained as a final product by coupling the cyanine dye to ACh via a PEG linker.

3.6. Data acquisition and analysis

Electrophysiological data extracted from the ISO3 software were analyzed using Microsoft Excel 2010 and Origin 9.5 (OriginLab, Northhampton, USA). For fluorescence measurements, Zen 2010 fluorescence imaging software (Carl Zeiss Microscopy GmbH, Jena, Germany) was used. Imaging data were processed and analyzed using FIJI (Schindelin et al., 2012) (Java-based image processing program

inspired by National Institutes of Health), Microsoft Excel 2010 and Origin 9 (OriginLab, Northhampton, USA) software.

3.6.1. Electrophysiological data

Concentration-activation relationship curves were constructed by normalizing the current amplitude (*I*) obtained at successive concentrations of ligands with respect to the maximum current amplitude (I_{max}) obtained at the saturating concentration of ligands and were plotted as a function of ligand concentrations (x). The mean concentration-activation data were fitted with the Hill equation, which provides an estimate of EC_{50}, the concentration at which 50% of the channels are activated, and the Hill coefficient *H,* describing the slope of the curve (equation 1).

$$\boldsymbol{I/I_{max} = 1/[1 + (EC_{50}/A)]^{H}} \quad \textbf{(1)}$$

where *I* is the current amplitude, *A* the concentration of the agonist, EC_{50} the concentration of the ligand that produces a half-maximal response, and H the Hill coefficient. Unless otherwise stated, I_{max} was constrained to 1 because a maximal ligand concentration was used to define full ligand activity.

Desensitization kinetics and recovery from desensitization were analyzed with either a mono-exponential (equation 2) or a bi-exponential (equation 3) function based on curve fitting using Origin 9.5 (Origin Lab, Northampton, USA). To analyze the rate of onset of desensitization, the current data points were fitted from the point after the peak current was reached until the end of ligand application period.

The mono-exponential function is defined as:

$$\boldsymbol{y = y_0 + Ae^{-x/\tau_1}} \quad \textbf{(2)}$$

where y_o is the offset, *A* is the amplitude and τ is the decay time constant.

The bi-exponential function is defined as:

$$\boldsymbol{y = y_0 + A_1e^{-x/\tau_1} + A_2e^{-x/\tau_2}} \quad \textbf{(3)}$$

where y_o is the offset, A_1 and A_2 are the amplitudes for two different desensitization components. τ_1 and τ_2 are the respective decay time constants.

3.6.2. Image analysis

Confocal images obtained with the ZEN 2010 fluorescence imaging software were analyzed using the JAVA-based image processing software FIJI (ImageJ) (Schindeln et al., 2012).

The fluorescence intensity caused by fACh binding to the nAChR expressing cells was collected from an individual whole cell. Because cells were not perfectly stable in shape when flushed by the solution stream, a fixed region of interest (ROI) was not appropriate for time series analysis. Therefore, we used a high number of line profiles, integrated the fluorescence signals per line and summed them up. Figure 15 shows an exemplary image with three profiles. At least ten profiles were used per image.

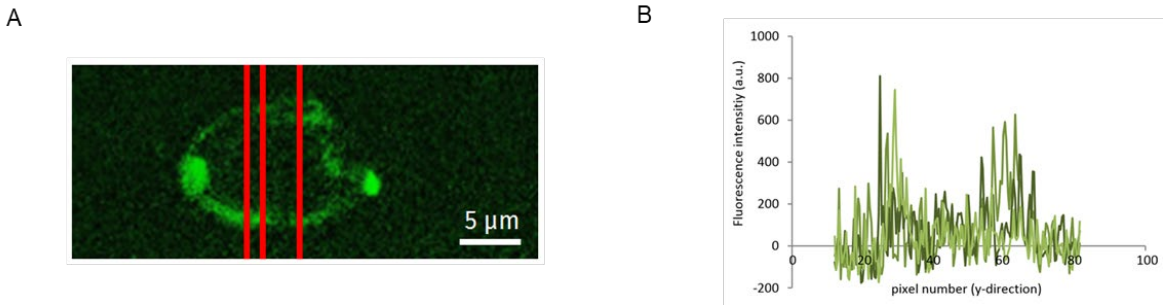

Figure 15. Image analysis

(A) Confocal image of a cell recorded 50 ms after being exposed to 10 µM fACh. The cell was attached to a patch pipette, lifted from the chamber bottom and positioned within the solution stream. Red lines indicate profiles used for analysis. (B) Fluorescence intensities along the red lines in (A).

In case of ligand application intervals, when fACh was also labeling the bath solution, a reference dye Dy647 was used for background subtraction (Biskup et al., 2007). Dy647 was not binding to the receptor or somewhere else on the cell surface (refer Figure 43) so that it behaved like unbound fACh, thus making it a good marker for background subtraction.

3.7. Statistical analysis

All data points are expressed as mean ± S.E.M. Statistical comparisons were done with Student's t-test and a $P < 0.05$ was considered as significant.

4. Results

Adult muscle-type nAChRs can exist in three interconvertible conformational states, i.e. closed, open or desensitized state (Katz and Thesleff, 1957; Krauss et al., 2000; Zouridakis et al., 2009, Papke, 2014). Numerous studies (Miyazawa et al., 2003; Purohit et al., 2007; Wells, 2008; Albuquerque et al., 2009, Unwin, 2013) have provided a clear understanding of receptor structure and mechanism of ligand binding. In the last decades, various approaches, such as time-resolved photolabeling (Averalo et al., 2005), incorporation of unnatural amino acids (Nowak et al., 1995), and variant fluorescence techniques (Dahan et al., 2004; Grandl et al., 2007; Fujimoto et al., 2008) have been applied to study the state-dependent structure-function relationship of nAChRs, however, a clear concept is still missing. Therefore, the present study is dedicated to the simultaneous investigation of ligand binding and channel gating in adult muscle-type nAChRs using an approach called confocal patch-clamp fluorometry (cPCF).

To investigate ligand binding and channel gating employing cPCF, prerequisites were needed to be checked and fulfilled. These prerequisites are:
(1) establishing the required experimental setup to perform electrophysiological and fluorescence recordings simultaneously in the whole-cell mode,
(2) studying detailed functional characteristics of three ligands, ACh, nicotine, and carbachol at muscle-type nAChRs and comparing them to choose a potential candidate for synthesizing its fluorescent derivative,
(3) testing a newly synthesized fluorescent derivative to study ligand binding and channel gating in adult muscle-type nAChRs.

4.1. Establishment of experimental setup

Typically, cells attached to the chamber bottom are used for performing whole-cell recordings. Previously it has been shown that lifted SH-EP1 cells (human epithelial cell line) expressing α4β2 AChRs yielded faster desensitization kinetics compared to cells attached to the chamber bottom. The authors explained this with a faster solution exchange across the cell membrane for lifted cells (Yu et al., 2009).

For validating this kinetic difference in HEK 293 cells expressing nAChRs, 50 µM of ACh (native ligand) was applied via a double-barreled application pipette for 1 s and current responses were recorded from lifted and cells attached to the chamber

bottom in separate experiments. Normalized current traces of lifted cells and cells attached to the chamber bottom is shown in Figure 16A. The mean peak current (9.21 ± 2.18 nA, n=5) obtained from lifted cells were similar to the mean peak current from cells attached to the chamber bottom (6.91 ± 1.37 nA, n=5; P=0.40). Hence, lifting of cells during the measurement did not affect maximum current response elicited by the receptor.

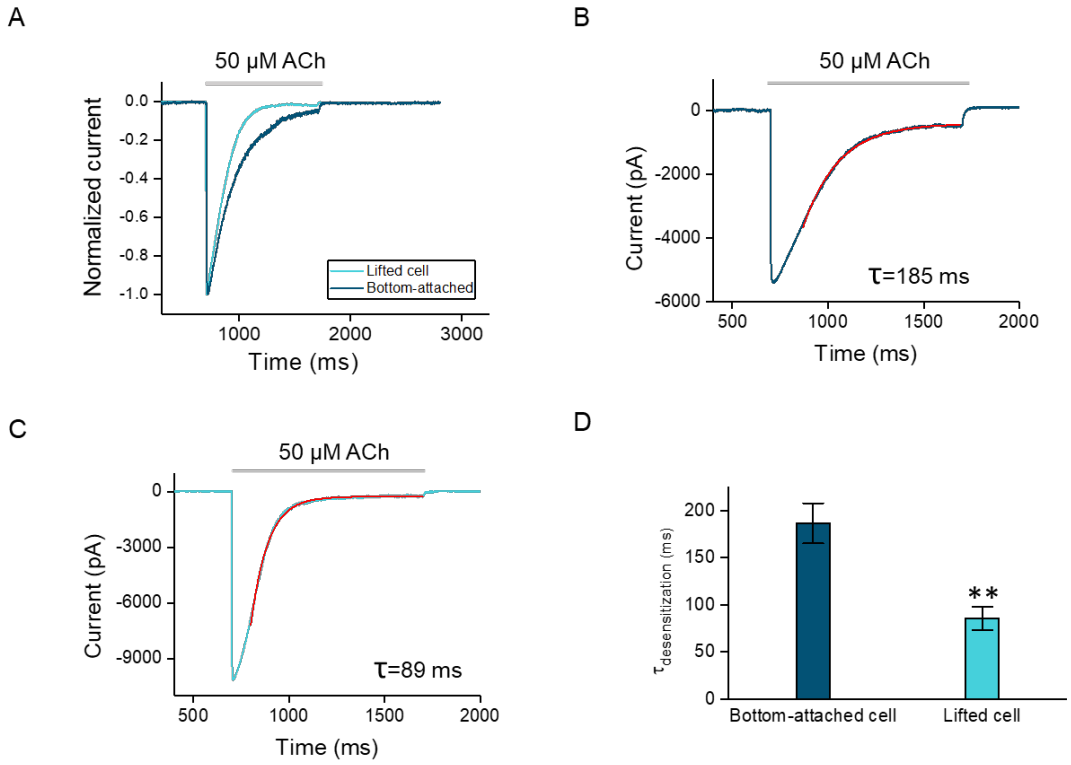

Figure 16. Current responses and kinetics of nAChRs in cells attached to the chamber bottom and lifted cells.

(A) Representative normalized current traces of nAChRs expressed in cells attached to the chamber bottom (dark blue) and lifted cell (light blue) showing faster desensitization kinetics in the lifted cell. Gray bar represents ligand application period. (B) Representative current trace of the lifted cell expressing nAChRs shows current decay fitted with mono-exponential function. (C) Representative current trace of cells attached to the chamber bottom expressing nAChRs shows current decay fitted with the mono-exponential fit. (D) Time course of desensitization kinetics. Data are means ± S.E.M. (n=5), Statistical t-test cell attached to the chamber bottom versus lifted cells: **, P ≤ 0.01.

Desensitization kinetics were compared by fitting a mono-exponential function to the current time courses (Figure 16B,C), yielding time constants of 186.2 ± 21.3 ms (n=5) in cells attached to the chamber bottom and 85.4 ± 12.8 ms (n=5; P<0.01) in lifted cells (Figure 16D). Hence, desensitization kinetics of the receptor was two times faster in lifted cells compared to cells attached to the chamber bottom. The accelerated desensitization kinetics supports the idea that the solution exchange was more rapid and uniform around lifted cells than around cells attached to the chamber bottom. Therefore, all experiments in the present study were conducted on lifted cells.

4.2. Selection of the most suitable candidate for cPCF experiments

In the present study, functional characteristics of ligands, ACh, nicotine, and carbamylcholine were investigated and compared to identify the most potential candidate for cPCF experiments. Analysis of functional characteristics, such as efficacy, potency, and affinity of the ligand was a fundamental step because the sensitivity of muscle-type nAChRs varies for different ligands. Since the action of the ligand on the receptor depends on two elementary events: affinity and efficacy (PG Strange, 2008), the potential candidate for cPCF experiments was sought to be chosen on this basis.

ACh (Figure 17), an ester of acetic acid and choline, is synthesized, stored and released by cholinergic neurons at the neuromuscular junction as well as at neuronal synapses.

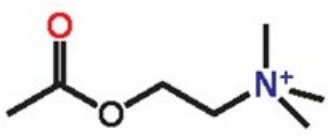

Figure 17. Chemical structure of ACh

It is axiomatic that selective binding of ACh at muscle-type nAChRs triggers channel activation that arises due to transmembrane conformational changes within the receptor protein, followed by a rapid desensitization (Karlin and Akabas, 1995; Grandl et al., 2007; Yu KD et al., 2009). This natural agonist is therefore widely used for activating nAChRs also in electrophysiological experiments. However, its utility is compromised by its susceptibility to hydrolysis (Wonnacott and Barik, 2007). From excised patches and single channel studies, it is evident that ACh is a highly efficacious agonist at muscle-type nAChR (Dilger and Brett, 1990; Akk and Auerbach, 1999; Lape et al., 2008). Hence, in the present study focal application of ACh on the lifted whole cell containing muscle-type nAChRs was done for determining functional properties.

Nicotine (3 (-)-1-methyl-2-(3-pyridyl)-pyrrolidine), a tobacco alkaloid, is a tertiary amine having a pyridine and a pyrrolidine ring (Figure 18). It is a prototypical exogenous ligand for both neuronal and muscle-type nAChRs. Nicotine acts on ganglionic nerve cells, adrenal medulla cells, at several sites of the central nervous system, and on neuromuscular junction (Roger L. Papke, 2014; Mishra et al., 2015). It activates and desensitizes all subtypes of nAChRs except two, $\alpha 9$ receptors and $\alpha 9\,\alpha 10$ receptors, where it acts as an antagonist (Wonnacott and Barik, 2007). Effects of the nicotine on neuronal nAChRs are well understood (Gourlay and Benowitz, 1997; Fenster et al., 1997; Rose et al., 1999, Paradiso and Steinbach, 2003; Xiu et al., 2009) whereas only a few studies so far investigated nicotinic effects on muscle-type nAChRs (Akk and Auerbach, 1999; Jadey et al., 2013).

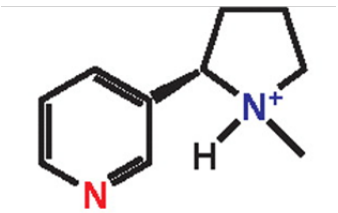

Figure 18. Chemical structure of nicotine

A comprehensive knowledge about the mechanism underlying the nicotine-induced gating of muscle-type nAChRs is still missing, since at muscle-type nAChRs, nicotine is described as a weak agonist (Zhou et al., 1999; Akk and Auerbach, 1999), a partial agonist (Jadey et al., 2013) or a full agonist (Beene et al., 2002). For this reason, macroscopic currents evoked by fast jumps of the nicotine concentration at adult muscle-type nAChRs was studied.

Carbamylcholine or carbachol (2-carbamoyloxyethyl-trimethyl-ammonium chloride) (Figure 19) is a choline carbamate formed by substituting the acetyl group with a carbamyl group on ACh. This modification makes it a relatively hydrolysis-resistant analog (Wonnacott and Barik, 2007). Carbamylcholine imitates the action of ACh and thus acts on the parasympathetic nervous system. It has been widely used for the treatment of glaucoma and ophthalmic surgeries. It is a non-selective cholinergic agonist, which acts on both muscarinic and nicotinic receptors, although more potent on muscarinic receptors. Single-channel studies reported that carbachol opens the nAChRs ~5 times slower in comparison to ACh (Akk and Auerbach; 1999). Moreover, the affinity of carbachol is stated to be 10 times less than ACh (Celie et al., 2004). However, carbachol is considered to be a strong agonist at this receptor since it has around 1300 times stronger affinity when the receptor exists in the open state in comparison to the closed state (Akk and Auerbach; 1999).

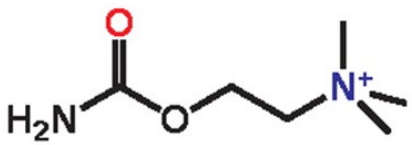

Figure 19. Chemical structure of Carbamylcholine

Notably, the presence of a carbamyl group instead of the acetyl group in carbachol increases its chemical stability. This might become the key property for reaching the main aim in the present study to relate ligand binding to channel gating employing the cPCF method. For this reason, the functional properties of carbachol were also explored.

Since ACh is the native ligand and highly efficacious agonist (Dilger and Brett, 1990; Akk and Auerbach, 1999; Lape et al., 2008) at muscle-type nAChRs, the functional characteristics of other two candidates, nicotine, and carbachol were compared with respect to the ACh in the present study.

4.2.1. Concentration-activation relationships

The concentration-activation relationship is a well-accepted mean for determining the two overall properties of a ligand, potency, and efficacy. These properties are also one of the important distinguishing factors for comparing different ligands regarding their functionality.

Sub-saturating concentrations and a saturating concentration of each ligand were applied via a double-barreled switch pipette as described earlier (refer 3.4.2). After applying one concentration, the cell was kept continuously in the ligand-free control solution for about a minute to complete the recovery of the receptor. Representative current traces monitored in lifted HEK 293 cells containing muscle-type nAChRs upon application of increasing concentrations of ACh, nicotine, and carbachol are shown in Figure 20.

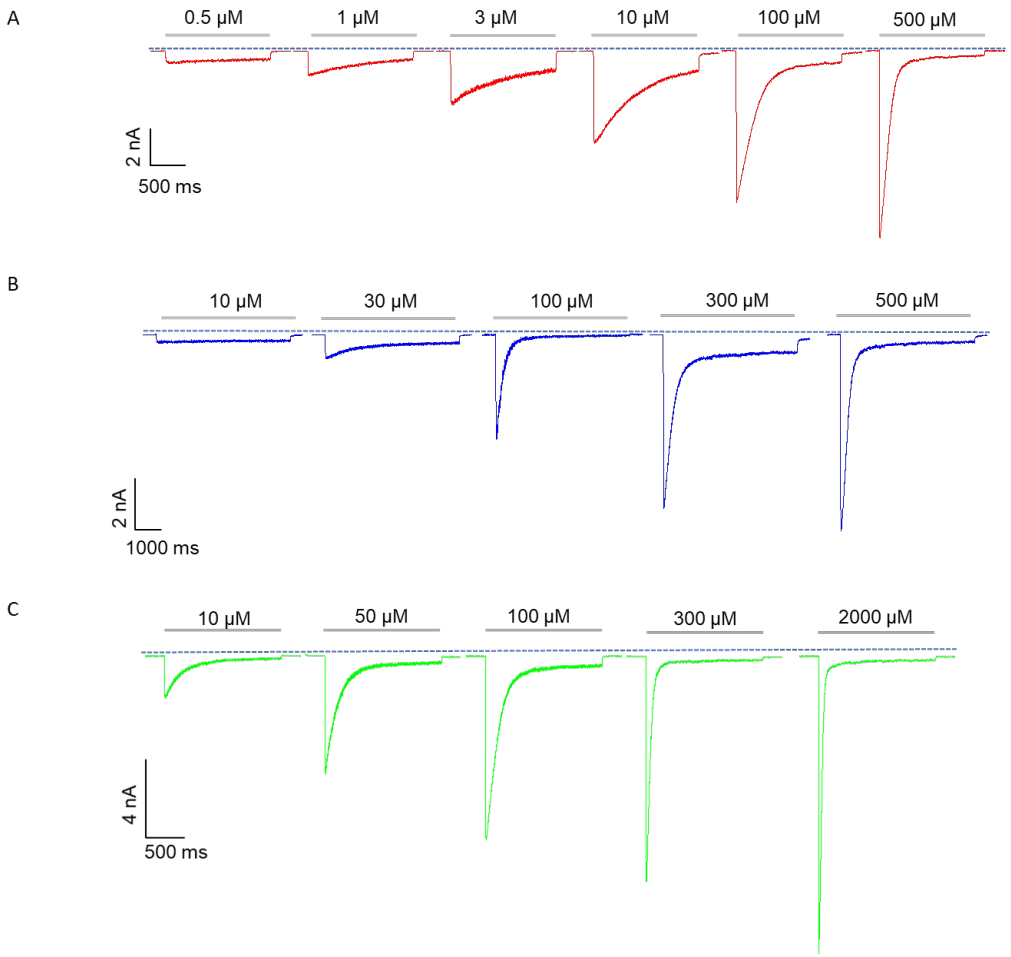

Figure 20. Activation of muscle-type nAChRs by different concentrations of ACh, nicotine, and carbachol.

Representative traces are demonstrating the inward current monitored from cells containing muscle-type nAChRs when varying concentrations of ACh (in red), nicotine (in blue), and carbachol (in green) were applied for the indicated time. Gray bar above each trace represents the application period of the ligand.

Current obtained at different concentrations of ACh (0.5 µM to 500 µM) and nicotine (10 µM to 500 µM) were normalized to their saturating concentration of 500 µM, carbachol current responses were normalized to its saturation concentration of 2000 µM (Figure 21). Mean data points were plotted against each concentration and fitted with the Hill function. ACh (EC_{50}=2.5 µM) was found to be about twenty-fold more potent than nicotine (EC_{50}=54.5 µM) and about thirty-fold more potent than carbachol (EC_{50}=73.2 µM) in activating muscle-type nAChRs at the membrane potential of -60 mV. The Hill-coefficient, H, for ACh, nicotine, and carbachol was 1.41,1.36, and 0.97, respectively.

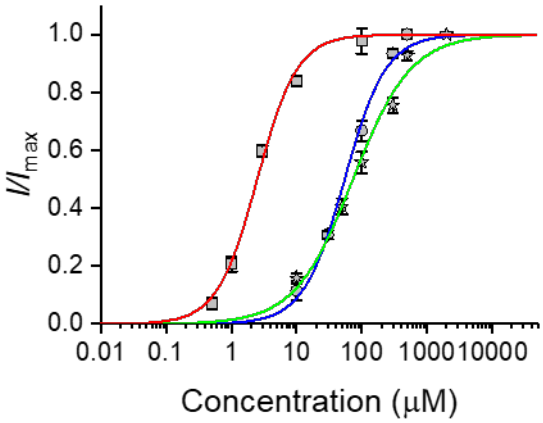

Figure 21. Comparison of concentration-activation relationship of ACh, nicotine, and carbachol in muscle-type nAChRs

Figure 21 shows the comparison of concentration-activation curves obtained for the three agonists, ACh, nicotine, and carbachol. Mean values of current responses obtained for the three agonists were fitted with the Hill function (Hill fit: red trace-ACh, blue trace-nicotine, and green trace-carbachol). When EC_{50} values were compared, the order of potency obtained is: ACh (EC_{50}=2.5 µM; H=1.41) > nicotine (EC_{50}=54.5 µM; H=1.36) > carbachol (EC_{50}=73.2 µM; H=0.97). Data are means ± S.E.M. for 4-13 cells.

In whole-cell recording, an attenuation of the peak current due to desensitization may lead to an underestimation of the peak currents particularly at higher concentrations of ligands and thereby to an underestimation of the EC_{50} values. Therefore, to correct potential artifacts due to the slow ligand application, back extrapolation of the falling phase of current was done up to the time point at which the ligand was applied to the channels. In this case, the obtained EC_{50} values for ACh, nicotine, and carbachol were 8.57 µM, 88.19 µM, and 114.25, respectively. The estimated Hill coefficient values are 0.73, 1.54, and 1.16, correspondingly.

Upon comparison with ACh, it was found that nicotine is a partial agonist whereas carbachol is a full agonist (Figure 22). When 500 µM of ACh and nicotine was applied in the same cell, nicotine produced about 58% of the maximum response evoked by the ACh whereas (Figure 22A, C) 2000 µM of carbachol produced a similar response

as produced by 500 µM of ACh (Figure 22B, C). Hence, ACh and carbachol, both were found to be similarly efficacious agonists at muscle-type nAChRs.

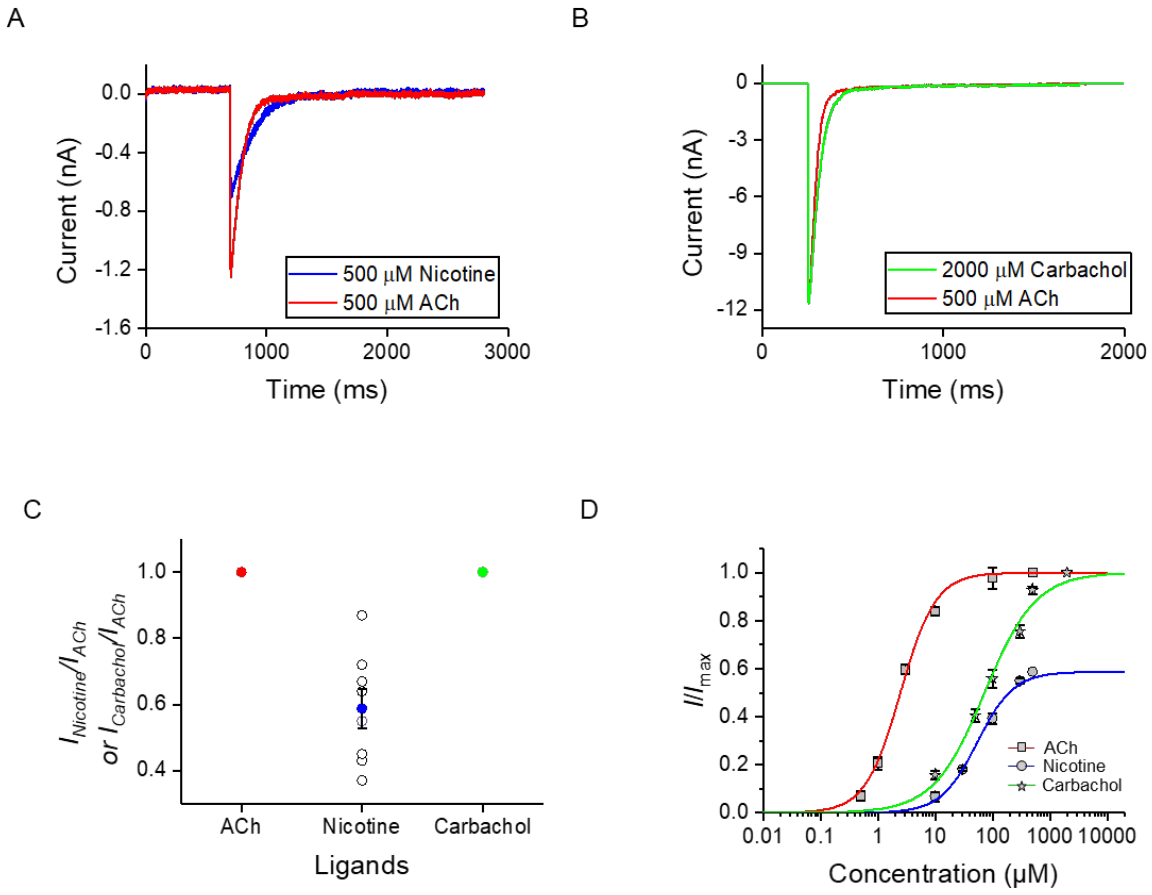

Figure 22. Comparison of the efficacy of ACh, nicotine, and carbachol

(A) Representative traces obtained by application of 500 µM of nicotine and ACh in the same cell. (B) A representative trace of 2000 µM of carbachol and 500 µM ACh in the same cell. (C) Efficacy comparison of all three agonists. Here, the data points were obtained by taking the ratio of maximum current amplitudes obtained upon application of 500 µM of nicotine and ACh in the same cell or 2000 µM carbachol and ACh in the same cell. The blue symbol represents the mean data obtained after nicotine application. Open symbols represent individual recordings. Green symbol represents mean data for carbachol. Open symbols representing individual recordings in case of carbachol are hidden behind the green symbol. (D) Concentration-activation curves with constrained I_{max} values: 1 for ACh, 0.58 for nicotine, and 1 for carbachol. For fit parameters, refer to Figure 21.

4.2.2. Comparison of desensitization induced by ACh, nicotine, and carbachol in muscle-type nAChRs

From numerous studies (Katz and Thesleff, 1957; Gross et al., 1991; Elenes and Auerbach, 2002, Paradiso and Steinbach, 2003; Giniatullin et al., 2005), it is believed that nAChRs undergo desensitization upon a prolonged ligand application. In the present study, it was observed that all three ligands desensitized the muscle-type nAChRs and that the extent of desensitization as well as the desensitization kinetics, depends on the agonist concentration.

Upon application of varying concentrations of ACh, nicotine, and carbachol, muscle-type nAChRs elicited a peak current followed by a current decay reaching a transient plateau. Desensitization accelerated with increasing concentration of ACh, nicotine, and carbachol. The time constant for the current decay upon exposure of various concentrations of ACh, nicotine, and, carbachol is reasonably fitted with a mono-exponential function in most of the cases suggest that there is only one predominant desensitized state (Figure 23A-C). In some cases of ACh, the falling phase of current was biphasic but was described by a single exponential for simplicity in comparisons.

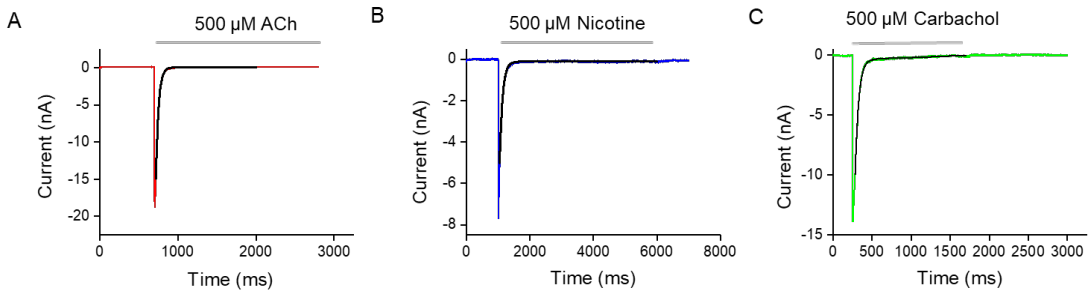

Figure 23. Desensitization of muscle-type nAChRs upon application of ACh, nicotine, and carbachol

Representative traces (ACh-red, nicotine-blue, and carbachol-green) showing current decay fitted with a mono-exponential function (fit in black) are illustrated. Gray bar above each trace indicates application time of the agonist.

To compare the desensitizing effect of all three ligands which work in different concentration ranges fairly, the time constants were plotted against the activation

level (fraction of activated channels derived from the concentration-activation relationship) rather than against the agonist concentration used in this study.

When time course of desensitization kinetics was compared at low activation levels (0.5 μM ACh, 10 μM nicotine, and 10 μM carbachol), it was found that ACh desensitized the channel about twice faster than nicotine ($\tau_{desensitization}$ for ACh at 0.5 μM=1090 ms; $\tau_{desensitization}$ for nicotine at 10 μM=2437 ms; P=0.0097) whereas almost five-fold slower than carbachol ($\tau_{desensitization}$ for ACh at 0.5 μM=1090 ms; $\tau_{desensitization}$ for carbachol at 10 μM=276 ms; P=0.0006). On the other hand, when the comparison was done at maximum activation or highest concentration range (500 μM ACh, 500 μM nicotine, and 2000 μM carbachol), ACh desensitized the channel about four-fold faster than nicotine ($\tau_{desensitization}$ for ACh at 500 μM=67 ms; $\tau_{desensitization}$ for nicotine at 500 μM=313 ms; P=0.0013) and three-fold slower than carbachol ($\tau_{desensitization}$ for ACh at 500 μM=67 ms; $\tau_{desensitization}$ for carbachol at 2000 μM=26 ms; P=0.0042) (Figure 24).

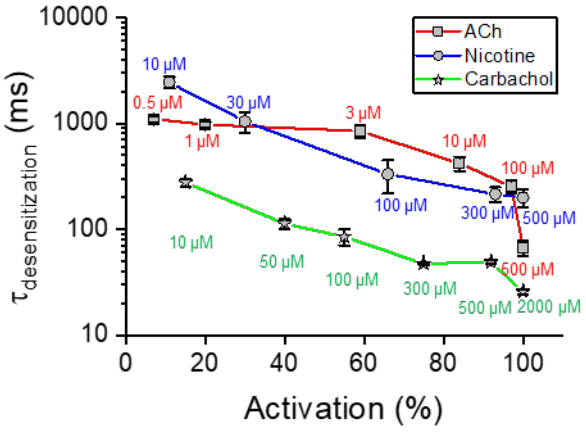

Figure 24. Comparison of desensitization kinetics

Time course of desensitization versus activation level is plotted in order to compare desensitization kinetics of the three ligands. The concentration of ligands at corresponding data points is indicated in the graph. At lower activation level, ACh mediated desensitization is two-fold faster (P=0.0097) than nicotine while five-fold slower (P=0.0006) than carbachol. Additionally, at higher concentrations, desensitization induced by ACh was four-fold faster (P=0.0013) than nicotine whereas three-fold slower (P=0.0042) than carbachol. Data are

means ± S.E.M. for 4-13 cells. Statistical t-test: P > 0.05=no asterisk, P ≤ 0.05=*, P ≤ 0.01=**, P ≤ 0.001=***.

Extent of desensitization with ACh, nicotine, and carbachol

The extent of desensitization (ED) of muscle-type nAChRs was determined from the steady-state to peak ratio (1-$I_{steady\text{-}state}/I_{peak}$). Mean values of the ED for ACh, nicotine, and carbachol were plotted against their respective concentrations and were fitted with the Hill equation. In this way, the concentration at which 50% of desensitization was reached was estimated. The estimated EC_{50} for ED for ACh, nicotine, and carbachol was 2.5 µM, 21.0 µM, and 2.13 µM and the Hill coefficient H was found to be 0.79, 2.02, and 1.04, respectively (Figure 25A-C). In case of carbachol, ED was relatively high at low concentrations which might indicate that the high percentage of channels underwent desensitization. Estimation of EC_{50} for ED in case of carbachol was based on an extrapolated fitting rather than the fit obtained from data points as it was in case of ACh and nicotine because the lowest concentration of carbachol at which current measurement was possible was 10 µM.

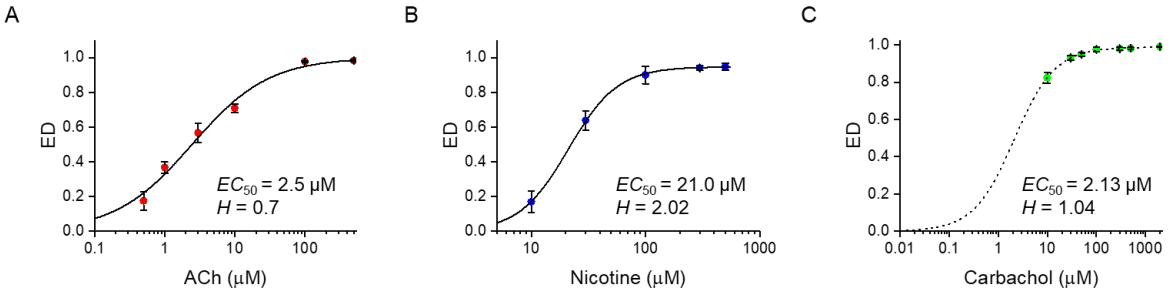

Figure 25. Concentration dependence of extent of desensitization

The graph represents the ED at different concentrations of ACh (red), nicotine (blue), and carbachol (green). The ED was boosted with increasing concentrations of indicated ligands. EC_{50} for ED of ACh, nicotine, and carbachol, as well as Hill coefficient, are indicated in the respective figures (A-C). Data are means ± S.E.M. for 5-7cells.

For comparison, the ED obtained from the three agonists is plotted against the activation level as shown in Figure 26. The ED was compared at lowest concentrations (0.5 µM ACh, 10 µM nicotine, and 10 µM carbachol) or at lowest

activation level and at saturating concentrations (500 µM ACh, 500 µM nicotine, and 2000 µM carbachol) or at maximum activation level. At the lowest activation level, the ED mediated by ACh is similar to nicotine (ED at 0.5 µM ACh=0.18 ± 0.05 and 10 µM nicotine=0.17 ± 0.06; P=0.94) but around five-fold lower than for carbachol (ED at 10 µM carbachol=0.83 ± 0.02; P=0.0003). On the contrary, the ED is similar at saturating concentrations for all three agonists (ACh=0.98 ± 0.005 and nicotine=0.95 ± 0.01; P = 0.11 and ACh=0.98 ± 0.005 and carbachol=0.99 ± 0.003; P=0.24). This suggests that the fraction of desensitizing channels is similar at saturating concentrations.

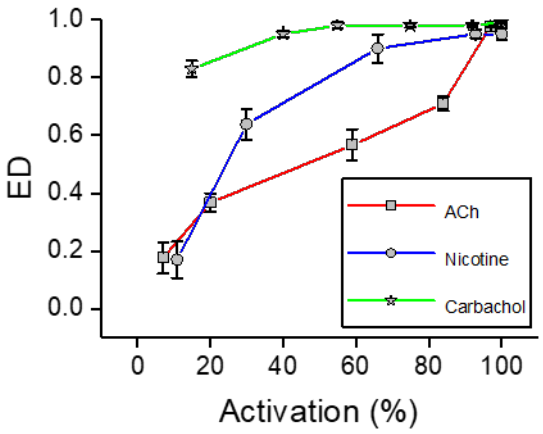

Figure 26. Comparison of the extent of desensitization

Data points obtained after assessment of the ED for all three agonists were plotted as a function of the activation level. At the lowest activation level, desensitization mediated by ACh is similar (P=0.94) to that of nicotine while approximately five-fold lower (P=0.0003) than that for carbachol. Further, at saturating concentrations of agonists, the ED mediated by all agonists are similar. Data are means ± S.E.M. for 3-13 cells. Statistical t-test: P > 0.05=no asterisk, P ≤ 0.05=*, P ≤ 0.01=**, P ≤ 0.001=***.

4.2.3. Recovery from desensitization caused by ACh, nicotine, and carbachol

Recovery of nAChRs from desensitization depends on the type of agonist, its concentration as well as on the duration of agonist exposure, which drives the receptor into the desensitized state (Reitstetter et al., 199; Wang and Sun, 2005). In the present study, recovery from desensitization mediated by ACh, nicotine, and carbachol was compared.

The time course of recovery from desensitization was estimated using a two-pulse protocol, containing a desensitizing pulse (D) and a test pulse. 10 μM ACh was used to activate nAChRs because at this concentration large and strong current signals were obtained without driving nAChRs into deeper desensitized states, which might take several hours to get recovered (Giniatullin et al., 2005). Similarly, 200 μM nicotine and 300 μM of carbachol were used to activate receptors since at this concentration they showed similar activation as obtained by ACh (see Figure 24). After application of desensitizing pulse of 10 μM in case of ACh, 200 μM in case of nicotine and 300 μM in case of carbachol, the test pulse of similar concentrations of ACh, nicotine, and carbachol (as indicated for desensitizing pulse) were applied after various intervals ranging from 0.1-6.5 s (Figure 27A-C).

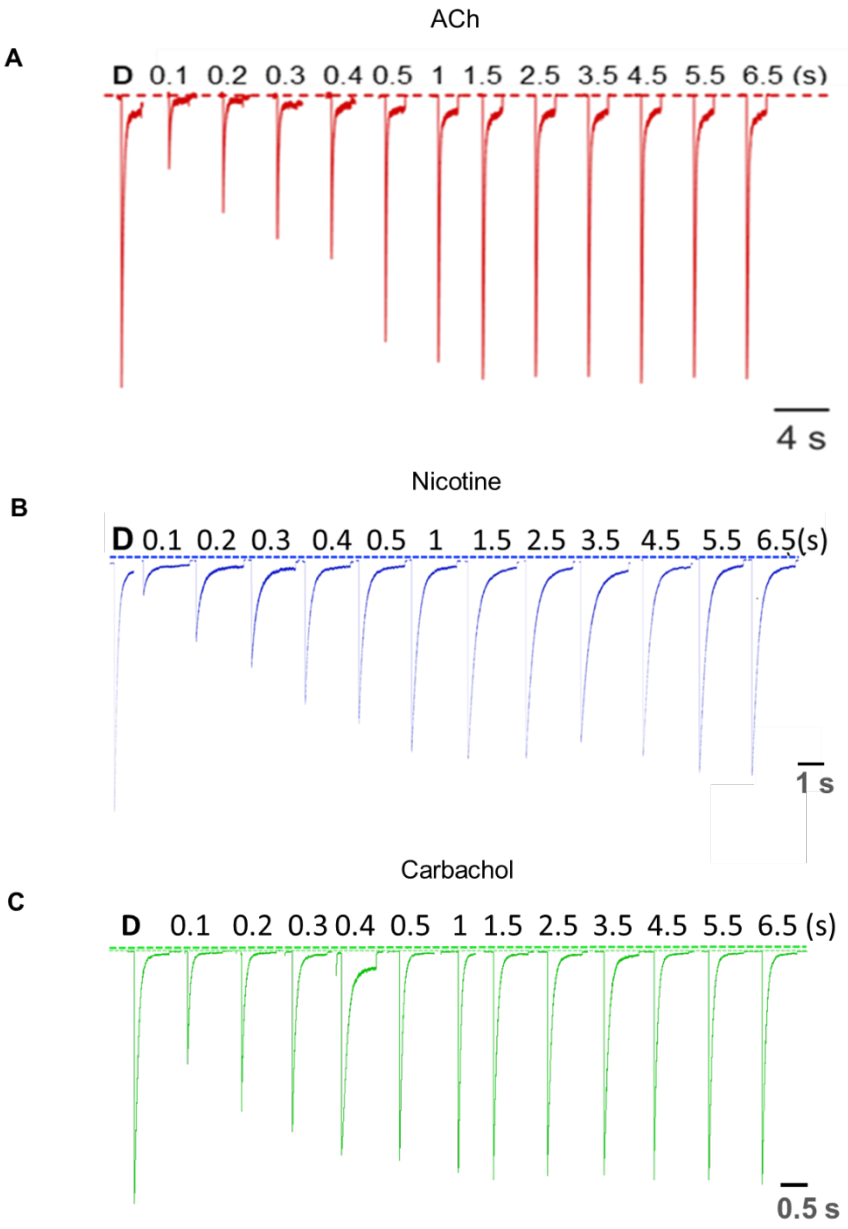

Figure 27. Two-pulse protocol to study recovery from desensitization induced by 10 µM ACh, 200 µM nicotine, and 300 µM carbachol

Representative recordings obtained by using a two-pulse protocol to study recovery from desensitization evoked by ACh, nicotine and, carbachol are shown. 10 µM ACh, 200 µM nicotine and 300 µM carbachol was applied for each desensitizing pulse (D) as well as for each test pulse at recovery intervals ranging from 0.1-6.5 s.

There was a waiting period between each pulse pair of at least 30 s to fully recover all channels. Current amplitudes of the test pulses were normalized to the current amplitude of the respective desensitizing pulses. The relative peak currents (I_{test} /

$I_{desensitization}$) were plotted against the interval time and were reasonably fitted with a mono-exponential function in case of all the three ligands, ACh, nicotine, and carbachol. The time course of recovery ($\tau_{recovery}$) obtained in case of ACh, nicotine, and carbachol were 0.3 s, 0.68 s, and 0.25 s, respectively. This suggested that the recovery from ACh-mediated desensitization is faster than the nicotine-mediated desensitization but slower than the carbachol-mediated desensitization (Figure 28).

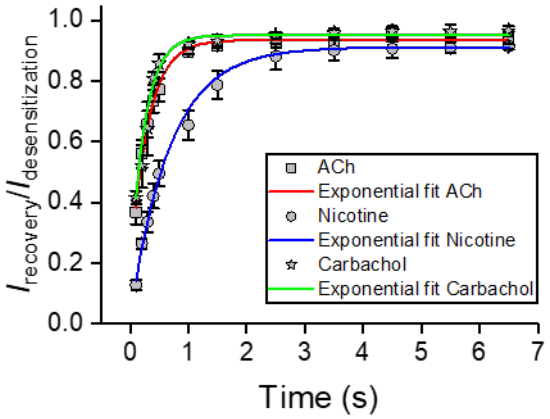

Figure 28. Recovery from agonists mediated desensitization

Data points obtained by analyzing recovery from agonist-mediated desensitization are plotted as a function of concentration. Recovery time constants for ACh, nicotine, and carbachol were 0.3 s, 0.68 s, and 0.25 s, respectively. Data are means ± S.E.M. for 3-13 cells.

100 % recovery was not possible in any of the cases. The maximum percentages of recovery from desensitization by ACh, nicotine, and carbachol were 95%, 91%, and 96%, respectively.

4.2.4. Block of nAChRs by ACh, nicotine, and carbachol

When concentrations (ACh: 2.5 mM and 3 mM; nicotine: 1 mM, 2 mM, and 5 mM; carbachol: 7 mM) higher than the saturating concentration of ACh (500 µM), nicotine (500 µM), and carbachol (2 mM) were applied to the cells containing muscle-type nAChRs, blocking of nAChRs was observed in all cases. In each case, saturating concentration as well as concentration higher than the saturating concentration were applied in the same cell for better comparison. The peak current amplitude declined

noticeably compared to the peak current obtained after application of the saturating concentration of ligands. As a result, a bell-shaped concentration-activation curve was obtained in case of all three ligands(Figure 29A-C).

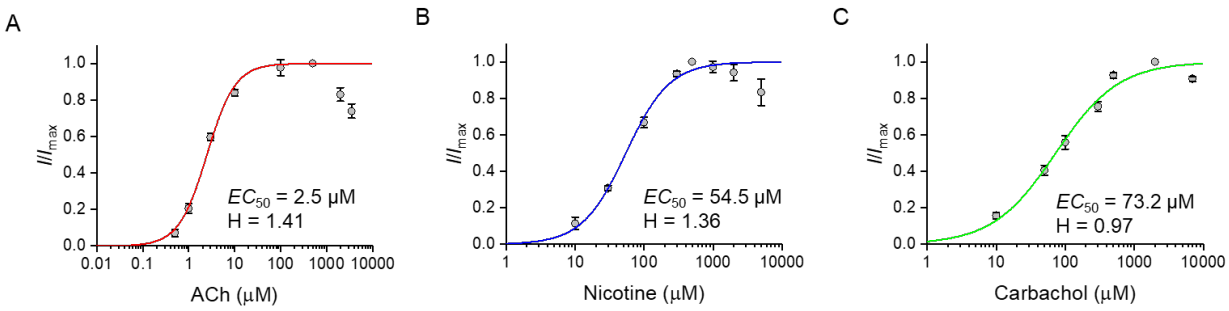

Figure 29. Attenuation in peak current at higher concentrations of ACh, nicotine, and carbachol

Normalized current responses are plotted as a function of indicated concentrations of ACh nicotine, and carbachol and fitted with the Hill equation (ACh-red fit, nicotine-blue fit, and carbachol-green fit). Bell-shaped concentration-activation relationship indicates blocking of the receptor at the concentration higher than the saturating concentration (500 µM in case of ACh and nicotine whereas 2 mM in case of carbachol). Data are means ± S.E.M. for 3-12 cells.

Removal of concentrations higher than saturating concentrations (blocking concentrations) of ACh (2.5 mM and 3 mM) and nicotine (1 mM, 2 mM, and 5 mM) gave rise to a rapid current increase called 'off-current' (Figure 30A), which suggests a reopening of channels which were formerly blocked (Maconochie and Steinbach, 1995). Therefore, the analysis of this off-current can be used to gain information about the nature of the block. Surprisingly, no 'off current' was observed in case of carbachol.

Experiments were designed to monitor block when different blocking concentrations of ligands at different exposure times, i.e. at 200 ms, 1000 ms, 2000 ms, and 5000 ms and at different membrane voltages (-60 mV & +60 mV) were applied. For quantification, the degree of block is calculated as the ratio of the current obtained after removal of ligand ($I_{off\text{-}current}$) to the current obtained in presence of ligand, ($I_{steady\text{-}state}$) (measured just before the washing phase) (Figure 30B). The decline in peak

current and a relative increase of the off current of muscle-type nAChRs with increasing blocking concentrations of nicotine (2 mM, 3.5 mM, and 5 mM) is shown in (Figure 30C).

$$\text{degree of block} = \frac{I_{off}}{I_{steady\text{-}state}}$$

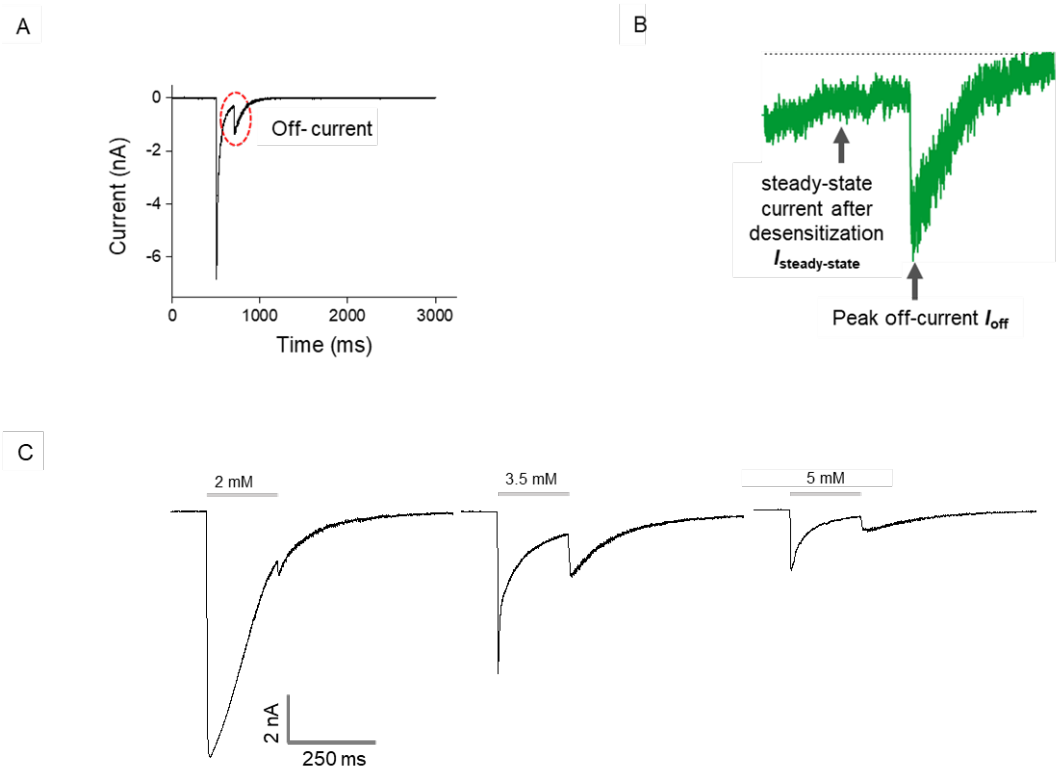

Figure 30. Block of muscle-type nAChRs at ligand concentrations higher than the saturating concentrations

(A) Representative current trace of nAChRs measured in response to 3.5 mM of ACh showing the off-current (red circled) when blocking concentration was washed off. (B) Magnification of the current shown in A, focussing on the off current. (C) Current traces represent peak current decline and a relative increase in off-current with increasing concentrations of nicotine.

Channel block was observed for ACh and nicotine at concentrations higher than the saturating concentrations at both -60 mV and +60 mV. Since no off-currents were

observed for carbachol at high concentrations at -60 mV, the block was compared for ACh and nicotine at -60 mV. The used time points were 200 ms, 1000 ms, 2000 ms, and 5000 ms and the concentrations 2 mM, 3.5 mM, and 5 mM (Figure 31). At 200 ms and at 1000 ms, the degree of block by nicotine is significantly higher than by ACh at 3.5 mM and 5 mM whereas there is no difference between the degree of block at 2 mM. Similarly, at 2000 ms and 5000 ms the degree of block is indistinguishable at the concentrations 2 mM, 3.5 mM, and 5 mM.

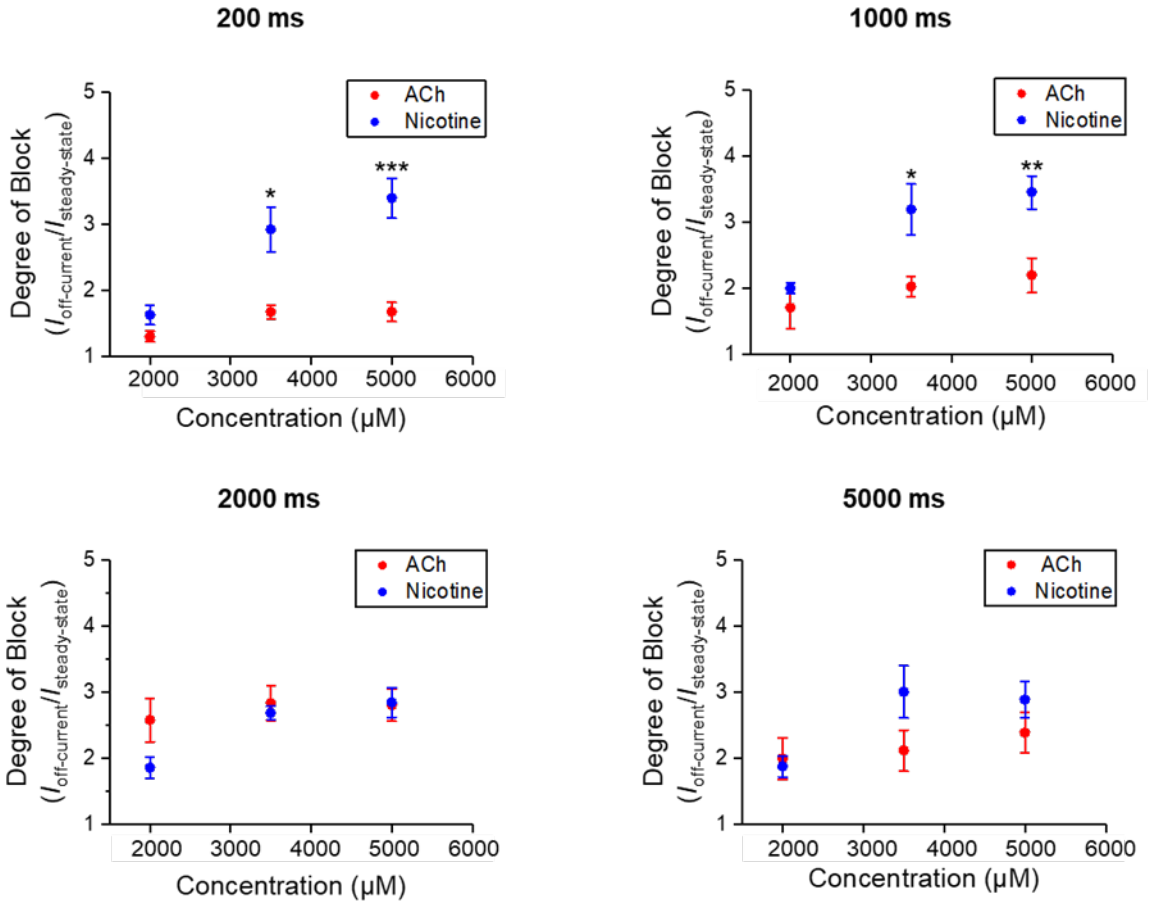

Figure 31. Concentration dependence of block of muscle-type nAChRs by ACh and nicotine

The degree of block is plotted as a function of concentration. At 200 ms, the block by nicotine is twice higher than by ACh at 3.5 mM (P=0.02) and 5 mM (P=0.0003). At 1000 ms, the block by nicotine is approximately 1.5 times higher than by ACh at 3.5 mM (P=0.04) and 5 mM (P=0.006). At 2000 ms and 5000 ms, the difference in the degree of block is insignificant amongst agonists. Data are means ± S.E.M. for 3-9 cells. Statistical t-test for ACh versus nicotine: P > 0.05=no asterisk, P ≤ 0.05=*, P ≤ 0.01=**, P ≤ 0.001=***.

The block by ACh and nicotine (each 5 mM) was also compared at -60 mV and +60 mV at different time points, using 200 ms, 1000 ms, 2000 ms and 5000 ms. A representative trace of the block by nicotine at both voltages is shown in Figure 32A. The block by nicotine is significantly higher than by ACh at -60 mv than at +60 mV at all time points (Figure 32B). Reduction of the block has been observed at +60 mV in comparison to the block at -60 mV in case of both ACh and nicotine. The voltage-dependent block was more pronounced for nicotine than for ACh.

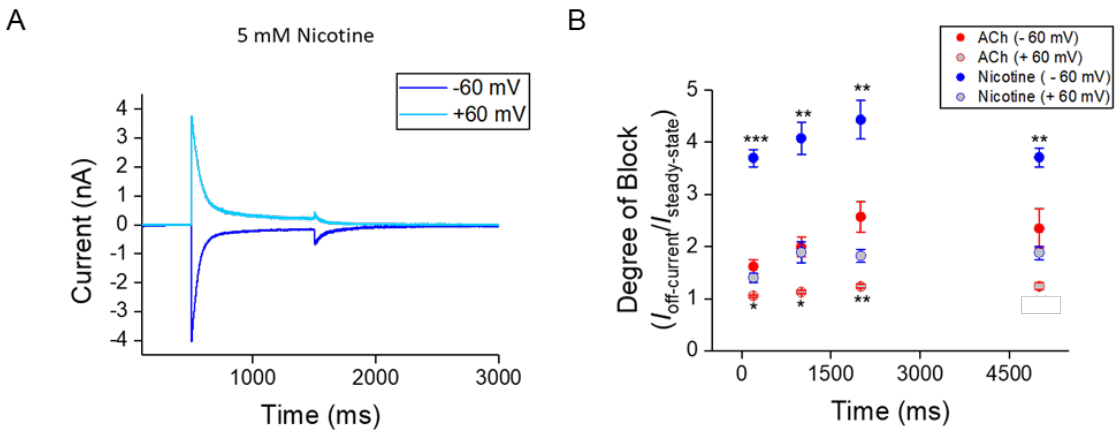

Figure 32. Voltage dependence of block of muscle-type nAChRs by ACh and nicotine

(A) Representative traces obtained after application of 5 mM nicotine at -60 mV (dark blue) and +60 mV (light blue) are shown. (B) Graph showing a comparison of the degree of block at -60 mV when 5 mM of ACh (filled red circles) and nicotine (filled blue circles) was applied at 200 ms, 1000 ms, 2000 ms and 5000 ms. At 200 ms, 1000 ms, and 2000 ms, block by nicotine is approximately two-fold higher than by ACh (P=0.00005, P=0.001, P=0.006, respectively), whereas the block by nicotine at 5000 ms is around 1.5 times higher than ACh (P=0.01). Block by ACh (void red circles) and nicotine (void blue circles) at +60 mV are also represented at 200 ms, 1000 ms, 2000 ms, and 5000 ms. The block by nicotine is significantly higher at 200 ms, 1000 ms and 2000 ms (P=0.02, P=0.03, and P=0.006, respectively). The difference in the degree of block at 5000 ms is insignificant (P=0.12). Data are means ± S.E.M. for 4-5 cells. Statistical t-test for ACh versus nicotine at -60 mV and +60 mV: P ≤ 0.05=*, P ≤ 0.01=**, P ≤ 0.00 =***.

4.2.5. Comparative chart of functional characteristics of three ligands ACh, nicotine, and carbachol

Comparison of functional properties of muscle-type nAChRs agonists, ACh, nicotine, and carbachol are summarized in a tabular form. As mentioned before the functional characteristics of nicotine and carbachol were compared with respect to ACh (refer 4.2).

Table 3: Comparison of functional characteristics of muscle-type nAChRs agonists: ACh, nicotine, and carbachol

Functional Characteristics	ACh	Nicotine	Carbachol
EC_{50}	2.5 μM	54.5 μM	73.2 μM
H	1.41	1.36	0.97
Efficacy	full agonist	partial agonist	full agonist
Desensitization at the lowest possible activation level	At 0.5 μM τ=1090 ms	At 10 μM τ=2437 ms	At 10 μM τ=276 ms
Desensitization at saturating or at the highest activation level	At 500 μM τ=67 ms	At 500 μM τ=313 ms	At 200 μM τ=26 ms
Extent of desensitization at the lowest possible activation level	0.18	0.17	0.83
Extent of desensitization at saturating or at the highest activation level	0.98	0.95	0.99

Recovery from desensitization	$\tau_{recovery}$=0.3 s	$\tau_{recovery}$=0.68 s	$\tau_{recovery}$=0.25 s
Blocking of nAChRs by agonist	attenuation of peak current is observed at a concentration higher than the saturating concentration (500 µM)	attenuation of peak current is observed at a concentration higher than the saturating concentration (500 µM)	attenuation of peak current is observed at a concentration higher than the saturating concentration (2000 µM)
Concentration-dependent block of nAChRs Degree of block ($I_{off\text{-}current}/I_{steady\text{-}state}$)		comparatively higher than ACh	not compared because no off-current was observed
Voltage dependent block of nAChRs at -60 mV and + 60 mV Degree of block ($I_{off\text{-}current}/I_{steady\text{-}state}$)		comparatively higher than ACh at both – 60 mV and + 60 mV	not compared because no off-current was observed

After comparing the functional characteristics of the three ligands, ACh is considered as the most suitable candidate for fluorophore-coupling and application in cPCF because it is most potent amongst the three ligands. Whereas ACh activates the receptors in a low concentration range, it blocks them in a very high concentration range (>500 µM). Apart from this, recovery of the receptor from the ACh induced desensitization gets completed within a reasonable time window of 2000 ms.

4.3. Selection of linkers for coupling a fluorophore to ACh

As mentioned under section 3.5, coupling a fluorophore directly to an agonist molecule will alter its properties. Hence, coupling a fluorophore to the ligand via a linker is a way to minimize the effect of one moiety on the other. Thereby, the structure and the length of a linker are crucial factors to be considered (Prescott et al., 1999; Shi et al., 2014). Different linkers of variable lengths were tested to find the most suitable one for coupling as shown in Figure 33.

Compounds in which the ester group of the ACh is replaced with an amide group are more stable and can be easily synthesized although they are less flexible and hydrophilic (Barlow et al., 1978). Therefore, they were considered in the testing strategy, although these compounds are expected to be less potential agonists. Two linker alternatives were tested: alkyl linkers and PEG linkers. Alkyl linkers were expected to be advantageous because it has been reported that when they are linked to the functional group, the characteristics of the functional group was not changed (Mallavadhani et al., 2014). PEG linkers were considered because they are non-toxic, hydrophilic, and highly flexible.

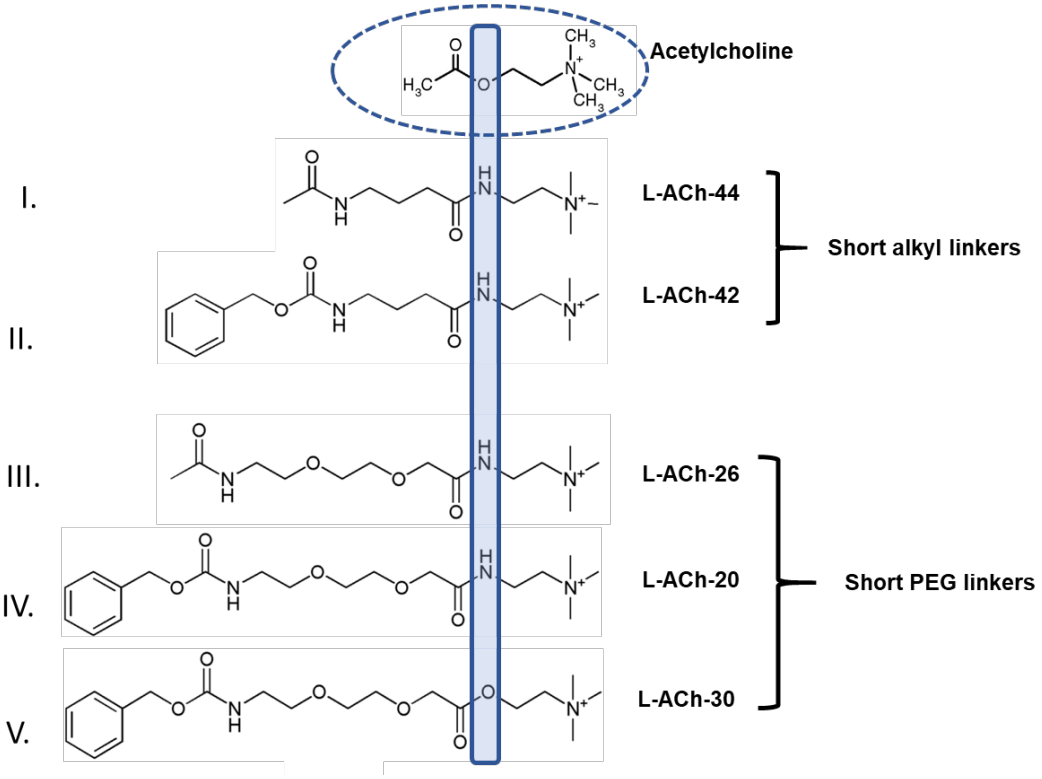

Figure 33. Different linkers coupled to ACh

Structures and names of the compounds used to identify the most appropriate linker chemistry. Chemical structure of acetylcholine is shown in the dotted circle. Acetyl amides and acetyl esters were used.

4.3.1. nAChR activation with linker-coupled ACh derivatives

When linker-coupled ACh (L-ACh) were applied to nAChRs, most of them did not produce a current response resembling a typical ACh-induced current. 50 µM of L-ACh (L-ACh-44, L-ACh-42, L-ACh-30, L-ACh-26, and L-ACh-20) were compared with 50 µM ACh (Figure 34A-B). Relative current (I_{Linker}/I_{ACh}) obtained were 0.04 ± 0.02 (L-ACh-44), 0.04 ± 0.003 (L-ACh-42), 0.10 ± 0.01 (L-ACh-30), 0.04 ± 0.01 (L-ACh-26), and 0.07 ± 0.02 (L-ACh-20). Only L-ACh-30 elicited a current with a desensitization kinetics (τ=253.66 ± 36.66 ms) resembling the current elicited by ACh (τ=44.93 ± 1.27 ms; P=0.40) as shown in Figure 35A-B. Hence, L-ACh-30 was selected for fluorophore coupling. However, the amplitude of this current was much smaller reaching a value of only 10 ± 1 % of that obtained with ACh.

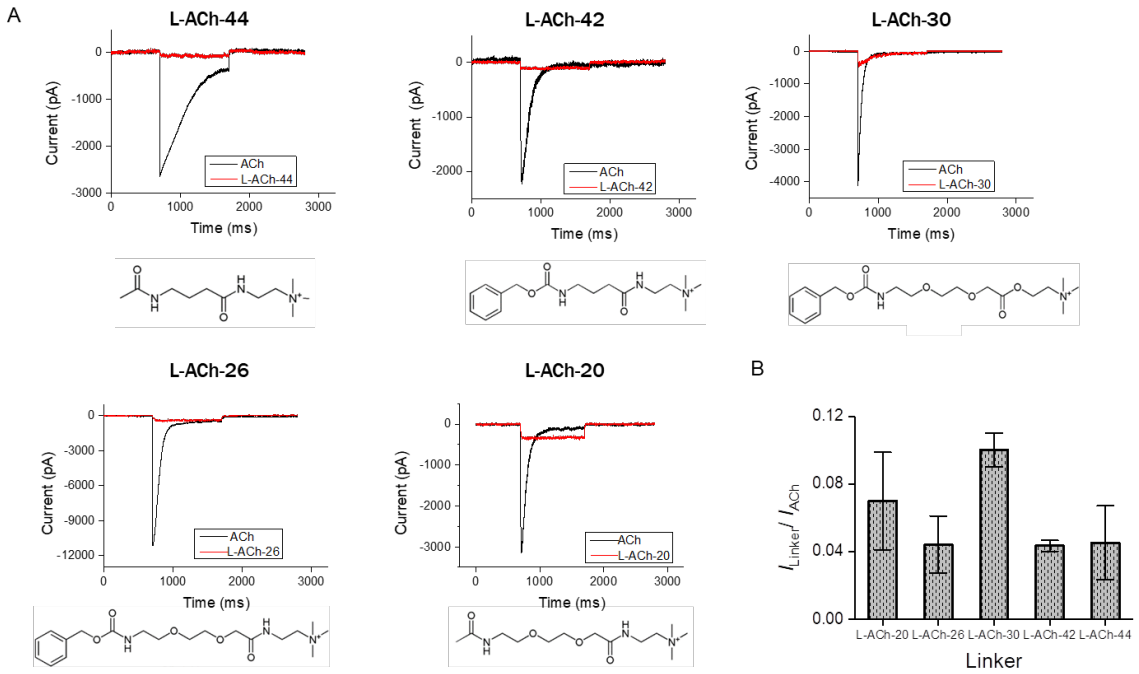

Figure 34. Current produced by nAChRs in response to different L-ACh

(A) Representative current traces obtained by 50 μM of the indicated L-ACh (in red) and 50 μM ACh (in black). (B) The relative current obtained from nAChRs in response to indicated linkers. Data are means ± S.E.M. for 3-5 cells.

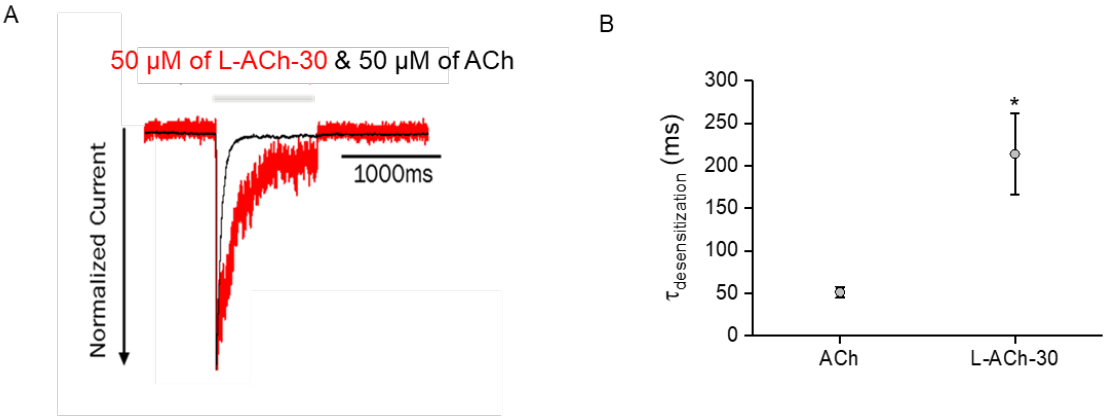

Figure 35. The current response induced by L-ACh-30

(A) A representative current trace monitored from the cell expressing nAChRs in response to 50 μM L-ACh-30 (in red) normalized with current obtained in response to 50 μM ACh (in black) is shown. Gray bar above the traces indicates application time of ligands. (B) L-ACh-30 showed similar activation kinetics. Data are means ± S.E.M. for 4 cells. Statistical t-test: P ≤ 0.05=*.

4.3.2. Testing of non-sulfonated Cy3-coupled L-ACh

Before coupling the L-ACh-30 with a sulfonated Cy3 dye, it was first coupled with the non-sulfonated Cy3 to develop the synthesis strategy and to perform the initial functional tests. Non-sulfonated Cy3-coupled L-ACh-30 was named herein as L-ACh-68A. In order to compare the current, 50 µM ACh and 50 µM L-ACh-68A were applied in the same cell. Current obtained in response to L-ACh-68A were normalized to the current obtained upon ACh application (Figure 36A).

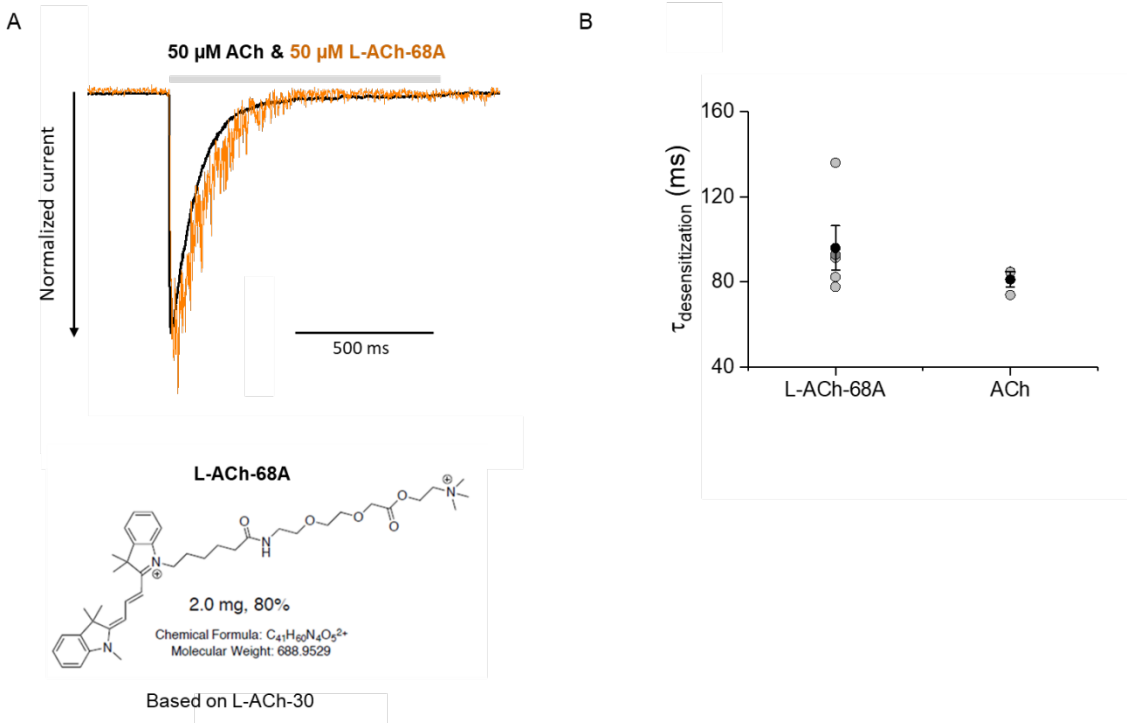

Figure 36. Current response induced by L-ACh-68A

(A) Normalized nAChRs current in response to the indicated concentration of ACh and L-ACh-68A (B) The graph shows the comparison between the time course of desensitization of L-ACh-68A (τ=96.05 ms) and ACh (τ=81.5 ms; P=0.23). Mean values are represented by black symbols and individual recordings by gray symbols. Similar mean values suggest that both agonists desensitize the receptor similarly. Data are means ± S.E.M. for 3-5 cells. Statistical t-test: P > 0.05=no asterisk.

Upon comparison, the difference in the time course of desensitization kinetics turned out to be insignificant, which indicates that L-ACh-68 A (τ=96.05 ms) desensitizes the

receptor similarly as ACh (τ=81.5 ms; P=0.23) (Figure 36B). Hence, obtained desensitization kinetics upon application of non-sulfonated Cy3 coupled to L-ACh-30 (Figure 36A) is more similar to the kinetics of untagged ACh in comparison to the desensitization kinetics of L-ACh-30 (τ=253.66 ms) alone (Figure 35A).

Despite the similar desensitization kinetics of currents produced by L-ACh-68A and ACh, employment of L-ACh-68A was not feasible because of the lipophilic nature of non-sulfonated Cy3 (Figure 37).

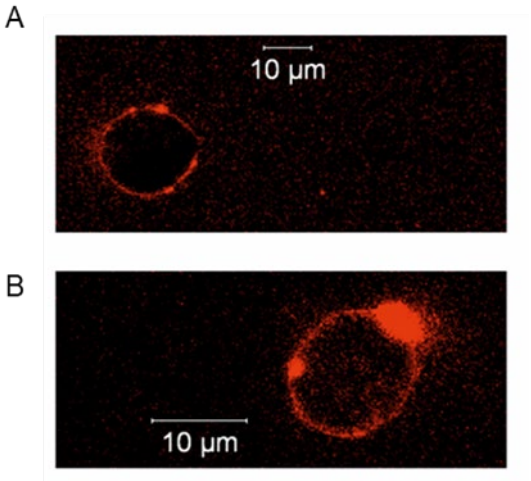

Figure 37. L-ACh-68A coupled with non-sulfonated Cy3 is lipophilic

(A) Control cell exposed to 10 µM non-sulfonated Cy3-ACh. (B) nAChR expressing cell exposed to 10 µM non-sulfonated Cy3-ACh.

Therefore, sulfonated Cy3 was coupled with L-ACh-30 following the same strategy for performing cPCF experiments. The new compound synthesized was named as fACh or Cy3-ACh (Figure 38).

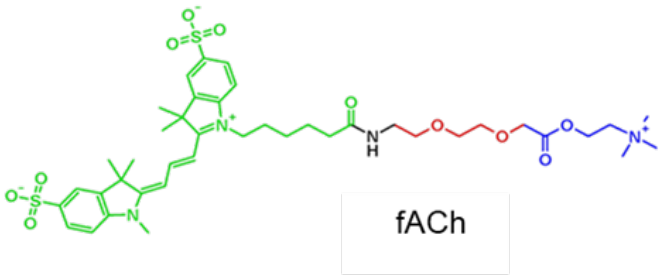

Figure 38. Chemical structure of fACh

Blue part in the structure represents ACh, red part represents PEG linker, and green part represents sulfonated Cy3.

4.4. Relating ligand binding and channel gating using fACh

4.4.1. Electrophysiological characterization of fACh

Different concentrations of fACh (0.5 to 500 μM) were applied to the lifted cells containing adult muscle-type nAChRs for 1 s to monitor fACh-elicited concentration-dependent inward currents. Current amplitude increased with increasing concentrations of fACh, 500 μM was found to be the saturating concentration (Figure 39).

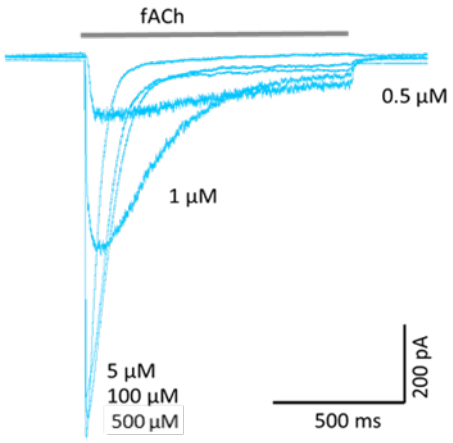

Figure 39. Concentration-dependent inward currents of fACh
Representative current traces obtained upon application of indicated concentrations of fACh for 1 s is shown. The smallest current response was obtained with 0.5 µM and the maximum current response was obtained by 500 µM.

To assure that fACh closely mimics the native ligand ACh, the potency and efficacy of fACh was compared with ACh. Varied concentrations of fACh and ACh for 1 s were applied to determine the concentration-activation relationship. Peak current values obtained for each concentration were normalized to the saturating concentration of 500 µM in both cases. Mean data points were plotted against each concentration and were fitted with the Hill equation (Figure 40A). The estimated concentration of ACh which can produce a half-maximal response (EC_{50}) was 2.4 µM and Hill coefficient, H was 1.4. The respective values for fACh were 0.99 µM and 1.8. This indicates that fACh is twice as potent than ACh. For better comparison of efficacy, the saturating concentration of 500 µM of both ACh and fACh was applied in the same cell. Similar current responses were obtained from both ligands, suggesting that fACh is similarly efficacious as ACh ($I_{fACh,max}/I_{ACh,max}$=0.97 ± 0.1) (Figure 40B).

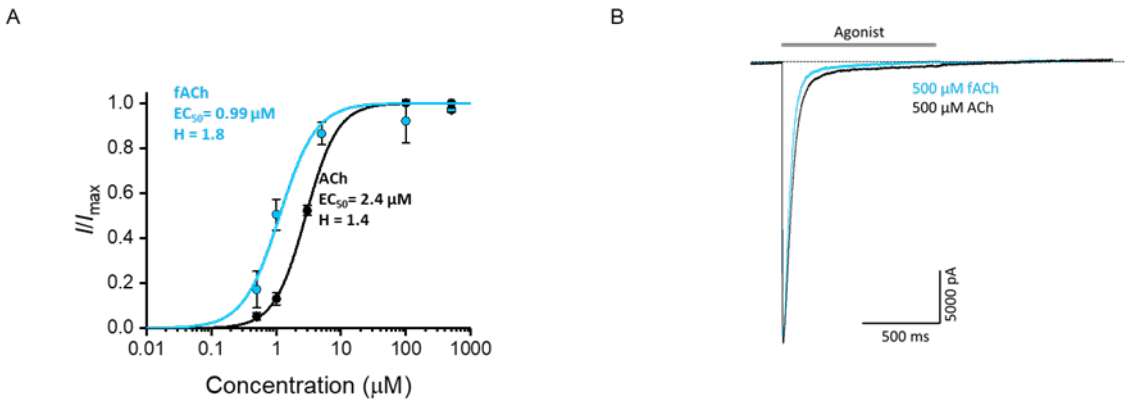

Figure 40. Potency and efficacy of fACh in comparison to ACh

(A) Relative current versus concentration graph. fACh is twice as potent as ACh. Mean data points were plotted against their corresponding concentrations and were fitted with the Hill equation. Obtained concentration-response curves of ACh (in black) and fACh (in blue) is shown. Upon estimation of EC_{50} values, fACh (EC_{50}=0.99 µM) was found to be twice as potent as ACh (2.4 µM). The Hill coefficient of ACh and fACh was 1.4 and 1.8, respectively. Data are means ± S.E.M. for 3-7 cells. (B) fACh and ACh have similar efficacy. Current traces obtained upon application of 500 µM ACh and fACh in the same cell is shown.

4.4.2. Establishing cPCF experiments with fACh

Both fluorescence and electrophysiological recordings were carried out simultaneously in cPCF experiments. When applying fACh, a non-specific fluorescence signal in the traditional patch-pipettes (pipettes used for electrophysiological recordings in this study) that were empty (no cells attached to them) was observed. Therefore, there was a need to find the most suitable pipette condition that allows for the lowest unspecific fluorescence signal, which would lead otherwise to misinterpretation of experimental results.

Tested pipettes with different glass types and configuration were named as I, II, III, and IV (specifications are given in Figure 41B). The protocol of fACh application is shown in Figure 41A. Figure 41B represents a comparison of fluorescence intensities at three different time points: (a) before application of fACh (b) 50 ms after fACh application, and (c) 13 s after fACh application. Glass type ‘IV’ was found to be best suitable for further cPCF experiments as it gives the lowest unspecific fluorescence

signal in comparison to other glass types. Furthermore, it turned out that avoiding fire-polishing of the glass pipettes reduced the unspecific fluorescence (Figure 41C).

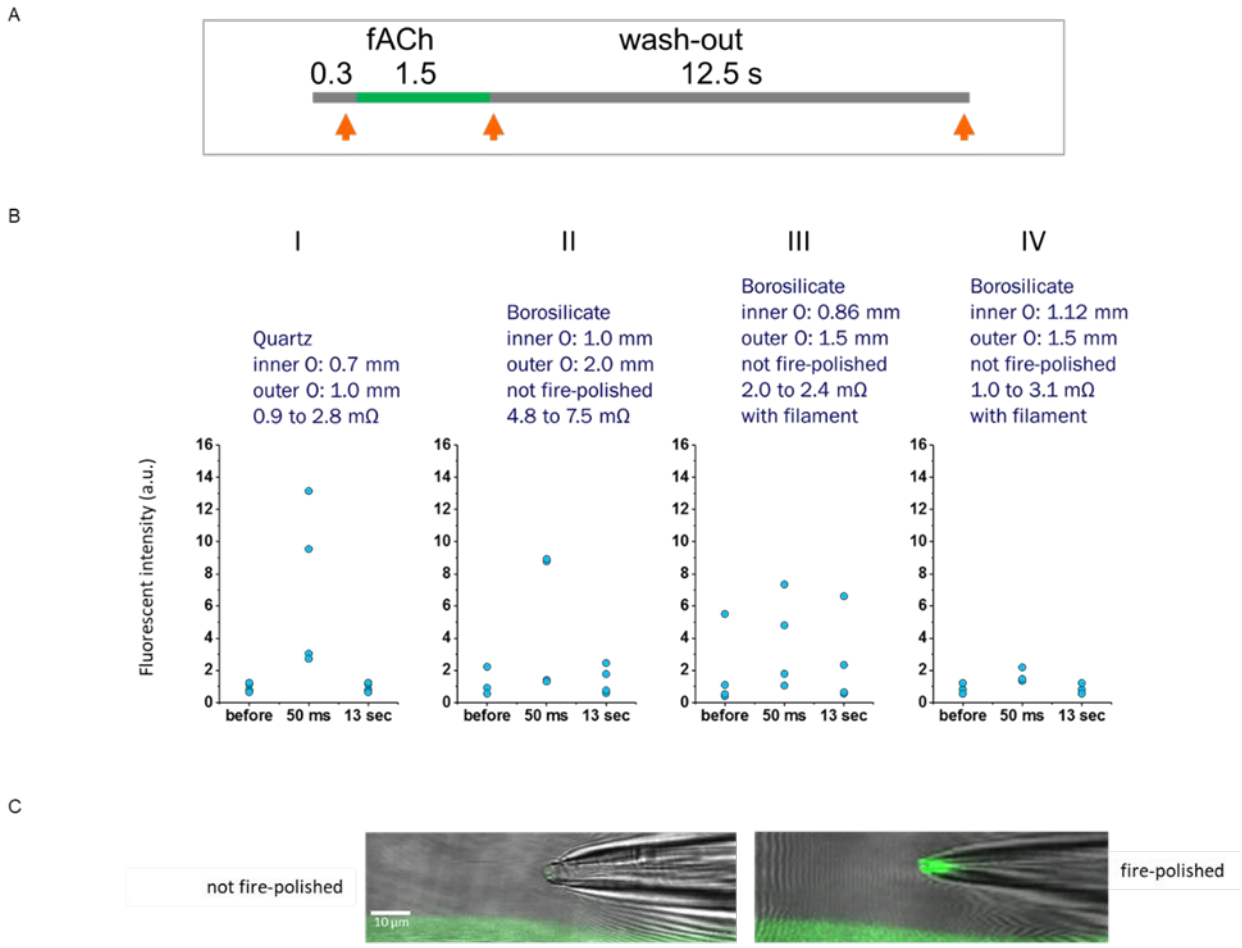

Figure 41. Comparison of patch pipettes with different glass types and configuration
(A) Application protocol of fACh (B) Indicated glass types having indicated configurations (I-IV) were tested to find the most suitable glass pipette for cPCF experiments. Graphs representing fluorescence intensity at three-time points: before application of fACh, 50 ms after application and 13 s after application (wash-out phase). Glass type IV is best suitable for further cPCF experiments as it produced the lowest signals. Transfected cells caused a signal of ~10 a.u. under the same conditions (for comparison see Figure 43). (C) Fire-polishing caused even higher non-specific fluorescence signal. The glass used was borosilicate having inner diameter 1.12 mm and outer diameter 1.5 mm. Pipette resistance was between 1 to 3 MΩ.

4.4.3. fACh binding to muscle-type nAChRs

To check if fACh is able to bind to muscle-type nAChRs, 10 µM fACh was applied to transiently transfected HEK 293 cells attached to the cell culture coverslip used for cultivation. A pronounced membrane staining only in cells carrying the receptor was found. To identify transfected and non-transfected cells cytosolic CFP was used as a transfection marker. Thus, fACh was found to bind to nAChRs (Figure 42).

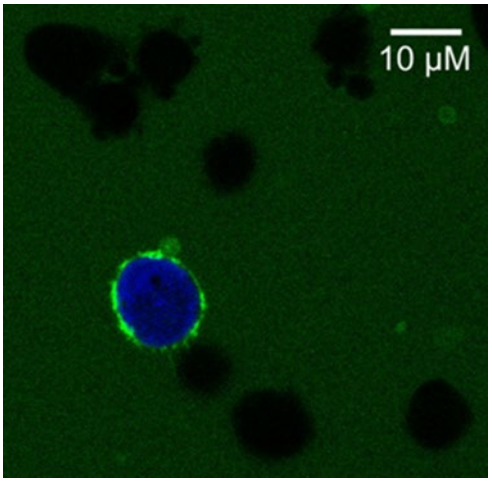

Figure 42. fACh binds to nAChRs

The confocal image represents binding of fACh (fluorescent signal) only to the cell expressing nAChRs (in this case stained blue because of CFP was used as a transfection marker). All other cells appearing in black are control cells because they do not express the receptor.

To study the reversibility of fACh binding, washing-in and washing-out experiments on lifted control cells and transfected cells were performed. As shown for cells attached to the chamber bottom (Figure 42) high fluorescent signals were obtained only in case of transfected cells whereas in control cells fluorescence signals were negligible (Figure 43A). Upon washing, the intensity decreased. These results indicate reversibility of the signal, thus of ligand binding (Figure 43B).

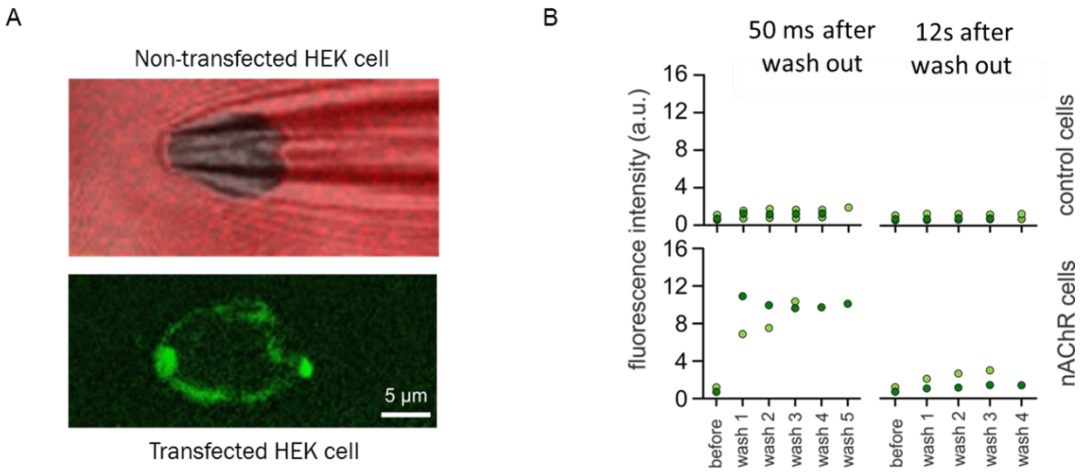

Figure 43. Fluorescence intensity increases due to binding in transfected cells
(A) fACh yielded a fluorescence signal after binding to adult muscle-type nAChRs in HEK 293 cells which are absent in control cells. Red fluorescence in the non-transfected cell arose from the background dye Dy647, which is used to identify the position of the cell and for background subtraction (see Materials and Methods). (B) Graphs representing the specificity of the fluorescence signal obtained 50 ms (left panels) and 12 s (right panels) after switching from 10 µM fACh to control solution, respectively. Quantification was done in the washing out phase to get rid of the background signal caused by unbound fACh. Data points represent individual recordings (n=3 for controls, n=2 for transfected cells).

4.4.4. PCF applications using fACh

Two different protocols (I and II) were used for measuring fluorescence signals after application of fACh (Figure 44): Protocol I had a scan time of 100 ms and a high sampling rate (10 Hz). Protocol II had a scan time of 800 ms and a lower sampling rate of 1.3 Hz. Lower sampling rate provides an advantage of increased scan time per image that ultimately yields an increased number of pixels. Hence, better image resolution can be obtained. Protocol I was applied for washing-in and protocol II for washing-out fACh (Figure 44).

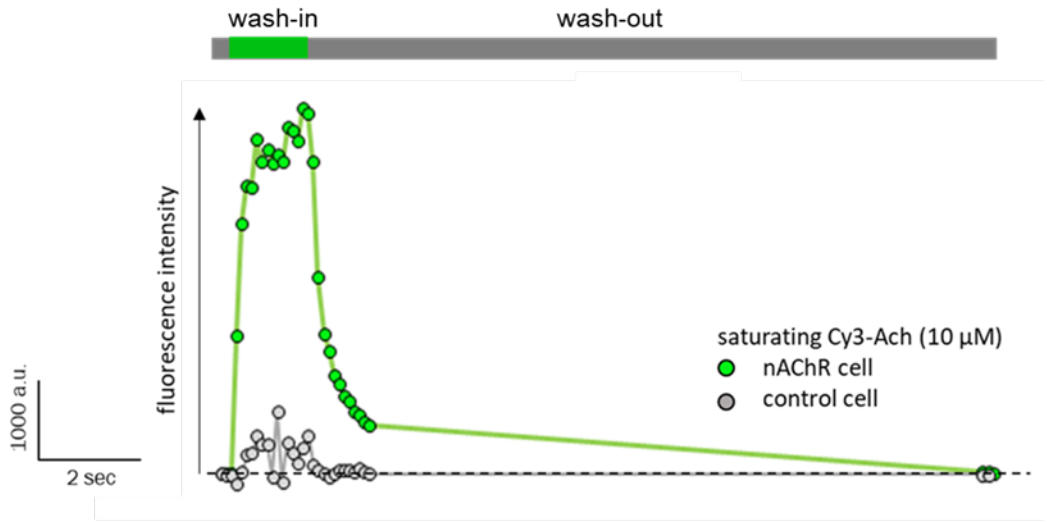

Figure 44. Protocols for fluorescence signal measurements

Two protocols were used to monitor fluorescence signals. Protocol I was used for washing-in and protocol II for washing-out. Green symbols represent the time course of the fluorescence intensity in a transfected cell (mean of 4 traces of the same cell). Grey symbols represent a respective time course in a control cell.

After confirming that fACh mimics the agonistic behavior of native ACh binding to muscle-type nAChRs in a specific and reversible way and defining the experimental settings, started to test whether fACh is useful to study nAChR gating was tested.

Application 1: Monitoring the kinetics of agonist binding and unbinding

10 µM fACh was applied to transfected cells to monitor binding as well as unbinding. Both the binding and unbinding process could be reasonably fitted with a bi-exponential function. Initial fast components of binding as well as unbinding were too fast to be resolved at a sampling rate of 10 Hz. Nevertheless, the slower phases could be described more thoroughly, yielding a time constant for the slow component of binding of 286 ± 81 ms and for the slow component of unbinding of 1652 ± 323 ms (Figure 45).

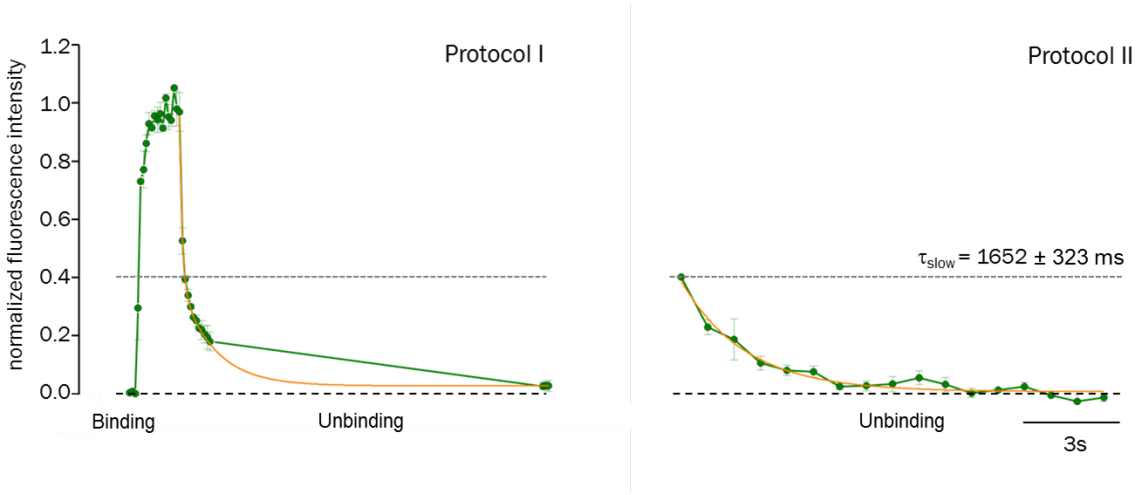

Figure 45. fACh binding and unbinding follow bi-exponential time course
fACh binding and unbinding to the nAChR. The data points of four traces were averaged. In protocol I, faster events were not resolved at a sampling rate of 10 Hz. In protocol II, the sampling rate was set to 1.3 Hz.

Application 2: Relating agonist binding to desensitization

Upon application of 10 µM fACh, a steep increase in the fluorescence intensity was followed by a slow phase approximating a constant value. This slow binding component might reflect that the receptor enters into the desensitized state. Concerning the current, the falling phase (desensitization), recorded simultaneously with fluorescence recording, could also be reasonably described by a bi-exponential function and it turned out that the time course of the slow component of desensitization ($\tau_{slow,\ desensitization}$=356 ± 26 ms) was similar to that of binding ($\tau_{slow,\ binding}$=286 ± 81 ms). Figure 46 shows an overlay of current trace (inverted) and fluorescence signal to demonstrate this kinetic similarity.

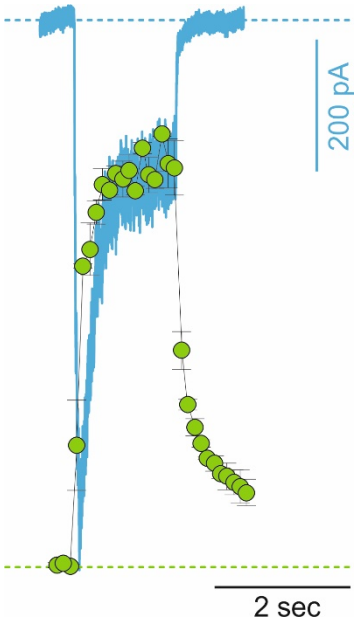

Figure 46. Slow phase of the fluorescence increase is similar to the slow phase of desensitization

Superposition of fluorescence (green) and a current signal (blue). The slow component of fluorescence increase ($\tau_{slow,\ binding}$=286 ± 81 ms) and slow component of current desensitization ($\tau_{slow,\ desensitization}$=356 ± 26 ms) show similar kinetics. Data are mean ± S.E.M. of 4 traces.

Application 3: Relating ligand unbinding to recovery from desensitization

The time course of the unbinding phase of fACh and time course of the recovery from the ACh mediated desensitization were compared to investigate if recovery from desensitization correlates with agonist unbinding. It turned out that the slow component ($\tau_{slow,\ unbinding}$) of unbinding (τ=1652 ± 323 ms) (refer Figure 46) was much slower than the time course of recovery from desensitization (τ=300 ms) (refer Figure 28 for ACh). This suggests that the recovery from desensitization is independent of the dissociation of at least one agonist molecule from the receptor.

5. Discussion

The muscle-type nAChR is one of the best-studied cell surface receptors. It is involved in synaptic transmission at the neuromuscular junction (Kistler et al., 1982; Stroud and Moore, 1985) and served as an archetype for a better understanding of allosteric mechanisms of ligand-gated ion channels (Changeux, 1990; Prince and Sine; 1999). Several classical biophysical methods such as crystallography, electron microscopy, electrophysiology, ion flux assays, ligand-binding assays, and single-channel recordings have provided deep insight into structure and function of this receptor but the knowledge about their interrelationship is relatively poor (Karlin, 2002; Lester, 2014). There are several questions which are still to be answered, such as whether binding of a ligand at one binding site can open the channel or both binding sites are needed to be occupied, or whether there are intermediate states when the receptor proceeds through electrophysiologically defined states (closed, open and desensitized states). Various complex kinetic models have been proposed so far to unravel the state-dependent relationships, but most of them are based on indirect information about binding. Experimentally obtained binding data could validate existing kinetic models or lead to new ones.

New fluorescence approaches, such as time-resolved photolabeling (Averalo et al., 2005), use of fluorescent unnatural amino acids (Nowak et al., 1995), fluorescent ligands (Grandl et al., 2007, Krieger et al., 2008; Fujimoto et al., 2008; Schmauder et al., 2011) or fluorophore-coupled receptors (Dahan et al., 2004) in combination with electrophysiology provided new insights into the state-dependent relationships but a clear concept is still missing. The present study is intended to contribute to a better understanding by modifying and using a confocal patch-clamp fluorometry (cPCF) technique (refer to 5.1) to study agonist binding and activation behavior simultaneously. Using a fluorescent agonist and the whole-cell configuration has provided an advantage to directly monitor state-dependent ligand binding under best possible physiological conditions, without relying on any structural modifications of the receptor.

5.1. Newly modified cPCF technique

Until now, PCF (Zheng and Zagotta, 2000) or cPCF has been used in combination with excised *Xenopus laevis* oocytes patches in the inside-out configuration to study

state-dependent conformational changes and ligand binding in CNG, and HCN channels (Biskup et al., 2007; Kusch et al., 2012) and in the outside-out configuration to study channel gating in BASIC channels (Schmidt et al., 2014). In the present study, this technique was modified to study ligand binding to an extracellularly controlled ion channel in the whole-cell configuration.

The outside-out configuration could have been an alternative for studying ligand binding to extracellular binding sites. This possibility was ruled out because HEK 293 cells were chosen as a heterologous expression system, which would allow only small patches with a low fluorescence and current signal. As this technique demands high signal to noise ratio, it was decided to collect data from whole cells in the present study.

The mammalian HEK 293 cell line has been chosen as a heterologous expression system over non-mammalian cells (*Xenopus laevis* oocytes) though those cells are reported to be more advantageous in terms of expression level and in providing a suitable environment for proper maintenance of physiological functions (Korngreen, 2016). Additionally, differences in channel properties of nAChRs expressed in oocytes compared to those expressed in mammalian cells have also been reported (Grassi et al., 1995; Sivilotti et al., 1997; Lewis et al., 1997; Millar, 2009).

The experiments were done on lifted cells rather than on cells attached to the chamber bottom after attainment of the whole-cell mode because faster desensitization kinetics was observed in lifted cells (85.42 ms) in comparison to the desensitization kinetics of cells attached to the chamber bottom (186.24 ms). Hence results support the idea proposed by Yu and coworkers in 2009 that application of ligand solutions to lifted cells results in homogenous and faster solution exchange.

Besides that, a specific glass pipette (Borosilicate glass inner diameter:1 mm; outer diameter: 1.5 mm) was used for cPCF experiments because other glass pipettes (different glass types and configurations; refer 4.4.2 for details) produced more non-specific fluorescence upon ligand application. In earlier cPCF studies with excised patches, the fluorescent signal was estimated from the patch that lies inside the patch pipette rather than at the very tip, therefore, glass type and configuration was not a major issue. Further, fire polishing of the pipette was also avoided in the present study because it increased the non-specific fluorescence signal. The reasons for this phenomenon are not clear.

5.2. Selection of a potential agonist for cPCF experiments

For relating ligand binding and channel gating of nAChR using cPCF experiments, the prerequisite was to synthesize a fluorescence agonist that could closely mimic the properties of the native ligand ACh. To choose the most suitable candidate for fluorophore coupling, the electrophysiological characteristics of three unmodified agonists, ACh, nicotine, and carbachol, under whole-cell conditions, which includes the concentration-activation relationship, the desensitization behavior and the ability to block the channel were compared first. ACh was chosen because it is the native, highly efficacious agonist of muscle-type nAChRs (Dilger and Brett, 1990; Akk and Auerbach, 1999; Lape et al., 2008). Nicotine, a plant alkaloid is the name-giving agonist of the nAChR as its primary target and was, therefore, an interesting agonist to be studied. Carbachol is a synthetic choline ester and a strong agonist (Akk and Auerbach, 1999). It is chemically more stable than ACh because of the presence of a carbamyl group instead of an acetyl group (Wonnacott and Barik, 2007).

5.2.1. Potency and efficiency of the potential candidates

The concentration-activation relationships of the three ligands were compared to determine the most potent and most efficient agonist amongst them. Upon comparison, ACh was found to be most potent. It was twenty-fold more potent than nicotine and thirty-fold more potent than carbachol. Further, ACh and carbachol have similar efficacy, while nicotine could produce only 58% of the maximum current produced by ACh at 500 µM. Hence, results support previous reports showing that ACh and carbachol are full agonists whereas nicotine is a partial agonist for the receptor (Dilger and Brett, 1990; Akk and Auerbach, 1999, Jadey et al., 2013, Celie et al., 2004). However, nicotine was also considered as a full agonist at muscle-type nAChRs in an earlier study (Beene et al., 2002).

In previous studies, the estimated EC_{50} values of ACh (via single-channel, whole-cell or excised patch studies) at muscle-type nAChRs range between 7- 28 µM (Dilger and Brett, 1990; Cooper et al., 1996; Akk and Auerbach, 1999; Brownlow et al., 2001; Hatton et al., 2003; Jonosson et al., 2006, 2009; Papke et al., 2010). However, in the present study, a smaller EC_{50} of 2.49 ± 0.15 µM was found. Reasons behind varying

EC_{50} values might be the use of different techniques, particularly the method of ligand application.

For whole-cell recordings, it is assumed that due to the agonist application time slower than the time needed for channel activation, the peak current might be compromised by the fast onset of desensitization superimposing with activation. Maconochie and Steinbach (1995) proposed a back-extrapolation method for the peak-reduction correction. However, they found that back-extrapolation will lead to an overestimation of the data. In this study, back-extrapolation of the falling phase of the current using exponential function until the time point at which ligand was applied was also done. When mean data points obtained after extrapolation were fitted with the Hill equation, a slight right shift of the concentration-activation curve was found. The corrected EC_{50} value for ACh (8.57 µM) was around four-fold higher than the empirically obtained EC_{50} value (2.4 µM). The Hill-coefficient, H, obtained before and after correction was 1.41 and 0.73, respectively. Thus, the true EC_{50} value of ACh is expected to lie between 2.4 µM and 8.57 µM.

In case of nicotine and carbachol, to the best of our knowledge, the concentration-activation relationships were not deduced for muscle-type nAChRs from whole-cell configuration till date. Herein, an EC_{50} value for nicotine of 54.5 µM; H = 1.36 and for carbachol of 73.2 µM; H= 0.97 was found. Interestingly, these values were also lower than the previously reported values estimated by single-channel recordings (Akk and Auerbach, 1999; Marshall et al., 1991). Single-channel studies have reported EC_{50} values for nicotine ranging from hundreds of micromolar to even millimolar range (Yost and Winegar, 1997; Akk and Auerbach, 1999; Jadey et al., 2013). EC_{50} for carbachol is laying in hundreds of micromolar range (Marshall et al., 1991; Akk et al., 2005). After correction by back-extrapolation in case of nicotine and carbachol, slightly higher EC_{50} value were estimated ($EC_{50\ \text{nicotine}}$ = 88.19 µM; $EC_{50\ \text{carbachol}}$ = 114.25 µM). The obtained Hill coefficient, H after extrapolation for nicotine and carbachol was 1.54 and 1.16 respectively. In comparison to ACh, only slight increase in the extrapolated EC_{50} values for nicotine and carbachol led to suggest that the rising phase of the current in case of nicotine and carbachol were only slightly compromised by desensitization. This was unexpected because knowledge about the desensitization behavior obtained herein would suggest a higher effect of desensitization on the peak current for carbachol and a similar effect for nicotine

compared to ACh (see next paragraph). Further experiments are needed to solve this discrepancy.

Regarding the usability of PCF recordings, the comparison of potency and efficacy makes the native ACh the most suitable candidate amongst the three tested ligands for fluorophore coupling because it would require the lowest concentrations range.

5.2.2. ACh, nicotine, and carbachol-induced desensitization in muscle-type nAChRs

To study the agonist-mediated desensitization kinetics, the falling phase of the current was fitted with an exponential function. For all three ligands, the current was best fitted with a mono-exponential function indicating the presence of at least one predominant desensitized state. Desensitization mediated by ACh and nicotine were fast and found to be similar whereas carbachol-induced desensitization was fastest of all. This supports a previous study showing that carbachol mediated-desensitization of muscle-type nAChRs is much faster than ACh-mediated desensitization in BC3H-1 cells in out-side out patch (Dilger and Liu, 1992).

Some studies reported one or two possible components of desensitization time-course (Dilger and Liu, 1992; Paradiso and Brehm, 1998; Jahn et al., 2001) while four to five components of desensitization time-course were also reported (Elenes and Auerbach, 2002). However, the number of intermediate states of desensitization remains still unclear (Figure 47) (Reitstetter et al., 1999).

Paradiso and Brehm (1998) interpreted the reason behind the mono-exponential time course of desensitization. According to them, receptors first accumulate in a ‘shallow state’ of desensitization before entering into deeper states, therefore, the transition into the other states is electrically silent and cannot be predicted.

Also, the ED ($1-I_{steady\text{-}state}/I_{desensitization}$) differed for the three agonists. At lower concentrations of agonists (0.5 µM ACh, 10 µM nicotine, and 10 µM carbachol) or at the lowest percentage of activation (refer 4.2.2 for details) the ED was observed to be similar in case of ACh and nicotine (fraction of channels which underwent desensitzation: 0.5 µM ACh = 0.18 ± 0.05 and 10 µM nicotine = 0.17 ± 0.06) whereas it was observed to be 5-times higher in case of carbachol (fraction of channels which underwent desensitization: 0.83 ± 0.02). However, the ED was observed to be similar

at saturating concentrations of all three agonists or at maximum activation percentage of all agonists (fraction of channels which underwent desensitization: 500 µM ACh = 0.98 ± 0.005, 500 µM nicotine = 0.95 ± 0.01, and 2000 µM carbachol = 0.99 ± 0.003). To describe the concentration dependence of the ED, the Hill equation was fitted to the data. It was found that EC_{50} for ED for ACh (2.5 µM) and for carbachol (2.12 µM) were similar and significantly lower than for nicotine (21.0 µM).

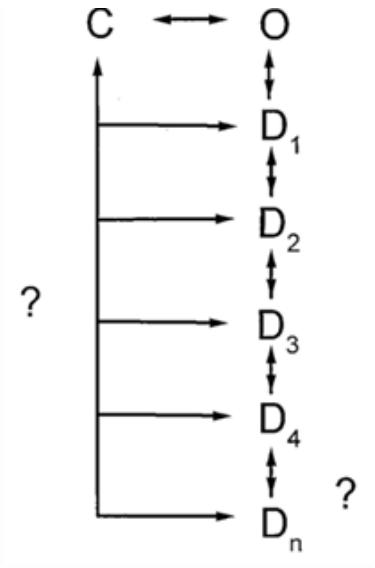

Figure 47. A simple model showing different states of desensitization of nAChRs.
In this kinetic model, 'C' represents the closed state, 'O' represents the open state and D_1 to D_n represent n intermediate states of desensitization (adapted from Reitstetter et al., 1999).

Interestingly, the concentration at which half of the channel population gets activated and the concentration at which half of the channel population underwent desensitization in case of ACh was similar. However, this was not the case for nicotine and carbachol. The EC_{50} for ED is 2.12 µM for carbachol supported previously reported values (Feltz and Trautmann, 1980).

The data about desensitization kinetics and ED support the idea that desensitization behavior depends on the type of agonist which drives the channel into desensitization (Reitstetter et al., 1999; Giniatullin et al., 2005). Carbachol caused the fastest desensitization and was able to drive a high fraction of the channel population into desensitization even at very low concentrations. Nicotine and ACh behaved very

similar regarding their ability to desensitize, however, nicotine needed a higher a concentration to drive the receptor to the same extent.

Recovery from desensitization of muscle-type nAChRs mediated by the three agonists was monophasic. Recovery from carbachol-mediated desensitization was faster ($\tau_{recovery}$ = 0.25 s) than from ACh and nicotine-mediated desensitization ($\tau_{recovery}$ = 0.30 s, $\tau_{recovery}$ = 0.68 s, respectively). After providing maximum time-interval of 6.5 s for recovery, the fractions of channels that got recovered were ~95%, ~91%, and ~96% for ACh, nicotine, and carbachol respectively.

Several studies reported that recovery of muscle-type nAChRs from agonist-mediated desensitization is independent of the nature of the agonist (Katz and Thesleff, 1957; Feltz and Trautmann, 1982) whereas other studies reported that rates of recovery from agonist mediated-desensitization depend on the nature of agonists that drives the receptor into the desensitized state as well as on the exposure time of agonists (Dilger and Liu, 1992; Reitstetter et al., 1999).

Regarding the time-course of recovery, one study reported monophasic time courses (Dilger and Liu, 1992) of muscle-type nAChRs while another reported biphasic recovery (Paradiso and Brehm, 1998). It is speculated that the reason behind the monophasic recovery, in this case, is due to the electrically silent deeper desensitized states and the presence of only one prominent desensitized state. Fractional percentage of recovery from the ACh, nicotine, and carbachol mediated desensitization also supports the fact that some percentage of channel went under deeper desensitization and might take longer time periods to get fully recovered.

It is noteworthy that carbachol rapidly and strongly desensitizes the receptor even in a low concentration range, albeit desensitized receptors recover very quickly from carbachol mediated desensitization. For the purpose of studying the relationship between agonist binding and receptor desensitization, all three agonists tested are interesting candidates because desensitization is well pronounced in all of them.

5.2.3. Acetylcholine and nicotine-induced channel block

Block of muscle-type nAChRs by agonists of the receptor is due to rapid self-antagonism that has been ascribed to a mechanism in which agonists occludes the ion channel pore if present in a concentration higher than the saturating concentration

(Sine and Steinbach, 1984; Maconochie and Steinbach, 1995). Additional binding to binding sites elsewhere than in the αδ and αε binding sites would be a major problem for fluorescence binding studies. Therefore, it was required to test in which concentration range a channel block has to be expected for the three candidates.

After application of high concentrations (above saturating concentrations) of the three agonists, off-currents (current monitored in wash-out phase due to reopening of the channels which were formerly blocked during application phase) were recorded at a transmembrane voltage of -60 mV in case of ACh and nicotine only. In case of carbachol, off-currents were not observed even at a very high concentration of 7 mM and hence, it might be interesting for future research.

To describe the blocking behavior in more detail, the degree of block at different concentrations (concentration range: 2 mM to 5 mM), different application times (200 ms to 5000 ms) and different voltages (-60 mV and +60 mV) were estimated. The block induced by nicotine is concentration dependent, whereas block by ACh was not in the concentration range tested herein. Both ACh and nicotine block were observed to be time-independent within the range tested (200 ms to 5000 ms) in the present study but have a strong dependence on voltage.

From the appearance of off-currents only at concentrations higher than the lowest saturating concentration, it is concluded that for binding studies additional binding of the agonist to a binding site within the channel pore should not be a major issue because the lowest saturating concentration can be chosen for the experimental settings.

5.3. Relating ligand binding and channel gating using fACh

Fluorophore-coupled agonist molecules are well suitable tools to study ligand binding to receptor binding sites by directly measuring their emission intensities using fluorescence microscopy approaches (Biskup et al., 2007; Kusch et al. 2010; Schmauder et al., 2011; Bhargava et al., 2013). An important prerequisite is a fluorophore and a coupling strategy, which does not negatively affect the agonist's behavior.

Since the early 70’s of the last century, attempts were made to couple fluorophores such as dansyl (Cohen and Changeux, 1973; Waksman et al., 1980) and pyrene

(Barrantes et al., 1975), N-7(4-nitrobenzo-2-oxa-1,3-diazole) (Jürss et al., 1979) to the native ligand ACh and its analogs. However, the applicability of these fluorescent compounds was not well-suited for fluorescence studies, such as cPCF, because they either yielded fluorescent antagonists after fluorophore coupling or weak fluorescent agonists with moderate affinities (Waksman et al., 1980; Jurss et al., 1979). Also, some fluorescent agonists had a short fluorescent lifetime or an inappropriate emission wavelength (Fujimoto et al., 2008). In 2008, Fujimoto and colleagues reported the synthesis of a fluorescent derivative called Cy3-acylcholine, with Cy3 as the fluorophore showing significantly improved biophysical features. However, the yield of this synthesis was very low, about 0.06% (Wu et al., 2009). Also, Krieger and co-workers in 2008, reinvestigated pharmacological properties of previously synthesized fluorescent acylcholines, as well as, newly synthesized fluorescent acylcholine by them, were also investigated *on embryonic* nAChRs. The fluorescent acylcholine compounds either gave no or lower responses than unmodified ACh.

As an alternative, agonists other than ACh were chemically modified. In 2007, Grandl and colleagues synthesized five fluorescent analogs of the agonist epibatidine where it was either fluorescently tagged by coumarin dye, Atto dye or cyanine dye (EPB-Cou, EPB-Cl-Cou, EPB-Atto610, EPB-Cy3, and EPB-Cy5). In 2011, Schmauder and co-workers used epibatidine-Cy5 to study activation kinetics in muscle-type nAChRs at the single molecule level. However, use of epibatidine-Cy5 was avoided in this study because Grandl and colleagues (2007) have reported that the affinity of fluorescent derivatives of epibatidine for muscle-type nAChRs was decreased by three orders of magnitude in comparison to the untagged epibatidine. Apart from this, epibatidine has reverse site selectivity, i.e., unlike native ligand ACh, epibatidine binds more tightly to the αε binding site than to the αδ site (Prince & Sine, 1999; Dahan et. al, 2004).

For this reason, in the present study, it was intended to synthesize and test a newly synthesized fluorophore-coupled ACh (fACh) in cPCF experiments. The syntheses were realized in cooperation with the Plested lab (FMP Berlin), ChiroBlock GmbH (Wolfen, Germany) and Abcam (Cambridge, UK). At first, (through electrophysiology) several ACh-derivatives modified by different chain-like structures to serve in the next synthesis step as linkers between ACh and fluorophore (L-ACh) were tested. A PEG linker was found to be more appropriate in electrophysiological experiments than

alkyl linkers. A second interesting observation was the dependence of functional properties on the length of the linker. The longer the length of the linker, the lower was the current signal. A correlation of the pharmacological features and the length and structure of the linker was described before (Krieger et al., 2008).

In the next step, a non-sulfonated Cy3 was coupled to this ACh-linker derivative (L-ACh-68A). L-ACh-68A was used to optimize the synthesis strategy and to perform the first electrophysiological experiments. Coupling the dye improved the functional properties compared to derivatives just carrying the linker alone.

After having confirmed that the test compound L-ACh-68A is able to activate the channel, Cy3-ACh (fACh) was synthesized following the same strategy. Before applying newly synthesized fACh in cPCF experiments, the ability to activate muscle-type nAChRs was examined by patch-clamp experiments and was compared with ACh. Upon application of successive concentrations of fACh, increase in current amplitudes was monitored. When fACh was compared with untagged ACh, fACh was found to be similarly efficient as ACh. Additionally, fACh is twice as potent as ACh. Interestingly, similar results were also found by Grandl and co-workers in 2007 in case of epibatidine that was coupled by Cy5. Epibatidine-Cy5 was also found to be a full agonist as epibatidine but twice as potent as epibatidine at muscle nAChR (gain of function mutant of δS268K).

After confirmation that fACh is a suitable agonist at muscle-type nAChR, it was used in cPCF experiments. Herein, the usage of fACh for three different applications has been proposed:

Application 1: Monitoring agonist binding and unbinding

Using a fluorescently tagged ACh in combined fluorescence and electrophysiological recordings is a suitable tool to study agonist binding and unbinding while simultaneously monitoring the channel activity. Upon both washing in and washing off fACh, two components in the fluorescent signal was found. The fast components in both processes were too fast to be resolved under the technical conditions. However, the slow processes could be analyzed. A slow component of binding of 286 ± 81 ms and a slow component of unbinding of 1652 ± 323 ms was found.

It is speculated that the two components of the unbinding kinetics might reflect different affinities of the two binding sites, αδ and αε, as reported earlier on the basis of electrophysiological data (Arias, 2000; Unwin, 2005; Kalamida et al., 2007; Wonnacott and Barik, 2007) or time-resolved fluorescence spectroscopic data (Martinez et al., 2000). The fact that these two components cover around 50% each is supporting this idea. However, it cannot be ruled out that two different channel population exist, showing a fast and a slow unbinding behavior. Future experiments employing mutated receptors with only one functional binding sites or application of site-specific blockers to wildtype receptors could help gaining more insights into this problem.

Application 2: Relating agonist binding to desensitization

Because PCF allows for simultaneously measuring agonist binding and activation levels of the channel, fACh can be used to study desensitization-dependent agonist binding. Relating agonist binding and activation was not possible with the approach used herein because both activation and the first phase of binding were too fast to be resolved.

Like the fluorescence signal, the simultaneously recorded current trace was also reasonably fitted with a bi-exponential function. The slow phase of binding ($\tau_{binding,\ slow}$ = 286 ± 81 ms) and slow phase of desensitization ($\tau_{desensitization,\ slow}$ = 356 ± 26 ms) were found to be similar. The similarity in the time course of desensitization (slow component) and time course of binding (slow component) supports the idea reported earlier on the basis of patch-clamp experiments that the binding affinity increases during desensitization (Elenes et al., 2006).

Application 3: Relating unbinding to recovery from desensitization

Furthermore, fACh can be used to study recovery from desensitization. The time course of recovery ($\tau_{recovery}$ = 300 ms approx.) of muscle-type nAChRs was compared from ACh-mediated desensitization and the slow component of unbinding of fACh ($\tau_{unbinding,\ slow}$ = 1652 ± 323 ms). Recovery from desensitization is five times faster than agonist dissociation from one of the two binding sites. From this, it can be speculated that the remaining bound ligand is not involved in the recovery from desensitization

as the desensitization is already completed and a new activation process can be started.

In these experiments, untagged ACh was used in lieu of fACh for recovery experiments because of cost-effectiveness. The fact that fACh is twice as potent as ACh cannot be neglected when evaluating this application. For better comparison, future experiments using fACh instead of ACh to study the recovery time course would help to study this relationship even more thoroughly.

Although fACh is a suitable tool for relating ligand binding and channel gating in whole-cell configuration, a major limitation is its chemical instability in solution. Performing experiments immediately after dissolving fACh in the buffer may overcome this problem. The reason for the instability is the acetyl group which is prone to hydrolysis (Wonnacott and Barik, 2007). The carbamate group of carbachol is more stable (Wonnacott and Barik, 2007); hence, fluorescent derivatives of carbachol can be used in cPCF experiments to unravel functional aspects of nAChR gating. Additionally, a fluorescent derivative of carbachol might be useful for studying functions of muscarinic receptors because carbachol is a potent agonist to muscarinic ACh receptors as well (Wonnacott and Barik, 2007).

Despite various advantages of cPCF, the experimental demand for sampling rate higher than 10 kHz to resolve faster components of binding and unbinding of fACh limits its application. Although higher sampling rates can be achieved, resolution of the captured image will be compromised in this case. Photon counting is a potential alternative to this problem; however, this approach does not offer a strategy to subtract the signal of unbound ligands from the membrane-bound ligands. Although every method has some advantages and pitfalls, direct monitoring of agonist binding using cPCF allows for direct investigation of ion channel functions that are so far basically relying on electrophysiological data. It can provide new information to shed light on the complex nAChR gating behavior.

6. Conclusions

In the present study, the cPCF technique was used to investigate functional properties of muscle-type nAChR in real time. Electrophysiological properties of the agonists, i.e. nicotine and carbachol were compared with the properties of the native ligand ACh to find the most suitable ligand for synthesizing its fluorescent derivative. Surprisingly, concentration-activation curves for nicotine and carbachol in whole-cell configuration for muscle-type receptors was derived for the first time in the present study. In comparison to the previous data obtained from single-channel studies, lower EC_{50} values for all the three agonists were estimated in the present study. Additionally, it was also found that nicotine is a partial agonist but carbachol is a full agonist. Both agonists are moderately potent at this receptor.

ACh was found to be the most efficacious and potent agonist at this receptor in comparison to nicotine and carbachol. Therefore, ACh was selected for synthesizing its fluorescent derivative and named it ‘fACh’. By using fACh, cPCF experiments were performed for the first time in the whole-cell configuration in the present study to study muscle-type nAChRs functions.

As a result, it was found that both binding and unbinding of agonist to the receptor is a biphasic process which supports the previously proposed idea based on electrophysiological data that the two binding sites have different affinities. The time course of the increase in fluorescent signal due to binding was found to be similar to the slow phase of desensitization which was recorded simultaneously with fluorescence recordings. The observations corroborate the previous result that during desensitization, the affinity of the receptor for the ligand increases.

Hence, the feasibility of synthesis and employment of fluorescence agonists to shed light on the functionality of nAChRs and Cys-loop superfamily, without affecting the receptor by genetic or chemical fluorophore tagging has been successfully demonstrated in the present study. Apart from ACh, fluorescent derivatives of nicotine and carbachol can also be synthesized for fluorescence studies. Though nicotine and carbachol activate nAChRs competitively in a higher concentration range than ACh, both can be used for wash-out unbinding experiments.

References

Abraham, D. J. (2003). Burger's medicinal chemistry and drug discovery, *John Wiley & Sons, Inc.*, New Jersey.

Adams, P. R. & Sakmann, B. (1978). Decamethonium both opens and blocks endplate channels. *Proceedings of the National Academy of Sciences*,**75(6)**:2994-2998.

Adams, P. R. (1976). Drug blockade of open end-plate channels. *The Journal of Physiology*, **260**:531-552.

Akk, G. & Steinbach, J. H. (2003). Activation and block of mouse muscle-type nicotinic receptors by tetraethylammonium. *The Journal of Physiology*, **551(1)**:155-168.

Akk, G. & Auerbach, A. (1996). Inorganic, monovalent cations compete with agonists for the transmitter binding site of nicotinic acetylcholine receptors. *Biophysical Journal*, **70(6)**:2652-2658.

Akk, G. & Auerbach, A. (1999). Activation of muscle nicotinic acetylcholine receptor channels by nicotinic and muscarinic agonists. *British journal of pharmacology*,**128(7)**:1467-1476.

Akk, G. & Steinbach, J. H. (2005). Galantamine activates muscle-type nicotinic acetylcholine receptors without binding to the acetylcholine-binding site. *The Journal of Neuroscience*, **25(8)**:1992-2001.

Akk, G., Milescu, L. S., & Heckmann, M. (2005). Activation of heteroliganded mouse muscle nicotinic receptors. *The Journal of Physiology*, **564(2)**:359-376.

Albuquerque, E. X., Pereira, E. F., Alkondon, M., & Rogers, S. W. (2009). Mammalian nicotinic acetylcholine receptors: from structure to function. *Physiological reviews*, **89(1)**:73-120.

Arevalo, E., Chiara, D. C., Forman, S. A., Cohen, J. B., & Miller, K. W. (2005). Gating-enhanced Accessibility of Hydrophobic Sites within the Transmembrane Region of the Nicotinic Acetylcholine Receptor's δ-Subunit A TIME-RESOLVED PHOTOLABELING STUDY. *Journal of Biological Chemistry*, **280(14)**:13631-13640.

Arias, H. R. (1996). Luminal and non-luminal non-competitive inhibitor binding sites on the nicotinic acetylcholine receptor. *Molecular Membrane Biology*,**13(1)**:1-17.

Arias, H. R. (2000). Localization of agonist and competitive antagonist binding sites on nicotinic acetylcholine receptors. *Neurochemistry International*, **36(7)**:595-645.

Arias, H. R., Feuerbach, D., Targowska-Duda, K. M., & Jozwiak, K. (2010). Catharanthine alkaloids are noncompetitive antagonists of muscle-type nicotinic acetylcholine receptors. *Neurochemistry International*, **57(2)**:153-161.

Auerbach, A. (1993). A statistical analysis of acetylcholine receptor activation in Xenopus myocytes: stepwise versus concerted models of gating. *The Journal of Physiology*, **461**:339-78.

Auerbach, A. (2015). Activation of endplate nicotinic acetylcholine receptors by agonists. *Biochemical Pharmacology*, **97(4)**:601-608.

Baker, J. G., Hall, I. P., & Hill, S. J. (2003). Pharmacology and direct visualisation of BODIPY-TMR-CGP: a long-acting fluorescent β2-adrenoceptor agonist. *British journal of pharmacology*, **139(2)**: 232-242.

Baker, J. G., Middleton, R., Adams, L., May, L. T., Briddon, S. J., Kellam, B., & Hill, S. J. (2010). Influence of fluorophore and linker composition on the pharmacology of fluorescent adenosine A1 receptor ligands. *British Journal of Pharmacology*, **159(4)**:772-786.

Barlow, R. B., Bremner, J. B., & Soh, K. S. (1978). The effects of replacing ester by amide on the biological properties of compounds related to acetylcholine. *British Journal of Pharmacology*, **62(1)**:39-50.

Barrantes, F. J., Sakmann, B., Bonner, R., Eibl, H., & Jovin, T. M. (1975). 1-Pyrene-butyrylcholine: a fluorescent probe for the cholinergic system. *Proceedings of the National Academy of Sciences*, **72(8)**:3097-3101.

Beene, D. L., Brandt, G. S., Zhong, W., Zacharias, N. M., Lester, H. A., & Dougherty, D. A. (2002). Cation− π interactions in ligand recognition by serotonergic (5-HT3A) and nicotinic acetylcholine receptors: The anomalous binding properties of nicotine. *Biochemistry*, 41(32): 10262-10269.

Benowitz, N. L. & Gourlay, S. G. (1997). Cardiovascular toxicity of nicotine: implications for nicotine replacement therapy. *Journal of the American College of Cardiology*, **29(7)**:1422-1431.

Bhargava, Y., Nicke, A., & Rettinger, J. (2013). Validation of Alexa-647-ATP as a powerful tool to study P2X receptor ligand binding and desensitization*. Biochemical and Biophysical Research Communications*, **438(2)**:295-300.

Biskup, C., Kusch, J., Schulz, E., Nache, V., Schwede, F., Lehmann, F., Hagen, V., & Benndorf, K. (2007). Relating ligand binding to activation gating in CNGA2 channels. *Nature*, **446(7134)**:440-443.

Boyd, N. D. & Cohen, J. B. (1980). Kinetics of binding of [3H] acetylcholine to Torpedo postsynaptic membranes: association and dissociation rate constants by rapid mixing and ultrafiltration. *Biochemistry*. **19(23)**:5353-5358.

Brejc, K., van Dijk, W. J., Klaassen, R. V., Schuurmans, M., van der Oost, J., Smit, A. B., & Sixma, T. K. (2001). Crystal structure of an ACh-binding protein reveals the ligand-binding domain of nicotinic receptors. *Nature*, **411(6835)**:269-276.

Brownlow, S., Webster, R., Croxen, R., Brydson, M., Neville, B., Lin, J. P., Vincent, A., Newsom-Davis, J., & Beeson, D. (2001). Acetylcholine receptor δ subunit mutations underlie a fast-channel myasthenic syndrome and arthrogryposis multiplex congenita. *Journal of Clinical Investigation*, **108(1)**:125.

Cash, D. J. & Hess, G. P. (1980). Molecular mechanism of acetylcholine receptor-controlled ion translocation across cell membranes. *Proceedings of the National Academy of Sciences* **77(2)**: 842-846.

Celie, P. H., van Rossum-Fikkert, S. E., van Dijk, W. J., Brejc, K., Smit, A. B., & Sixma, T. K. (2004). Nicotine and carbamylcholine binding to nicotinic acetylcholine receptors as studied in AChBP crystal structures. *Neuron*, **41(6)**:907-914.

Changeux, J. P. (1990). The TiPS lecture the nicotinic acetylcholine receptor: an allosteric protein prototype of ligand-gated ion channels. *Trends in Pharmacological Sciences*, 11(12): 485-492.

Changeux, J. P. (2012). The nicotinic acetylcholine receptor: The founding father of the pentameric ligand-gated ion channel superfamily. *The Journal of Biological Chemistry*, **287(48)**:40207-40215.

Changeux, J. P. & Edelstein, S. J. (1998). Allosteric Receptors after 30 Years. *Neuron*, **21**:959-980.

Changeux, J. P. & Edelstein, **S. J.** (2001). Allosteric mechanisms in normal and pathological nicotinic acetylcholine receptors. *Current Opinion in Neurobiology*, **11(3)**:369-377.

Changeux, J. P., Galzi, J. L., Thiery, A. D., & Bertrand, D. (1992). The functional architecture of the acetylcholine nicotinic receptor explored by affinity labelling and site-directed mutagenesis. *Quarterly Reviews of Biophysics*, **25(4)**:395-432.

Cohen, J. B. & Changeux, J. P. (1973). Interaction of a fluorescent ligand with membrane-bound cholinergic receptor from Torpedo marmorata. *Biochemistry*, **12(24)**:4855-4864.

Colquhoun, D. & Ogden, D. C. (1988). Activation of ion channels in the frog end-plate by high concentrations of acetylcholine. *The Journal of Physiology*, **395**:131-159.

Connolly, J., Boulter, J., & Heinemann, S. F. (1992). α4-β2 and other nicotinic acetylcholine receptor subtypes as targets of psychoactive and addictive drugs. *British Journal of Pharmacology,* **105(3)**:657-666.

Cooper, J. C., Gutbrod, O., Witzemann, V., & Methfessel, C. (1996). Pharmacology of the nicotinic acetylcholine receptor from fetal rat muscle expressed in Xenopus oocytes. *European Journal of Pharmacology*, **309(3)**:287-298.

Dahan, D. S. Dibas, M. I, Petersson, E. J., Auyeung, V. C., Chanda, B., & Bezanilla, F. (2004). A fluorophore attached to nicotinic acetylcholine receptor M2 detects productive binding of agonist to the αδ site. *Proceedings of the National Academy of Sciences*, **101(27)**:10195-10200.

Dale, H. H. (1914). The action of certain esters and ethers of choline, and their relation to muscarine. *The Journal of Pharmacology and Experimental Therapeutics*, **6(2)**:147-190.

Dilger, J. P. & Brett, R. S. (1990). Direct measurement of the concentration-and time-dependent open probability of the nicotinic acetylcholine receptor channel. *Biophysical Journal*, **57(4)**:723-731.

Dilger, J. P. & Liu, Y. (1992). Desensitization of acetylcholine receptors in BC3H-1 cells. *Pflügers Archiv European Journal of Physiology*, **420(5)**:479-485.

Edelstein, S. J., Schaad, O., Henry, E., Bertrand, D., & Changeux, J. P. (1996). A kinetic mechanism for nicotinic acetylcholine receptors based on multiple allosteric transitions. *Biological cybernetics*, **75(5)**: 361-379.

Elenes, S. & Auerbach, A. (2002). Desensitization of diliganded mouse muscle nicotinic acetylcholine receptor channels. *The Journal of Physiology*, **541(2)**:367-383.

Elenes, S., Ni, Y., Cymes, G. D., & Grosman, C. (2006). Desensitization Contributes to the Synaptic Response of Gain-of-Function Mutants of the Muscle Nicotinic Receptor. *The Journal of General Physiology*, **128(5)**:615–627.

Engel, A. G., Lambert, E. H., Mulder, D. M., Torres, C. F., Sahashi, K., Bertorini, T. E., & Whitaker, J. N. (1982). A newly recognized congenital myasthenic syndrome attributed to a prolonged open time of the acetylcholine-induced ion channel. *Annals of Neurology*, **11(6):** 553-569.

Engel, A. G., Ohno, K., Milon, M., Wang, H. L., Nakano, S., Bouzat, C., Pruitt, J. N. II., Hutchinson, D. O., Brengman, J. M., Bren, N., Sieb, J. P., & Sine, S. M. (1996). New mutations in acetylcholine receptor subunit genes reveal heterogeneity in the slow-channel congential myasthenic syndrome. *Human Molecular Genetics*, **5(9):**1217-1227.

Feltz, A. & Trautmann, A. (1980). Interaction between nerve-related acetylcholine and bath applied agonists at the frog end-plate. *The Journal of Physiology*, **299(1)**:533-552.

Feltz, A. & Trautmann, A. (1982). Desensitization at the frog neuromuscular junction: a biphasic process. *The Journal of Physiology*, **322(1)**:257-272.

Fenster, C. P., Rains, M. F., Noerager, B., Quick, M. W., & Lester, R. A. (1997). Influence of subunit composition on desensitization of neuronal acetylcholine receptors at low concentrations of nicotine. *Journal of Neuroscience*, **17(15)**:5747-5759.

Francis, M. M. & Papke, R. L. (1996). Muscle -type nicotinic acetylcholine receptor delta subunit determines sensitivity to noncompetitive inhibitors, while gamma subunit regulates divalent Permeability. *Neuropharmacology*, **35(11)**:1547-1556.

Fujimoto, K., Yoshimura, Y., Ihara, M., Matsuda, K., Takeuchi, Y., Aoki, T., & Ide, T. (2008). Cy3-3-acylcholine: a fluorescent analogue of acetylcholine for single molecule detection. *Bioorganic & Medicinal Chemistry Letters*, **18(3)**:1106-1109.

Galzi, J. L. & Changeux, J. P. (1994). Neurotransmitter-gated ion channels as unconventional allosteric proteins. *Current Opinion in Structural Biology*, **4(4)**:554-565.

Giniatullin, R., Nistri, A., & Yakel, J. L. (2005). Desensitization of nicotinic ACh receptors: shaping cholinergic signaling. *Trends in Neurosciences*. **28(7)**:371-378.

Giraudat, J., Devillers-Thiery, A., Auffray, C., Rougeon, F., & Changeux, J. P. (1982). Identification of a cDNA clone coding for the acetylcholine binding subunit of *Torpedo marmorata* acetylcholine receptor. *The EMBO Journal*,**1(6)**:713-717.

Gotti, C. & Clementi, F. (2004). Neuronal nicotinic receptors: from structure to pathology. *Progress in Neurobiology*, **74(6)**:363-396.

Graham, F. L. & van der Eb, A. J. (1973). A new technique for the assay of infectivity of human adenovirus 5 DNA. *Virology*, 52(2):456-467.

Grandl, J., Sakr, E., Kotzyba-Hibert, F., Krieger, F., Bertrand, S., Bertrand, D., Vogel, H., Goeldner,M., & Hovius, R. (2007). Fluorescent Epibatidine Agonists for Neuronal and Muscle-Type Nicotinic Acetylcholine Receptors. *Angewandte Chemie*, **119(19)**:3575-3578.

Grassi, F., Palma, E., Mileo, A. M., & Eusebi, F. (1995). The desensitization of the embryonic mouse muscle acetylcholine receptor depends on the cellular environment. *Pflügers Archiv European Journal of Physiology* **430(5)**:787-794.

Grosman, C. & Auerbach, A. (2001). The dissociation of acetylcholine from open nicotinic receptor channels. *Proceedings of the National Academy of Sciences*, **98(24)**:14102-14107.

Gross, A., Ballivet, M., Rungger, D., & Bertrand, D. (1991). Neuronal nicotinic acetylcholine receptors expressed in Xenopus oocytes: role of the α subunit in agonist sensitivity and desensitization. *Pflügers Archiv European Journal of Physiology*, **419(5)**:545-551.

Grossman, C. & Auerbach, A. (2000). Asymmetric and independent contribution of the second transmembrane segment 12' residues to diliganded gating of acetylcholine receptor channels: a single-channel study with choline as the agonist. *The Journal of General Physiology*,**115(5)**: 637-651.

Gündisch, D. & Eibl, C. (2012). Nicotinic acetylcholine receptor ligands; a patent review (2006-2011) *Expert Opinion on Therapeutic Patents*, **21(12)**:1867-1896.

Gupta, S., Chakraborty, S., Vij, R., & Auerbach, A. (2016). A mechanism for acetylcholine receptor gating based on structure, coupling, phi, and flip. *The Journal of General Physiology*, **149(1)**:85-103.

Hatton, C. J., Shelley, C., Brydson, M., Beeson, D., & Colquhoun, D. (2003). Properties of the human muscle nicotinic receptor, and of the slow-channel myasthenic syndrome mutant εL221F, inferred from maximum likelihood fits. *The Journal of Physiology*, **547(3)**:729-760.

Heidmann, T. & Changeux, J. P. (1980). Interaction of a fluorescent agonist with the membrane-bound acetylcholine receptor from Torpedomarmorata in the millisecond time range: Resolution of an "intermediate" conformational transition and evidence for positive cooperative effects. *Biochemical and Biophysical Research Communications*, **97(3)**:889-896.

Heidmann, T., Bernhardt, J., Neumann, E., Changeux, J. P. (1983). Rapid kinetics of agonist binding and permeability response analyzed in parallel on acetylcholine receptor rich membranes. *Biochemistry*, **22(23)**:5452-5459.

Hess, G. P. (1993). Determination of the chemical mechanism of neurotransmitter receptor-mediated reactions by rapid chemical kinetic techniques. *Biochemistry*, **32(4)**:989-1000.

Jackson, M. B. (1989). Perfection of a synaptic receptor: kinetics and energetics of the acetylcholine receptor. *Proceedings of the National Academy of Sciences*, **86(7)**:2199-203.

Jadey, S., Purohit, P., & Auerbach, A. (2013). Action of nicotine and analogs on acetylcholine receptors having mutations of transmitter-binding site residue αG153. *The Journal of General Physiology*, **141(1)**:95-104.

Jahn, K., Mohammadi, B., Krampfl, K., Abicht, A., Lochmüller, H., & Bufler, J. (2001). Deactivation and desensitization of mouse embryonic-and adult-type nicotinic receptor channel currents. *Neuroscience Letters*, **307(2)**:89-92.

Jha, A. & Auerbach, A. (2010). Acetylcholine receptor channels activated by a single agonist molecule. *Biophysical Journal*, **98(9)**:1840-1846.

Jonsson, M, Dabrowski, M., Eriksson, L. (2009). Pharmacological characteristics of the inhibiton of nondepolarizing neuromuscular blocking agents at human adult muscle nicotinic acetylcholine receptor. *Anesthesiology*,**110(6)**:1244-1252.

Jonsson, M., Dabrowski, M., Gurley, D. A., Larsson, O., Johnson, E. C., Fredholm, B. B., Eriksson, L. I. (2006). Activation and inhibition of human muscular and neuronal nicotinic acetylcholine receptors by succinylcholine. *Anesthesiology*, **104**:724-733.

Jürss, R., Prinz, H., & Maelicke, A. (1979). NBD-5-acylcholine: fluorescent analog of acetylcholine and agonist at the neuromuscular junction. *Proceedings of the National Academy of Sciences*, **76(3)**:1064-1068.

Kachel, H. S., Patel, R. N., Franzyk, H., & Mellor, I. R. (2016). Block of nicotinic acetylcholine receptors by philanthotoxins is strongly dependent on their subunit composition. *Scientific reports*, **6**:38116.

Kalamida, D., Poulas, K., Avramopoulou, V., Fostieri, E., Lagoumintzis, G., Lazaridis, K., Sideri, A., Zouridakis, M., & Tzartos, S. J. (2007). Muscle and neuronal nicotinic acetylcholine receptors: Structure, function and pathogenicity. *FEBS Journal*, **274(15):**3799–3845.

Karlin, A. & Akabas, Y. H. (1995). Toward a structural basis for the function of nicotinic acetylcholine receptors and their cousins. *Neuron*, **15**:1231-1244.

Karlin, A. (2002). Emerging structure of the nicotinic acetylcholine receptors. *Nature Reviews Neuroscience*, **3(2)**:102-114.

Katz, B. & Thesleff, S. (1957). A study of the 'desensitization' produced by acetylcholine at the motor end-plate. *The Journal of Physiology*, **I38(1)**: 63-80.

Kistler, J., Stroud, R. M., Klymkowsky, M. W., Lalancette, R., & Fairclough, R. H. (1982). Structure and function of an acetylcholine receptor. *Biophysical Journal*, **37(1)**:371-383.

Korngreen A. (2016). Advanced Patch-Clamp Analysis for Neuroscientists*. Human Press (Springer)*.

Krauss, M., Korr, D., Herrmann, A., & Hucho, F. (2000). Binding properties of agonists and antagonists to distinct allosteric states of the nicotinic acetylcholine receptor are incompatible with a concerted model. *Journal of Biological Chemistry*, **275(39)**,30196-30201.

Krieger, F., Mourot, A., Araoz, R., Kotzyba-Hibert, F., Molgó, J., Bamberg, E., & Goeldner, M. (2008). Fluorescent agonists for the Torpedo nicotinic acetylcholine receptor. *ChemBioChem*, **9(7)**:146-1153.

Kudryavtsev, D., Shelukhina, I., Vulfius, C., Makarieva, T., Stonik, V., Zhmak, M., Ivanov, I., Kasheverov, I., Utkin, Y., & Tsetlin, V. (2015). Natural compounds interacting with nicotinic acetylcholine receptors: from low-molecular weight ones to peptides and proteins *Toxins*, **7(5)**:1683-1701.

Kusch, J., Biskup, C., Thon, S., Schulz, E., Nache, V., Zimmer, T., Schwede, F. & Benndorf, K. (2010). Interdependence of receptor activation and ligand binding in HCN2 pacemaker channels. *Neuron*, **67(1)**:75-85.

Kusch, J., Thon, S., Schulz, E., Biskup, C., Nache, V., Zimmer, T., Seifert, R., Schwede, F. & Benndorf, K. (2012). How subunits cooperate in cAMP-induced activation of homotetrameric HCN2 channels. *Nature Chemical Biology*, **8(2)**:162-169.

Lape, R., Colquhoun, D., & Sivilotti, L. G. (2008). On the nature of partial agonism in the nicotinic receptor superfamily. *Nature*, **454(7205)**: 722-727.

Lape, R., Krashia, P., Colquhoun, D., & Sivilotti, L. G. (2009). Agonist and blocking actions of choline and tetramethylammonium on human muscle acetylcholine receptors. *The Journal of Physiology*, **587(21)**:5045-5072.

Leisle, L., Chadda, R., Lueck, J. D., Infield, D. T., Galpin, J. D., Krishnamani, V., Robertson, J. L., & Ahern, C. A. (2016). Cellular encoding of Cy dyes for single-molecule imaging. *Elife*, **5**:1-20.

Lester, Robin A. J. (2014) Nicotinic Receptors, *Springer*, New York.

Lewis, T. M., Harkness, P. C., Sivilotti, L. G., Colquhoun, D., & Millar, N. S. (1997). The ion channel properties of a rat recombinant neuronal nicotinic receptor are dependent on the host cell type. *The Journal of Physiology*, **505(2)**:299-306.

Lindstrom, J. (1997). Nicotinic acetylcholine receptors in health and disease. *Molecular Neurobiology*, **15(2)**:193-222.

Lindstrom, J., Merlie, J., & Yogeeswaran, G. (1979). Biochemical properties of acetylcholine receptor subunits from *Torpedo californica*. *Biochemistry*, **18(21)**:4465-4469.

Liu, Y. U. & Brehm, P. (1993). Expression of subunit-omitted mouse nicotinic acetylcholine receptors in Xenopus laevis oocytes. *The Journal of Physiology*, **470(1)**: 349-363.

Lukas, R. J., Changeux, J. P., Novère, N. L., Albuquerque, E. X., Balfour, D. J. K., Berg, D. K., Bertrand, D., Chiappinelli, V. A., Clarke, P. B. S., Collins, A. C., Dani, J. A., Grady, S. R., Kellar, K. J., Lindstrom, J. M., Marks, M. J., Quik, M., Taylor, P. W. & Wonnacott, S. (1999). Current status of the nomenclature for nicotinic acetylcholine receptors and their subunits. *Pharmacological Reviews*, **51(2)**:397-401.

Lukas, R. J., Ke, L., Bencherif, M., & Eisenhour, C. M. (1996). Regulation by nicotine of its own receptors. *Drug development research*, **38**:136-148.

Lustig, L. R. (2006). Nicotinic acetylcholine receptor structure and function in the efferent auditory system. *The Anatomical Record. Part A, Discoveries in Molecular, Cellular, and Evolutionary Biology,* **288A(4)**:424–434.

Maconochie, D. J. & Steinbach, J. H. (1995). Block by acetylcholine of mouse muscle nicotinic receptors stably expressed in fibroblasts. *The Journal of General Physiology*, **106(1)**: 113-147.

Magleby, K. L. & Pallotta, B. S. (1981). A study of desensitization of acetylcholine receptors using nerve-released transmitter in the frog. *The Journal of Physiology*, **316**:225-50.

Mallavadhani, U. V., Sahoo, L., Kumar, K. P., & Murty, U. S. (2014). Synthesis and antimicrobial screening of some novel chalcones and flavanones substituted with higher alkyl chains. *Medicinal Chemistry Research*, **23(6)**:2900-2908.

Marshall C. G., Ogden, D. & Colquhoun, D. (1991). Activation of ion channels in the frog endplate by several analogues of acetylcholine. *The Journal of Physiology*, **433**:73-93.

Martinez, K. L., Corringer, P. J., Edelstein, S. J., Changeux, J. P., & Mérola, F. (2000). Structural differences in the two agonist binding sites of the Torpedo nicotinic acetylcholine receptor revealed by time-resolved fluorescence spectroscopy. *Biochemistry*, **39(23)**:6979-6990.

Middleton, R. J. & Kellam, B. (2005). Fluorophore-tagged GPCR ligands. *Current Opinion in Chemical Biology*, **9(5)**:517-525.

Middleton, R. J., Briddon, S. J., Cordeaux, Y., Yates, A. S., Dale, C. L., George, M. W., Baker, J. G., Hill, S. J., & Kellam, B. (2007). New fluorescent adenosine A1-receptor agonists that allow quantification of ligand-receptor interactions in microdomains of single living cells. *Journal of medicinal chemistry*, **50(4)**:782-793.

Millar, N. S. (2009). A review of experimental techniques used for the heterologous expression of nicotinic acetylcholine receptors. *Biochemical Pharmacology*, **78(7)**:766-776.

Mishra, A., Chaturvedi, P., Datta, S., Sinukumar, S., Joshi, P., & Garg, A. (2015). Harmful effects of nicotine. *Indian Journal of Medical and Paediatric Oncology: Official Journal of Indian Society of Medical & Paediatric Oncology*, **36(1)**:24.

Miyazawa, A., Fujiyoshi, M., & Unwin, N. (2003). Structure and gating mechanism of the acetylcholine receptor pore. *Nature*, **423(6943)**:949-955.

Miyazawa, A., Fujiyoshi, Y., Stowell, M., & Unwin, N. (1999). Nicotinic acetylcholine receptor at 4.6 angstrom resolution: Transverse tunnels in the channel wall. *Journal of Molecular Biology*, **288(4)**:765-786.

Molnar, C. & Gair, J. (2015). Concepts of Biology-1st Canaian edition.

Neher, E. & Steinbach, J. H. (1978). Local anaesthetics transiently block currents through single acetylcholine-receptor channels. *The Journal of Physiology*, **277**:153-176.

Neubig, R. R. & Cohen J. B. (1980). Permeability control by cholinergic receptors in Torpedo postsynaptic membranes: agonist dose-response relations measured at second and millisecond times. *Biochemistry*,**19(12)**:2770-2779.

Neubig, R. R., Boyd, N. D., & Cohen, J. B. (1982). Conformations of Torpedo acetylcholine receptor associated with ion transport and desensitization. *Biochemistry*, **21(14)**:3460-3467.

Nguyen, V. T., Ndoye, A., & Grando S. A. (2000). Novel human α9 acetylcholine receptor regulating keratinocyte adhesion is targeted by pemphigus vulgaris autoimmunity. *American Journal of Pathology*, **157(4)**:1377-1391.

Nowak, M. W., Kearney, P. C., Sampson, J. R., Saks, M. E., Labarca, C. G., Silverman, S. K., Zhong, W., Thorson, J., Abelson, J. N., Davidson, N., Schultz, P. G., Dougherty, D. A. (1995). Nicotinic receptor binding site probed with unnatural amino acid incorporation in intact cells. *Science-New York Then Washington*, **268(5209)**:439-439.

Ogden, D. C. & Colquhoun, D. (1985). Ion channel block by acetylcholine, carbachol and suberyldicholine at the frog neuromuscular junction. *Proceedings of the Royal Society of London*, **225(1240)**:329-55.

Oosterhuis, H. J., Newsom-Davis, J., Wokke, J. H., Molenaar, P. C., Weerden, T. V., Oen, B. S., Jennekens, F. G., Veldman, H., Vincent, A., & Wray, D. W. (1987). The slow channel syndrome: two new cases*. Brain*, **110(4):**1061-1079.

Papke, R. L. (2014). Merging old and new perspectives on nicotinic acetylcholine receptors *Biochemical Pharmacology*,**89(1)**:1-11.

Papke, R. L., Wecker, L., & Stitzel, J. A. (2010). Activation and inhibition of mouse muscle and neuronal nicotinic acetylcholine receptors expressed in Xenopus oocytes. *The Journal of Pharmacology and Experimental Therapeutics*, **333(2)**:501-518.

Paradiso, K. & Brehm, P. (1998). Long-term desensitization of nicotinic acetylcholine receptors is regulated via protein kinase A-mediated phosphorylation. *Journal of Neuroscience*, **18(22)**:9227-9237.

Paradiso, K. G. & Steinbach, J. H. (2003). Nicotine is highly effective at producing desensitization of rat α4β2 neuronal nicotinic receptors. *The Journal of Physiology*, **553(3)**: 857-871.

Paul, M., Kindler, C. H., Fokt, R. M., Dresser, M. J., Dipp, N. C. J. & Spencer, Y. C. The potency of new muscle relaxants on recombinant muscle-type acetylcholine receptors. (2002) *Anesthesia & Analgesia*, **94(3)**:597-603.

Peng, H., Ferris, R. L., Matthews, T., Hiel, H., Albaitero, A. L., Lustig, L. R. (2004). Characterization of the human nicotinic acetylcholine receptor subunit alpha (α) 9 (CHRNA9) and alpha (α) 10 (CHRNA10) in lymphocytes. *Life Sciences*, **76(3)**:263-280.

Perutz, M. F. (1989). Mechanisms of cooperativity and allosteric regulation in proteins. *Quarterly reviews of biophysics*, **22(2)**:139-237.

Prescott, M., Nowakowski, S., Nagley, P., & Devenish, R. J. (1999). The length of polypeptide linker affects the stability of green fluorescent protein fusion proteins. *Analytical Biochemistry*, **273(2)**:305-307.

Prince, R. J. & Sine, S. M. (1999). Acetylcholine and epibatidine binding to muscle acetylcholine receptors distinguish between concerted and uncoupled models. *Journal of Biological Chemistry*, 274(28):19623-19629.

Prince, R. J., Pennington, R. A., & Sine, S. M. (2002). Mechanism of tacrine block at adult human muscle nicotinic acetylcholine receptors. *The Journal of General Physiology*, **120(3)**:369-393.

Purohit, P., Mitra, A., & Auerbach, A. (2007). A stepwise mechanism for acetylcholine receptor channel gating. *Nature*, **446(7138)**:930-933.

Purohit, Y. & Grosman, C. (2006). Block of muscle nicotinic receptors by choline suggests that the activation and desensitization gates act as distinct molecular entities. *The Journal of General Physiology*,**127(6)**:703-717.

Raftery, M. A., Hunkapiller, M. W., Strader, C. B., & Hood, L. E. (1980). Acetylcholine receptor: complex of homologous subunits. *Science*, **208(4451)**:1454-1457.

Reitstetter, R., Lukas, R. J., & Gruener, R. (1999). Dependence of nicotinic acetylcholine receptor recovery from desensitization on the duration of agonist

exposure. *The Journal of Pharmacology and Experimental Therapeutics*, **289(2)**:656-660.

Reynolds, J. & Karlin, A. (1978). Molecular weight in detergent solution of acetylcholine receptor from *Torpedo californica*. *Biochemistry*, **17(11)**:2035-2038.

Rose, J. E., Behm, F. M., Westman, E. C., & Coleman, R. E. (1999). Arterial nicotine kinetics during cigarette smoking and intravenous nicotine administration: implications for addiction. *Drug and Alcohol Dependence*, **56(2)**:99-107.

Rose, R. H., Briddon, S. J., & Hill, S. J. (2012). A novel fluorescent histamine H1 receptor antagonist demonstrates the advantage of using fluorescence correlation spectroscopy to study the binding of lipophilic ligands. *British Journal of Pharmacology*, **165(6)**:1789-1800.

Ruff, R. L. (1976). Local anaesthetic alteration of miniature endplate currents and endplate current fluctuations. *Biophysical Journal*, **16(5)**: 433-439.

Saitoh, T., Oswald, R., Wennogle, L., & Changeux, J. P. (1980). Conditions for the selective labelling of the 66 000 dalton chain of the acetylcholine receptor by the covalent non-competitive blocker 5-azido-[3H] trimethisoquin. *FEBS Letter*,**116(1)**:30-36.

Sakmann, B., Patlak, J., & Neher, E. (1980). Single acetylcholine-activated channels show burst-kinetics in presence of desensitizing concentrations of agonist. *Nature*, **286(5768)**:71-73.

Salamone, F. N., Zhou, M., & Auerbach, A. (1999). A re-examination of adult mouse nicotinic acetylcholine receptor channel activation kinetics. *The Journal of Physiology*, **516(2)**:315-330.

Schindelin, J., Arganda-Carreras, I., Frise, E., Kaynig, V., Longair, M., Pietzsch, T., Preibisch, S., Rueden, C., Saalfeld, S., Schmid, B., Tinevez, J. Y., White, D. J., Hartenstein, V., Eliceiri, K., Tomancak, P., & Cardona, A. (2012). Fiji: an open-source platform for biological-image analysis. *Nature Methods*, **9(7)**:676-682.

Schmauder, R., Kosanic, D., Hovius, R., & Vogel, H. (2011). Correlated Optical and Electrical Single-Molecule Measurements Reveal Conformational Diffusion from Ligand Binding to Channel Gating in the Nicotinic Acetylcholine Receptor. *ChemBioChem*, **12(16)**: 2431-2434.

Schmidt, A., Lenzig, P., Oslender-Bujotzek, A., Kusch, J., Lucas, S. D., Gründer, S., & Wiemuth, D. (2014). The bile acid-sensitive ion channel (BASIC) is activated by alterations of its membrane environment. *PloS One*, **9(10)**:e111549.

Shi, W., Ogbomo, S. M., Wagh, N. K., Zhou, Z., Jia, Y., Brusnahan, S. K., & Garrison, J. C. (2014). The influence of linker length on the properties of cathepsin S cleavable 177 Lu-labeled HPMA copolymers for pancreatic cancer imaging. *Biomaterials*, **35(22)**:5760-5770.

Sine, S. M. & Steinbach, J. H. (1984). Agonists block currents through acetylcholine receptor channels. *Biophysical Journal*, **46(2)**: 277-283.

Sine, S. M. & Taylor, P. (1980). The relationship between agonist occupation and the permeability response of the cholinergic receptor revealed by bound cobra α-toxin. *The Journal of Biological Chemistry*, **255(21)**:10144-10156.

Sivilotti, L. G., McNeil, D. K., Lewis, T. M., Nassar, M. A., Schoepfer, R., & Colquhoun, D. (1997). Recombinant nicotinic receptors, expressed in Xenopus oocytes, do not resemble native rat sympathetic ganglion receptors in single-channel behaviour. *The Journal of Physiology*, **500(1)**:123-138.

Slater, C. R. (2017). The structure of human neuromuscular junctions: some unanswered molecular questions. *International Journal of Molecular Sciences*,**18(10):** 2183.

Strange, P. G. (2008). Agonist binding, agonist affinity and agonist efficacy at G protein-coupled receptors. *British journal of pharmacology*, **153(7)**:1353-1363.

Stroud, M. R. & Moore, F. J. (1985). Acetylcholine receptor structure, function and evolution. *Annual Review of Cell Biology*,**1**:317-351.

Unwin, N. (1995). Acetylcholine receptor channel imaged in the open state. *Nature*, **373(6509)**: 37-43.

Unwin, N. (2003). Structure and action of the nicotinic acetylcholine receptor explored by electron microscopy. *FEBS Letters*, **555(1)**:91-95.

Unwin, N. (2005). Refined structure of the nicotinic acetylcholine receptor at 4 a˚ resolution. *Journal of Molecular Biology*, **346(4)**: 967-989.

Unwin, N. (2013). Nicotinic acetylcholine receptor and the structural basis of neuromuscular transmission: insights from Torpedo postsynaptic membranes. *Quarterly Reviews of Biophysics*, **46(4)**:283-322.

Waksman, G., Changeux, J. P., & Roques, B. P. (1980). Structural requirements for agonist and noncompetitive blocking action of acylcholine derivatives on Electrophorus electricus electroplaque. *Molecular pharmacology*, **18(1)**:20-27.

Wang, H. & Sun, X. (2005). Desensitized nicotinic receptors in brain. *Brain Research Reviews* **48 (3)**:420-437.

Wells, G. B. (2008). Structural answers and persistent questions about how nicotinic receptors work. *Frontiers in bioscience: a journal and virtual library*, **13**:5479.

Williams, D. K., Stokes, C., Horenstein, N. A., & Papke, R. L. (2011). The effective opening of nicotinic acetylcholine receptors with single agonist binding sites. *The Journal of General Physiology*, **137(4)**: 369-384.

Wonnacott, S. & Barik, J. (2007). Nicotinic ACh receptors. *Tocris Bioscience Scientific Reviews*, **28**:1-20.

Wu, G., Raines, D. E., & Miller, K. W. (1994). A hydrophobic inhibitor of the nicotinic acetylcholine receptor acts on the resting state. *Biochemistry*, **33(51)**:15375-15381.

Wu, H., Kaur, G., & Griffiths, G. L. (2009). An improved synthesis of a fluorescent gabapentin–choline conjugate for single molecule detection. *Tetrahedron Letters*, **50(18)**:2100-2102.

Wu, J. & Lukas, R. J. (2011). Naturally-expressed nicotinic acetylcholine receptor subtypes *Biochemical Pharmacology*, **82(8)**:800-807.

Xiu, X., Puskar, N. L., Shanata, J. A., Lester, H. A., & Dougherty, D. A. (2009). Nicotine binding to brain receptors requires a strong cation–π interaction. *Nature*, **458(7237)**:534-537.

Yamodo, H. I., David, C. C., Cohen, J. B., & Miller, K. W. (2010). Conformational Changes in the Nicotinic Acetylcholine Receptor During Gating and Desensitization. *Biochemistry*, **49(1)** 646-656.

Yost, C. S. & Winegar, B. D. (1997). Potency of agonists and competitive antagonists on adult-and fetal-type nicotinic acetylcholine receptors. *Cellular and Molecular Neurobiology*, **17(1)**:35-50.

Yu, K. D., Liu, Q., Wu, J., & Lukas, R. J. (2009). Kinetics of desensitization and recovery from desensitization for human α4β2-nicotinic acetylcholine receptors stably expressed in SH-EP1 cell. *Acta Pharmacologica Sinica*, **30(6)**: 805-817.

Zheng, J. & Zagotta, W. N. (2000). Gating rearrangements in cyclic nucleotide-gated channels revealed by patch-clamp fluorometry. *Neuron*, **28(2)**:369-374.

Zhou M., Engel A., & Auerbach A. (1999). Serum choline activates mutant acetylcholine receptors that cause slow channel congenital myasthenic syndromes. *Proceedings of the National Academy of Sciences*, **96(18)**:10466-10471.

Zouridakis, M., Zisimopoulou, P., Poulas, K., & Tzartos, S.J. (2009). Recent advances in understanding the structure of nicotinic acetylcholine receptors. *IUBMB life*, **61(4)**,407-423.

Declaration

I hereby declare that:

1. I am aware of the current course of examination for doctoral studies of the Faculty of Medicine at Friedrich Schiller University of Jena, Germany.
2. I have researched and written the presented thesis myself, no passages of text have been taken from third parties or own exam papers without having been identified. All tools, personal notifications, and sources used by me have been indicated in the thesis.
3. My doctoral supervisor, Prof. Dr. Klaus Benndorf and Dr. Jana Kusch has supported me in selecting and analyzing the material.
4. The assistance of any doctoral consultant has not been utilized and no third parties have either directly or indirectly received monetary benefits from the presented work or from related contents of the submitted thesis.
5. I have not submitted the thesis as an examination paper for state or other academic examinations.
6. I have not submitted the same, largely similar or any different treatises to another university as dissertation.

Jena, ----------

(Abhilasha Ladha)

[German translation]

Ehrenwörtliche Erklärung

Ich erkläre hiermit, dass:

1. mir die geltende Promotionsordnung der Medizinischen Fakultät der Friedrich-Schiller-Universität Jena, Deutschland bekannt ist.
2. ich die vorliegende Arbeit selbst angefertigt habe, keine Textabschnitte von Dritten oder eigene Prüfungsarbeiten übernommen habe ohne diese zu kennzeichnen. Alle von mir verwendeten Hilfsmittel, persönlichen Mitteilungen und Quellen wurden in der Arbeit angegeben.
3. mein Betreuer Herr Prof. Dr. Klaus Benndorf und Dr. Jana Kusch mich bei der Auswahl und Analyse des Materials.
4. die Hilfe eines Promotionsberaters nicht in Anspruch genommen wurde und dass Dritte weder unmittelbar noch mittelbar geldwerte Leistungen von mir für Arbeiten erhalten haben, die im Zusammenhang mit dem Inhalt der vorgelegten Dissertation stehen.
5. ich die Dissertation noch nicht als Prüfungsarbeit für eine staatliche oder andere akademische Prüfung eingereicht habe.
6. ich die gleiche, eine in wesentlichen Teilen ähnliche oder eine andere Abhandlung bei einer anderen Hochschule als Dissertation nicht vorgelegt habe.

Jena, ----------

(Abhilasha Ladha)

Acknowledgements

It is my pleasure to acknowledge the role of several individuals who were instrumental in the completion of my Ph.D. research.

Firstly, I would like to express my sincere gratitude to my advisor Prof. Dr. Klaus Benndorf for the continuous support of my Ph.D. study and related research, for his patience and motivation. His guidance helped me in all the time of research and writing of this thesis.

I would like to express my special appreciation and thanks to my supervisor Dr. Jana Kusch. I appreciate all her contributions of time, ideas, and funding to make my Ph.D. journey productive and stimulating. The joy and enthusiasm she has for her research were contagious and motivational for me, even during tough times in the Ph.D. pursuit. Her advice on both research as well as on my career have been invaluable. I want to thank her wholeheartedly for encouraging my research and for allowing me to grow as a research scientist.

I would also like to acknowledge valuable inputs of Dr. Ralf Schmauder and Dr. Vasilica Nache who contributed to many helpful discussions. My sincere thanks also go to Prof. Dr. Thomas Zimmer for providing continuous support related to molecular biology. Many thanks to Karin Schoknecht and Sandra Bernhardt for lab assistance.

A handful of thanks goes to my lab fellows. It was a magnificent pleasure working with them. I am especially grateful to Dominik Lenz and Maik Otte for being my ‘German translators’.

A special thanks to my family: my parents, my in-laws, and to my brothers and sisters for supporting me spiritually throughout writing this thesis and my life in general.

These acknowledgments would not complete without mentioning the backbone of my life- Navin, my husband for not only his incredible love, patience, and understanding during my Ph.D. journey but also for providing me scientific inputs whenever needed during my thesis writing.

Last but not least, I want to thank ‘Almighty God’ for making this journey successful.

-Abhilasha Ladha

Curriculum Vitae and Publication List

Personal Details

Name, Nationality:	Abhilasha Ladha, Indian
Family status:	Married
Date of birth, Place:	17.06.1986, Varanasi, India
Email:	abhineuro@yahoo.com

Education and Research experience

From 03/2018:	Postdoctoral researcher at Institute of Physiology, Aachen, Germany
07/2013-12/2017:	Doctoral student at Institute of Physiology II, Jena, Germany (Supervisor: Prof. Dr. Klaus Benndorf and Dr. Jana Kusch)
01/2013 – 06/2013:	Scientific co-worker at Forschungszentrum Jülich, Jülich, Germany
9/2011 – 10/2012:	Research Assistant, School of Studies in Neuroscience, Jiwaji University, Gwalior, India
07/2009 – 08/2011:	M.Sc. Neuroscience, School of Studies in Neuroscience, Jiwaji University, Gwalior, India
07/2006 – 06/2009:	B.Sc., Boston College for Professional Studies, Jiwaji University, Gwalior, India

Achievements and Awards

1. One of the organizers of the 6th Young Physiologist Symposium, a subgroup of Deutsche Physiologist Gesellschaft, 28-29 September 2017.
2. Got ProChance 2016 travel award from FSU Jena to attend 61st Annual meeting Biophysical Society, New Orleans, USA, 10-16 Feb 2017.
3. Travel award from the German Physiological Society for attending the Young Physiologist Symposium (Leipzig, 2015 and Jülich, 2016).
4. Awarded by 'INSPIRE AWARD' by Department of Science & Technology, Government of India, 2012.
5. Topper of M.Sc. Neuroscience (2009-2011), School of Studies in Neuroscience, Jiwaji university, Gwalior, India.
6. Department of Biotechnology (DBT)-Studentship for master studies from the Government of India (2009 - 2011)
7. John-Miller travel award for attending the Annual Meeting of the Indian Academy of Neurosciences (Jaipur, 2010 and Lucknow, 2011)

Poster

Ladha, A., Martos, V., Plested, A. J. R., Kusch, J. A fluorescent agonist of the muscle nicotinic acetylcholine receptor. 61st Annual meeting Biophysical Society, New Orleans, USA (10-16 Feb 2017).

DOI: http://dx.doi.org/10.1016/j.bpj.2016.11.2982

Ladha, A., Schmauder, R., Kusch, J. Step-child nicotine: Effect of the name-giving agonist on muscle-type nicotinic acetylcholine receptor.59th annual meeting of Biophysical Society, Baltimore, U.S.A. (February 7-11, 2015).

DOI: http://dx.doi.org/10.1016/j.bpj.2014.11.2350

Ladha, A., Kushwaha, K., Tiwari, M., Patro, N., Patro, I. K. Differential neuroinflammatory response to bacterial and viral infection in hippocampus of neonatal rats. XXX annual meeting of Indian Academy of Neurosciences, Amritsar, India (October 28-30, 2012).

Singh, S., **Ladha, A.,** Patro, N., Patro, I. K. Phenotypic changes in astrocytes and microglia in aging brain. XXX annual meeting of Indian Academy of Neurosciences, Amritsar, India (October 28-30, 2012).

Scientific talk

Ladha, A., Martos, V., Plested, A. J. R., Kusch, J. Fluorescent acetylcholine derivative: A potential probe to study agonist binding and gating in nicotinic acetylcholine receptors. *Blitz presentation, FEBS/EMBO Lecture Course on Ion Channels and Transporters, May 14 – 20, 2017,* Erice, Italy.

Ladha, A., Martos, V., Plested, A. J. R., Kusch, J. Towards studying ligand binding and channel gating in nicotinic AChRs using Confocal PCF. *5th Symposium of Young Physiologists, September 22 – 23, 2016,* Forschungszentrum Jülich, Germany